DEVELOPMENT AND CHARACTERIZATION OF MOUSE MODELS OF HUMAN GLIOBLASTOMA

Qian Zhang

A dissertation submitted to the faculty of the University of North Carolina at Chapel Hill in partial fulfillment of the requirements for the degree of Doctor of Philosophy in the Department of Biochemistry & Biophysics, School of Medicine.

Chapel Hill
2006

Approved by

Advisor: Terry Van Dyke

Reader: Kinuko Suzuki

Reader: David Threadgill

Reader: Yue Xiong

Reader: Yi Zhang

ABSTRACT

QIAN ZHANG: Development and Characterization of Mouse Models of Human Glioblastoma
(Under the direction of Terry A. Van Dyke)

Glioblastoma multiforme (GBM) is a very challenging disease clinically because of lacking effective treatments. Accurate and accessible preclinical models of GBM are required to both understand these diseases and facilitate development of diagnostic tests and therapies. Recently, genetic mutations in human gliomas are better understood and techniques to generate genetically engineered mice (GEM) are more sophisticated, which makes it possible to mimic those mutations in the mouse in an accurate way. Here, we developed mouse models of human GBM by simulating most common genetic mutations in human GBMs, including abnormal RTK-Ras signal, Rb pathway, and Pten locus. In the beginning, the model was manipulated so that the mutation (K-Ras^{G12D}) was transferred to astrocytes using an hGFAP-Cre allele, which resulted in primary GBMs. This model is valuable for understanding the role of K-Ras overactivation in primary GBM's formation and cell-of-origin. However, developmental phenotypes other than GBM in this model restrict its further uses in mechanistic studies and combinations with other mutations. In subsequent models, we modified the strategy and generated an inducible system, in which genetic changes can be spatially and temporally induced in adult astrocytes, thus avoiding developmental defects. Induction is elicited by activation of CreERtam, expressed from the human GFAP promoter, after intraperitoneal 4OH-tamoxifen injection. With high penetrance and reproducible timing,

the combination of all three events induces tumors that possess all common histological features of human GBM, including brain invasion, high mitotic indexes, angiogenesis, and necrosis. Furthermore, analysis of event combinations provides insight into disease etiology. For example, without Pten inactivation, pRb inactivation and K-Ras activation predispose to high-grade astrocytic tumors that lack the necrotic phenotype characteristic of GBM. Neither activation of K-Ras nor inactivation of Pten alone produces detectable pathology, and thus are involved in tumor progression. In contrast, inactivation of pRb function initiates disease that does not progress to high-grade tumors. Because of their inducibility, high-penetrance and molecular and histological similarity to human high-grade astrocytomas, these models are extremely promising for both further mechanistic analyses and for preclinical studies, including the validation of potential drug targets and diagnostic and therapeutic development.

TABLE OF CONTENTS

LIST OF TABLES

LIST OF FIGURES

LIST OF ABBREVIATIONS

4-OHT	4-hydroxy-tamoxifen
AA	anaplastic astrocytoma
Areg	amphiregulin
Btc	betacellulin
CC	corpus callosum
CDK4	cyclin dependent kinase 4
CNS	central nervous system
EGF	epidermal growth factor
EGFR	epidermal growth factor receptor
Epgn	epiregulin
GAP	RasGTPase activating protein
GBM	glioblastoma, glioblastoma multiforme
GEM	genetically engineered mouse
GFAP	glial fibrillary acidic protein
H&E	hematoxylin and eosin
HB-EGF	heparin-binding EGF-like growth factor
HDAC	histone deacetylase
IHC	immunohistochemistry
IP	intraperitioneally
LOH	loss of heterozygosity
LV	lateral ventricle
MMAC1	mutated in multiple advanced cancers

MRA	magnetic resonance angiography
mTOR	mammalian target of rapamycin
Nrg1	neuregulin-1
NSCLC	non-small cell lung cancer
OB	olfactory bulb
PCR	polymerase chain reaction
PDGFR	platelet-derived growth factor receptor
PNET	primitive neuroectodermal tumors
PI3K	phosphatidylinositol 3'-kinase
Pten	phosphatase and tensin homology on chromosome ten
Rb	retinoblastoma
Rb_f	retinoblastoma family members
RMS	rostral migratory stream
RT-PCR	reverse transcription- polymerase chain reaction
RTKs	Receptor tyrosine kinases
Stat	signal transducer and activator of transcription
SV40	simian virus 40
SVZ	sub ventricular zone
SVZa	anterior sub ventricular zone
T121	first 121 amino acids of SV40 large T antigen
TGFa	transforming growth factor-a
TUNEL	terminal deoxynucleotidyltransferase mediated dUTP-end labeling
VEGF	vascular endothelial growth factor

WHO	world Health Organization
Wt	wild type
µm	micrometer

CHAPTER ONE

INTRODUCTION

Brain tumors greatly impact the quality of human life as the central nervous system (CNS) plays a fundamental role in the control of human behavior. In the CNS, two major cell types are neurons and glial cells, the latter including astrocytes and oligodendrocytes. Neurons and glial cells are very different despite the fact that they develop from the same neural stem cells in early development. Neurons play a central role in controlling the sense, reaction, cognition and other human activities, while glial cells function as supporting roles for neurons. The majority of primary brain tumors in the adult are derived from glial cells. Astrocytoma develops from astrocytes and oligodendrocytoma develops from oligodendrocytes; and all of them are called gliomas. Malignant glioma is a very challenging cancer clinically. Although not as prevalent as breast cancer and prostate cancer, the lethality of this cancer is among the highest. New cancer therapies have been developed due to breakthroughs in cancer biology and other science technologies in recent years, and many types of cancers can now be treated with a greatly increased rate of survival. However, this is not the case for malignant gliomas, for which the situation has not changed in decades. To understand this unique tumor mechanism and develop meaningful therapies for this disease, preclinical models are necessary.

1.1 Features of Gliomas

The most common gliomas are astrocytomas, including the most advanced form, glioblastoma multiforme (GBM). Astrocytomas account for 75% of human gliomas (CBTRUS, 2006). According to the WHO grading system, astrocytomas are divided into four grades according to the histopathology of tumor.

1.1.1 Grade I astrocytoma

Pilocytic astrocytoma, or grade I astrocytoma, is the most common brain tumor in children and young adults. It accounts for about 5.7% of all gliomas (CBTRUS, 2006). This tumor is found in the cerebellum, optic nerve, chiasm and the hypothalamus. Classic pilocytic astrocytomas have the structures of cystic cavity and mural nodule. Typical histological features of pilocytic astrocytoma are bipolar cells with Rosenthal fibers that are immuno-reactive to GFAP (glial fibrillary acidic protein) and loose multi-polar cells with microcysts and granular bodies that stain poorly with GFAP. GFAP is a component of the astrocytic intermediate filament that is used as a marker for mature astrocytes. In the normal brain, the proliferation rate is nearly 0%. Pilocytic astrocytoma is a slow-growing tumor with a low rate (<1%) of mitosis, and no necrosis. This type of tumor is well circumscribed, is usually not infiltrative and has no tendency to be malignant (Kleihues and Cavenee, 2000). Genetically, pilocytic astrocytoma is associated with neurofibromatosis type 1(NF1), especially optic pathway gliomas (Listernick et al., 1999). It is always curable using surgery with or without radiation therapy and 80% of patients survive more than 20 years after diagnosis.

1.1.2 Grade II Astrocytoma

Diffusive astrocytoma, also referring to low-grade diffuse astrocytoma of adults, is grade II astrocytoma that accounts for 1.7% of human gliomas (CBTRUS, 2006). Diffusive astrocytoma can occur in any region of the brain, but the most common locations are the frontal and temporal lobes. Less often, it may be found in the brain stem and the spinal cord. This type of astrocytoma rarely affects the cerebellum. Diffusive astrocytoma has moderate cellularity and sometimes cells with atypical nuclei are found. Tumor cells are in a loosely structured background and infiltrate the surrounding tissues (Kleihues and Cavenee, 2000;Maher et al., 2001).

Astrocytoma at this stage is well differentiated demonstrated by the fact that most cells are immuno-reactive to GFAP and S100 (an acidic protein widely used as a glial marker), though the latter is not related to the diagnosis (Kleihues and Cavenee, 2000). Nestin, which is an intermediate filament protein and a marker for neural precursors, is usually not detected at this stage (Kleihues and Cavenee, 2000). Diffusive astrocytoma grows slowly with a mitotic rate of about 2.5%, and is detected by Ki67/MIB-1 (proteins expressed in the proliferating cells) immuno-histochemistry (IHC) labeling (Kleihues and Cavenee, 2000). A mutation in p53 is one of the most frequent genetic changes at this stage and occurs in about 75% of diffusive astrocytomas (Watanabe et al., 1997). Other mutations include overexpression of PDGFRα (platelet-derived growth factor receptor alpha) (Hermanson et al., 1992), LOH (loss of heterozygosity) of 10p (on chromosome 10) (Ichimura et al., 1998), LOH of 22q (Huang et al., 1996) and loss of chromosome 6 (Miyakawa et al., 2000). Surgical resection and radiotherapy are treatments for diffusive astrocytomas, but these tumors tend to recur because the tumor cells can't be removed completely.

1.1.3 Grade III astrocytoma

Anaplastic astrocytoma (AA) is a grade III astrocytoma in the WHO grading system, and accounts for 7.9% of human gliomas (CBTRUS, 2006). Anaplastic astrocytoma always develops from low-grade astrocytoma, so the location of these tumors is correspondent to those of grade II astrocytomas with a preference for the cerebral hemispheres. The significant features of anaplastic astrocytoma are nuclear atypia, high mitotic activity, and higher cellularity than diffusive astrocytoma. The mitosis rate is about 5-10% according to Ki67/MIB-1 IHC labeling. Another histological feature is the presence of secondary structures of Scherer: peri-nuclear and peri-vascular satellitosis that was discovered by Scherer in 1938 (Kleihues and Cavenee, 2000;Maher et al., 2001).

Although the majority of anaplastic astrocytoma cells are GFAP positive, lack of GFAP expression is observed in some cells. At the same time, nestin expression in some tumor cells is more common at this stage reflecting the dedifferentiated status of the cells. The most frequent genetic change at this stage is p53 mutation with an incidence of more than 90% (Watanabe et al., 1997). Other mutations include $p16^{INK4a}$ (a cell cycle regulator) deletion, RB (retinoblastoma) alterations, $p14^{ARF}$ (a cell cycle regulator) deletion, CDK4 (cyclin-dependent kinase 4) amplification, Pten (phosphatase and tensin homolog deleted on chromosome ten) mutation and LOH of 10q on chromosome 10. Standard treatments for anaplastic astrocytoma are surgery plus radiation therapy, or surgery plus radiation therapy and chemotherapy. However, the cure rate is very low for anaplastic astrocytoma, which has the tendency to progress to the highly malignant glioblastoma. The average length of survival after diagnosis is approximately 2 years.

1.1.4 Grade IV astrocytoma

Grade IV astrocytoma is also called glioblastoma or glioblastoma multiforme (GBM), which accounts for 50.7% of human gliomas (CBTRUS, 2006). As indicated by the name, GBM is highly heterogeneous, with many different cell components (astrocytes, oligodendrocytes, spindle cells and others) and diversified cell morphologies (poorly differentiated, fusiform, round or pleomorphic cells). Two common variants of GBM are gliosarcoma and giant cell glioblastoma. The majority of GBM cells are nestin immuno-reactive but expression of GFAP is always found in a subset of tumor cells. GBMs occur frequently in the sub-cortical white matter of the cerebral hemispheres with a preference in the temporal, parietal, frontal and occipital lobes. Tumors are most often located in the temporal-frontal lobe and rarely in the cerebellum or brain stem. Due to the invasive properties of GBM, it can infiltrate the other hemisphere and subsequently form certain pattern like a butterfly (Kleihues and Cavenee, 2000). Angiogenesis and necrosis are two hallmark features of human GBMs (Maheret al., 2001), which are not observed in the lower grades of astrocytomas. Other key histological features include highly anaplastic glial cells and a high level of mitosis. Although necrosis is a hallmark feature of GBM, apoptosis is not always found (Tachibana et al., 1996).

Glioblastomas can develop from lower grade astrocytoma after many years or *de novo* with a clinical history shorter than 3 months (Kleihues and Ohgaki, 1997). These are called secondary GBM (mean age=45) and primary GBM (mean age=62) respectively (Ohgaki et al., 2004). Although they are indistinguishable histologically, primary GBM and secondary GBM harbor different genetic changes. In primary GBM, frequent mutations include LOH of 10p/10q, EGFR (epidermal growth factor receptor) amplification/overexpression, MDM2

(transformed 3T3 cell double minute 2; p53-binding protein) overexpression, Pten mutation and $p16^{INK4a}$ deletion. In secondary GBM, common mutations include p53 mutations, PDGF-A (platelet-derived growth factor)/PDGFR-α overexpression, Rb alteration and LOH 10q. GBMs are usually not curable using standard treatments such as surgery, radiotherapy and chemotherapy. The prognosis for GBM patients is very poor and the median survival is 9-12 months (Reilly and Jacks, 2001;de Bruin et al., 2003).

1.2 Genetics of gliomas

1.2.1. Mutations in the cell cycle machinery

1.2.1.1 Rb pathway: $p16^{INK4a}$-CDK4-pRb

Rb (Retinoblastoma) is a major regulator of the G1 to S transition in the cell cycle. In quiescent cells, Rb protein binds to E2F transcription factor and eliminates its ability to transcriptionally activate multiple genes that facilitate DNA synthesis in cell proliferation (Roussel, 1999). The Rb protein activity is controlled by two components in the Rb pathway, $p16^{INK4a}$ and CDK4. CDK4 acts directly and $p16^{INK4}$ acts indirectly. Upon binding to cyclin D1, CDK4 phosphorylates the Rb protein and releases it from the E2F transcription complex, thus promoting cell proliferation. CDK4 is counter- controlled by $p16^{INK4a}$, which binds to CDK4 and inhibits the functional CDK4-cyclin D1 complex, resulting cell cycle arrest (Sherr and Roberts, 1999) (Fig 1).

$p16^{INK4a}$--CDK4--Rb is a linear pathway, so mutations in any step disrupt its function. Alterations of Rb, including deletion of the Rb locus and methylation of the Rb promoter, result in loss of Rb protein expression (Henson et al., 1994;Ichimura et al., 1996;Ueki et al., 1996;Nakamura et al., 2001b). Rb gene promoter methylation is more frequent in secondary glioblastoma than in primary glioblastoma, with incidences of 43% and 14% respectively

(Nakamura et al., 2001b). This mutation could possibly be a late event in glioblastoma progression, since it is not found in low-grade astrocytoma. Second, amplification of CDK4 is found in 11-15% of glioblastomas. Third, homozygous deletion of the $p16^{INK4a}$ gene occurs in 33%-68% of human GBM and is more frequent in primary than in secondary GBM (Henson et al., 1994;Ueki et al., 1996). Interestingly, those mutations are mutually exclusive. In total, approximately 70-80% of human gliomas harbor mutations of components in the Rb pathway.

1.2.1.2. p53 pathway: $p16^{Arf}$-MDM2-p53

p53, also known as the guardian of genome, is an important tumor suppressor gene. Loss-of-function mutations of p53 are common in a wide spectrum of human cancers, including astrocytoma (Levine et al., 1991). p53 is a major regulator of the cellular response to stress such as DNA damage, viral onco-protein expression or hypoxia (Levine, 1997). Under stress conditions, stabilized p53 causes cell cycle arrest in the G1-S and G2-S transitions or apoptosis if the damage is not corrected (Levine, 1997;Hansen and Oren, 1997;Bates and Vousden, 1996). Thus, inhibition of p53 function leads to uncontrolled cell growth and genomic instability. MDM2 is a negative regulator of p53, which makes it a pro-oncogene. In normal situations, MDM2 inhibits the transcriptional function of p53 by escorting p53 to the cytoplasm and inducing the ubiquitin-mediated degradation of p53 protein. $p14^{Arf}$ (human homolog of mouse $p16^{Arf}$) facilitates p53's function by inhibiting MDM2, thus stabilizing the p53 protein (Harris and Levine, 2005) (also see Fig1).

All three members of the $p14^{Arf}$-MDM2-p53 pathway are frequently mutated in glioblastomas. p53 mutations are usually found in secondary glioblastomas at a greater than 65% incidence, but are rarely found in primary glioblastomas (Kleihues and Cavenee, 2000).

Also, according to biopsy studies, mutations in this pathway seem to occur in the early stages of secondary GBMs, such as low-grade astrocytomas or anaplastic astrocytomas (Ohgaki et al., 2004;Watanabe et al., 1996;Watanabe et al., 1997). Most mutations of p53 occur at the hotspot codons 248 and 273 in secondary GBM (Kleihues and Cavenee, 2000). In addition, low expression levels of p53 protein are found in low-grade gliomas due to the methylation of the p53 promoter region (Amatya et al., 2005). Loss of $p14^{ARF}$ expression, due to either gene deletion or promoter methylation occurs in about 76% of gliomas with no bias toward either of the two types of GBM (Nakamura et al., 2001a). MDM2 amplification/overexpression occurs in about 50% of primary glioblastomas and is not frequent in the secondary glioblastomas (Reifenberger et al., 1993;Ghimenti et al., 2003;Biernat et al., 1997). MDM2 and p53 mutations are mutually exclusive, suggesting an alternative or compensate mechanism to inactivate p53 pathway.

1.2.2. RTKs: EGFR and PDGFR

Receptor tyrosine kinases (RTKs) regulate important cell behaviors including cell growth, differentiation and survival. When they receive signals from the extracellular ligands, RTKs are self-phosphorylated at the tyrosine sites, which in turn activate multiple downstream signal cascades leading to changes in cell activities. Two common RTKs mutated in human gliomas are EGFR and PDGFR.

EGFR mutations are hallmark genetic changes in glioblastoma, mainly in primary GBMs and rarely in secondary GBMs. The mutations of EGFR include EGFR amplification and overexpression, both of which generate high levels of EGFR protein (Wong AJ et al., 1987;Chaffanet et al., 1992). Amplification of EGFR is always accompanied by the alterations in the EGFR gene structure. Approximately 20-50% of EGFR amplifications have

a deletion in exons 2-7 producing a truncated extracellular domain variant of EGFR, called EGFRvIII. EGFRvIII is constitutively active at threshold levels because of two reasons: first, it is lack of a ligand-binding domain and in an activated status; second, its activity can't be down-regulated (Huang et al., 1997). EGFR amplification occurs in about 40% and EGFR overexpression occurs in about 60% of primary glioblastomas.

Abnormal PDGF signal is always found in low-grade astrocytomas and secondary GBMs. Both PDGFR ligand and receptor overexpression are increased in human astrocytomas, suggesting stimulation of the ligand-receptor loop by autocrine or paracine factors (Nister et al., 1988). PDGFR has two isoforms: PDGFR-α and PDGFR-β and two ligands: PDGF-A and PDGF-B. PDGF-A and PDGFR-α overexpression is found about 60% of low-grade astrocytomas and amplification of PDGFR-α is found in about 16% of glioblastomas (Kleihues and Ohgaki, 1999). It has been noted that expression of PDGFR-β in GBMs is related to the proliferation of endothelial cells inside tumors (Plate et al., 1992;Hatva et al., 1995).

Both EGFR and PDGFR signals play important roles in glial development, which may provide clues as to why they are involved in the tumorigenesis of glioblastoma. The function of EGFR in glial development is complex, but the basic fact is that EGF-EGFR signaling is related to the development/differentiation of astrocytes (Burrows et al., 1997;Weickert and Blum, 1995). In addition, EGFR contributes to maintenance of the neural stem cell compartment that resides in the ventricular/subventricular zone, in aspects of proliferation (Fricker-Gates et al., 2000), differentiation and migration (Doetsch et al., 2002). In contrast, PDGF-PDGFR signaling is related to oligodendrocyte development, since PDGFR-α level is decreased when glial progenitors differentiate into oligodentrocytes (Calver et al., 1998).

Figure 1. Important molecular pathways in human glioblastoma.

A. Gene mutations in cell cycle control pathways are frequent in human GBMs. The Ink4a locus encodes two genes, $p16^{INK}$ and $p14^{ARF}$ that inhibit the Rb and p53 pathways respectively. Both pathways are involved in cell cycle arrest. Rb controls the G1 to S transition in the cell cycle by binding to E2F. This activity is negatively regulated by CDK4, which phosphorylates the Rb protein. Hyperphosphorylated Rb releases E2F, which in turn transcriptionally activates the DNA replication machinery thus allowing the cell cycle to progress. In the lower arm, p53 regulates cell cycle arrest in both the G1 and G2 phase; it also induces apoptosis when cells are exposed to stress such as encountering genomic instability. p53 activity is inhibited by MDM2, which escorts p53 to the cytoplasm and induces p53 degradation mediated by ubiquitin.

B. Gene mutations in the signal transduction pathway are frequent in human glioblastoma. RTKs including EGFR and PDGFR are frequently mutated in GBMs. Two main downstream pathways are Ras and PI3K. Ras promotes cell proliferation by signaling through the p-ERK mitogenic pathway; Ras also sends signals to the cell survival pathway via the PI3K-Akt pathway. PI3K phosphorylates PIP2 to make PIP3 due to its kinase activity, which is antagonized by Pten. Pten is a tumor suppressor gene that is frequently inactivated in GBMs. The Akt pathway, signaling through mTOR and others, is implicated in apoptosis and cell proliferation.

In this figure, oncogenes are represented by ovals and tumor suppressor genes are represented by rectangles.

A. Cell cycle control

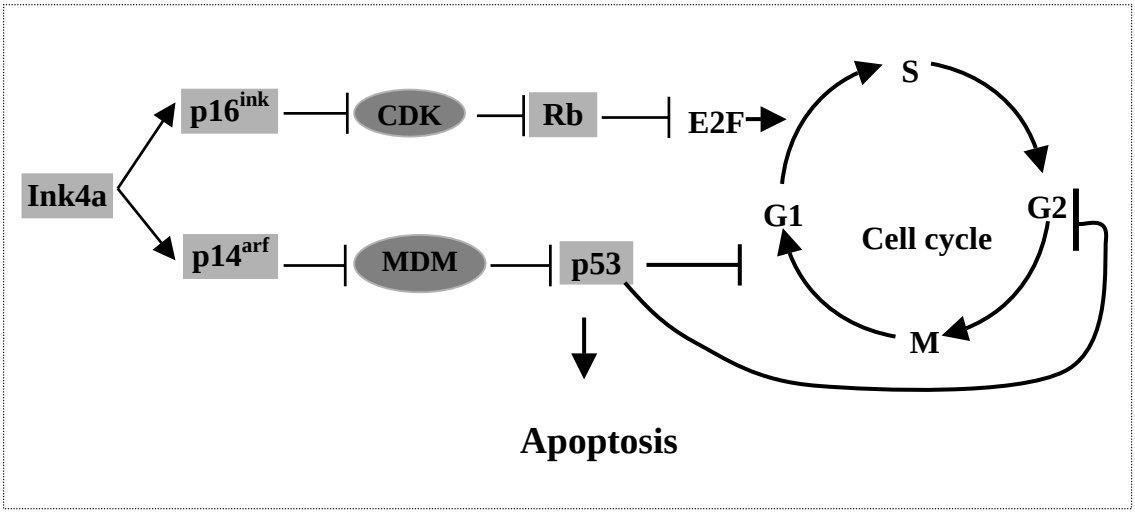

B. Signal transduction pathway

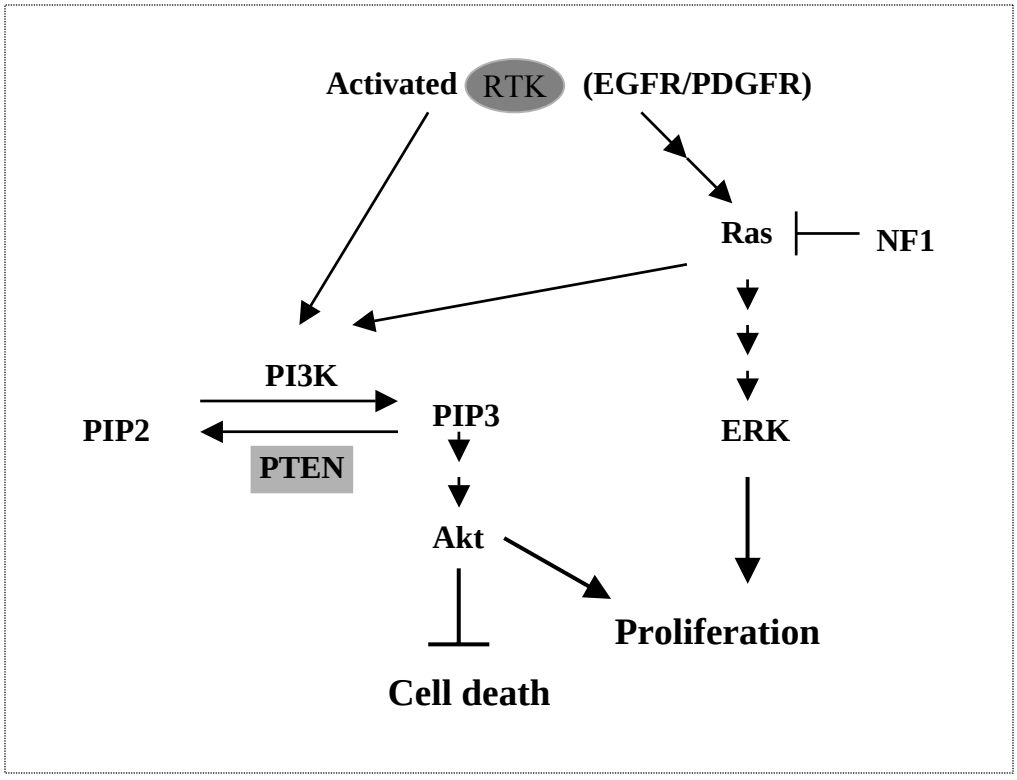

1.2.3. LOH on Chromosome 10 and Pten mutations

The most frequent genetic change in glioblastoma is the loss of heterozygosity (LOH) on chromosome 10, which occurs in approximately 60-80% of human GBMs (Ohgaki, 2005). LOH on chromosome 10 is the only identified mutation with a similar frequency in primary and secondary glioblastomas, suggesting its contribution to the common features of both GBMs. LOH mutations on chromosome 10 are loss of entire chromosome 10, or deletion of 10p14-p15, 10q23-24 or 10q25-pter (Karlbom et al., 1993;Rasheed et al., 1995). Deletions on chromosome 10 are more severe in primary glioblastomas than in secondary glioblastomas: primary GBMs are associated with LOH of the entire chromosome 10; while deletion is restricted to 10q in secondary GBMs (Fujisawa et al., 2000). LOH on chromosome 10 is a later event in GBM progression since it is not usually found in the lower grades of astrocytoma. LOH on chromosome 10, which could be concurrent with other genetic changes, is the only genetic change relating to the shorter survival time of human patients (Ohgaki et al., 2004). The mechanism causing LOH on chromosome 10 is not yet clear.

Multiple deletion loci on chromosome 10 indicate that several tumor suppressor genes are involved in the GBM progression (Ichimura et al., 1998). The candidate genes at these loci (Fujisawa et al., 2000) include Pten at 10q23.3 (Li and Sun, 1997;Steck et al., 1997;Li et al., 1997), LGI1 at 10q24 (Chernova et al., 1998), BuB3 at 10q24-26 (Cahill et al., 1999), MXI1 at 10q25.1 (Eagle et al., 1995;Wechsler et al., 1997), Hours-neu at 10q25.1 (Nakamura et al., 1998), DMBT1 at 10q26.1 (Mollenhauer et al., 1997) and KLF6 at 10p15-15 (Jeng and Hsu, 2003). Among those genes, Pten garners the most attention, and significant progress in understanding its function has been made in recent years. About 15-40% of human GBMs harbor Pten mutations, suggesting that Pten is involved in GBM progression (Knobbe et al.,

2002). The mutations of Pten include nonsense mutations, truncated mutations due to stop codons resulting from nuclear acid insertion or deletion, missense mutations, in frame deletions, splicing mutations and point mutations in the 5' UTR (Ohgaki et al., 2004).

Pten is a tumor suppresser gene, the alternative name of which is MMAC1 (mutated in multiple advanced cancers) or TEP1 (tensin-like phosphatase) (Li et al., 1997;Steck et al., 1997;Li and Sun, 1997). Pten was first cloned in 1997 due to the fact that LOH on the loci close to 10q23 are highly frequent in the multiple advanced cancers, including glioblastoma and others cancers such as prostate carcinomas (Steck et al., 1997;Li et al., 1997). Functional studies of Pten showed that Pten is a lipid phosphatase. The most established activity of Pten is to remove a phosphate from PIP_3, a molecular messenger signaling to Akt (protein kinase B; downstream of PI3-kinase) pathway, thus antagonizing the function of PI3K (phosphoinositide-3 kinase) (see Fig1). Once Akt is activated, it can regulate several important cell activities, including apoptosis, as well as cell cycle control, cell migration/invasion, cell growth, angiogenesis and glucose metabolism (Altomare and Testa, 2005). The functions of Pten in glioblastoma are strongly related to the PI3K/Akt pathway. By resisting the activity of PI3K/Akt, Pten inhibits G1 cell-cycle progression dependent on pRb's controlling of the cell cycle. The anti-apoptosis function of Pten is dependent on Akt and Pten mutations may be related to the hypoxia in GBMs, which in turn activates HIF1 (hypoxia-inducible factor-1) and then VEGF (vascular endothelial growth factor) resulting in angiogenesis. All of those are also related to the PI3K/Akt pathway (Xiao et al., 2002;Knobbe et al., 2002).

1.3. Ras pathway in gliomas

Ras protein is a 21kD small molecule, which functions as a molecular switch, occupying a central position in the networks of cell signaling. Ras pathways regulate multiple cell activities involving proliferation, differentiation, apoptosis, cell migration and angiogenesis. Ras protein is recycled between an active form, RasGTP when bound to GTP, and an inactive form, RasGDP when bound to GDP, which makes it an on-off switch in the control of signal pathways. The conversion of an inactive RasGDP to an active RasGTP is facilitated by GEF (guanine nucleotide exchange factor). Conversely, the conversion of an active RasGTP to an inactive RasGDP is facilitated by GAP (GTPase activating proteins). GAP catalyzes the GTPase function of Ras protein, and is a negative regulator of Ras, thus it is a potential tumor suppressor gene, such as NF1 (neurofibromin 1). Loss of NF1 is found in several related tumors, typically neurofibroma and optical nerve astrocytoma (Listernick et al., 1999).

The direct involvement of Ras in tumorigenesis is demonstrated by the fact that Ras mutations occur in about 30% of human cancers. Ras mutations are found in 90% of pancreatic cancers and 50% of colon cancers as well as significant percentages in many other tumors. Ras genes are sarcoma viral oncogene homologs, including K-Ras homolog to Kirsten sarcoma virus, H-Ras homolog to Harvery sarcoma virus and N-Ras isolated from neurobalstoma (Chang et al., 1982;Shimizu et al., 1983;Hall et al., 1983). Among them, K-Ras is mutated most frequently in human cancers (Bos, 1989). At the same time, K-Ras also plays an important role in embryonic development as shown by the observation that homozygous deletion of K-Ras is embryonic lethal (Koera et al., 1997). Mutations in Ras usually occur at amino acids 12, 13 and 61. These mutations disable the GTPase function of

Ras, resulting in a constitutively activated Ras since it is locked as an active from of RasGTP.

Ras is also involved in tumorigenesis indirectly. Although mutation of Ras proteins are usually not observed in human gliomas, increased levels of activated Ras are common in malignant astrocytoma (grade III and grade IV astrocytomas) associated with abnormal upstream RTK signals (Tuzi et al., 1991;Guha et al., 1997;Knobbe et al., 2004). Several lines of evidence indicate that Ras is related to the advanced stage of GBM progression: first, an increased level of RasGTP is associated with EGFR and PDGFR in high grade astrocytoma (Guha et al., 1997); secondly, mouse models with Ras mutations developed GBM-like morphology (Reilly et al., 2000;Holland et al., 2000;Ding et al., 2001;Zhu et al., 2005). One of the most studied downstream events of the activated Ras pathway is the mitogenic pathway, which signals through the Raf-MEK-ERK and leads to cell proliferation (Pruitt and Der, 2001). Another significant downstream event of the Ras pathway is the PI3K-Akt pathway which contributes to cell survival (Rodriguez-Viciana et al., 1994;Rodriguez-Viciana et al., 1997). In addition, the Ras pathway also contributes to angiogenesis by up-regulating VEGF that possibly signals through the PI3K pathway (Arbiser et al., 1997) or EGFR (Casanova et al., 2002).

Figure 2. Summary of genetic pathways and cell-of-origin in the evolution of primary and secondary glioblastomas.

Glioblastomas (GBMs) either develop from low-grade astrocytomas (secondary glioblastomas), or develop *de novo* (primary glioblastomas). Although these two types of GBM are indistinguishable histologically, they harbor different genetic mutations. This figure illustrates a step-wise progression of related genetic changes, either over-expression of pro-oncogenes or loss-of-function mutations of tumor suppressor genes. In the early stage of secondary GBMs, p53 and PDGFR signals are frequently mutated, which is rare in primary GBMs. In contrast, EGFR and MDM2 mutations are common in primary GBMs but not in secondary GBMs. LOH on chromosome 10 is a common mutation in both GBMs. On the other hand, Pten mutation is more frequent in primary GBMs and Rb alteration is more frequent in secondary GBMs. It is possible that GBMs develop either from mature astrocytes or from neural precursors.

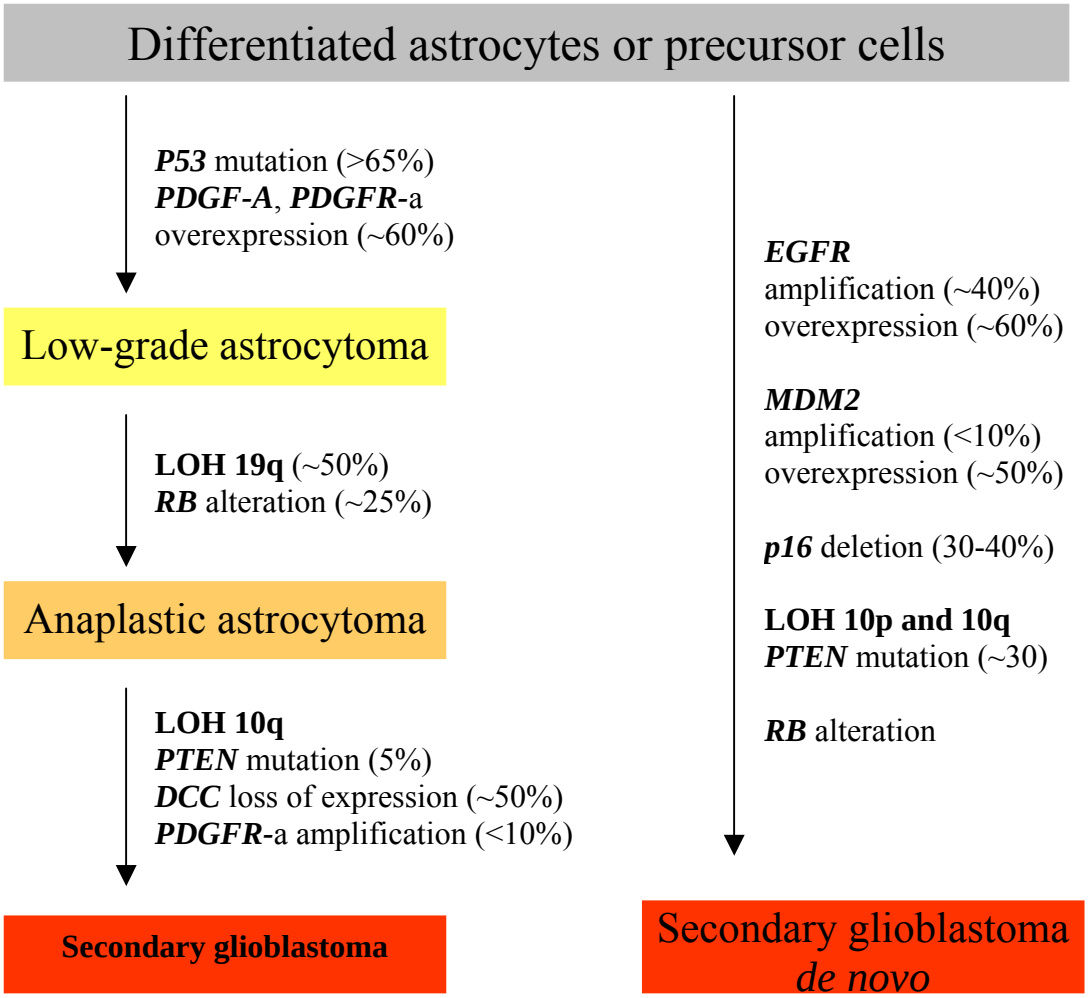

Adapted from: WHO Pathology & Genetics, Tumors of the Nervous System

1.4. Astrocytoma Mouse models

Animal models of human gliomas have been used for mechanism studies and therapy tests for many years. The earlier glioma models were generated either by chemical mutagen treatment (Swenberg et al., 1971), or by transplantation of glioma cells from established cell lines, originally obtained from human or rodent tumors, into an immuno-deficient mouse or rat. This is called a xenograft or allograft (Shapiro et al., 1979;Kobayashi et al., 1980). Most preclinical tests have been done using those conventional models. However, there are some drawbacks with these models. For example, the particular genetic mutations are unclear in those models, which could restrict their use in the emerging new therapies targeting molecular pathways. Also, in the xenograft or allograft models, tumors do not elicit an immune reaction from the host and tumor morphologies differ from human cases. The discrepancies between animal models and human disease limit the translation of test results to clinical applications using those models.

Recently, the knowledge of the genetic mutations found in human gliomas is increasing and the techniques to generate genetically engineered mice (GEM) are more sophisticated, which makes it possible to mimic those mutations in the mouse in a very accurate way. Several mouse models of human astrocytoma have been generated by manipulating genetic changes using different approaches, as summarized in table 1.

All of these models were generated by mimicking the most common genetic changes in human cases including mutations in cell cycle control pathway and signal transduction pathway: inactivation of Rb_f by T_{121} (first 121 amino acids of SV40 large T antigen) which resulted in grade III astrocytoma (Xiao et al., 2002); loss of p53 function by p53 gene deletion together with Nf1 deletion resulted in grade II-IV astrocytoma (Reilly et al.,

2000;Zhu et al., 2005); overexpression of mutant H-Ras resulted in grade II-III astrocytoma or GBM-like lesion depending on dose (Ding et al., 2001); over expression of v-src (oncogene of Rous sarcoma virus), resembling the abnormal EGFR/PDGFR signal, resulted in grade II-IV astrocytoma with a very low penetrance (Weissenberger et al., 1997). It seems that the most efficient way to model grade IV astrocytoma (GBM) is to introduce mutations in both the cell cycle control pathway and the signal transduction pathway at the same time. Interestingly, combined mutations from both pathways always result in GBM phenotype, like p53/Nf1 and Ink4a-Arf $^{-/-}$/K-Ras. This suggests that multiple genetic mutations from both pathways and their cooperation could be critical for GBM formation.

Another consideration in the generation of mouse models is that what cells are suitable targets for genetic mutation. Currently, there are two theories about the cell-of-origin in glioblastoma formation (Figure2). First, based on the fact that secondary glioblastoma can evolve from grade II or grade III astrocytoma, during which tumor cells lose GFAP expression but gain nestin expression gradually, it is possible that mature astrocytes are the original targets for tumorigenesis. GFAP promoter was used broadly in current astrocytoma mouse models to target genetic mutations to mature astrocytes, such as transgenic mutant H-Ras, T_{121} and v-src models (Weissenberger et al., 1997;Ding et al., 2001;Xiao et al., 2002). In those models, there was nestin expression in the tumor cells, suggesting astrocytes may undergo de-differentiation when transformed. However, the GFAP promoter also regulates gene expression in neural stem cells in the early developmental stage, which makes results using these models inconclusive. Second, most GBM cells are positive for nestin and do not necessarily develop from low-grade astrocytoma, such as primary GBM. It is hypothesized that GBMs can arise from neural precursors, which differentiate into astrocytes as well as

oligodentrocytes, of which the latter is present in some GBMs. GBM models have been generated successfully by targeting mutations to Nestin positive neural precursor cells, supporting the idea that these precursors are the cell-of-origin. For example, transduction of viruses carrying K-Ras and Akt oncogenes to nestin expressing cells leads to GBM formation (Holland et al., 2000).

Overall, mouse models help us understand the mechanism of glioma genesis and progression both on the molecular level and the cellular level, which is difficult to achieve by following human cases. In addition, mouse models can speed up therapy testing by offering testable systems for certain drugs. However, GEM models have not been widely used in preclinical testing, and one of the reasons could be that drawbacks of the current mouse models limit further application in therapeutic uses.

Table 1. Astrocytoma mouse models.

Targeted mutations	Targeted cells	Tumor developed	Phenotype	Reference
v-src	Astrocyte (GFAP+)	Grade II, III IV (GBM) astrocytoma	14.4% penetrance; developmental phenotype such as retarded growth, cerebellar ataxia and hydrocephalus	Weissenberger J, 1997 oncogene
$Nf1^{+/-}$ $+p53^{+/-}$ in cis	All cells	Grade II, III and IV (GBM) astrocytoma	Severity and penetrance is background strain dependent	Reilly KM, 2000 Nat Genet
K-Ras+Akt	Progenitor (nestin+)	Glioblastoma multiforme (WHO IV)	Mutations were introduced in P1; GBM developed when targeting to Nestin expressing cells, but not GFAP expressing cells; ~25% penetrance	Holland EC, 2000 nature genetics
V12Ha-Ras	Astrocyte (GFAP+)	Grade II, III astrocytomaat low dose;GBM at high dose	Developmental defects; Severity of phenotype is dose dependent; GBM only in mouse with high dose of Ras, which died early and can't be germline transmitted;	Ding H, 2001 cancer res
T121 (inactivated Rb_f)	Astrocyte (GFAP+)	Grade III astrocytoma	Diffusive anaplastic astrocytoma with 100% penetrance; Pten, but not p53 contribute to tumor progression; developmental defects	Xiao A, 2002 cancer cell
Ink4a-$Arf^{-/-}$ +K-Ras with or without Akt	Astrocytes (GFAP+) or progenitor (nestin+)	Glioblastoma multiforme (WHO IV)	Mutations were introduced in P1; GBM developed both from GFAP and nestin expressing cells	Uhrbom L, 2002 cancer res
$Nf1^{+/-}$ $+p53^{+/-}$	All cells	Glioblastoma multiforme (WHO IV)	GBM with neuronal differentiation; neural precursors suspected to be origin of tumorigenesis	Zhu Y, 2005 Cancer cell

1.5. Test of potential therapies on genetically-engineered mouse models

Conventional therapy choices for human malignant gliomas include surgical resection, radiotherapy and chemotherapy. However, those treatments don't favor the improvement of prognosis for patients. Thus, researchers have been motivated to explore new therapies for this disease. In the last few years, the knowledge of molecular aberrations in human gliomas has advanced rapidly. Accordingly, recent interest in novel therapy development is mainly focused on targeted molecular therapy. This also is a trend with other solid tumors, which may allow for a personalized approach to which is based on the individual's specific tumor mutations.

Therefore, reliable GEM models are essential for testing targeted molecular therapies. GEM models mimic certain genetic changes in human cases, which make every model specific to a certain targeted molecular therapy. Second, GEM models have similar histology to human cases, thus the results are more comparable with results of trials possibly being more reproducible in humans. Third, GEM models generate a consistent phenotype, which will help assess the outcome of various therapies.

Current targeted molecular therapies include small molecular inhibitors, gene therapy and immunotherapy.

1.5.1. Molecular inhibitors

EGFR as a target for cancer treatment has attracted a lot of attention in recent years. High levels of EGFR have been found in multiple cancers, including non-small-cell lung cancer (NSCLC), breast, colorectal, head and neck, prostate, and renal cancers, and primary GBM. Gefitinib (ZD 1839, Iressa) and Erlotinib (OSI-774, Tarceva) are two drug inhibitors of EGFR, which have generated promising results in clinical trials. The FDA has approved

Gefitinib for NSCLC treatment due to significant clinical responses in a subset of patients (Fukuoka et al., 2003;Kris et al., 2003;Pao and Miller, 2005). In malignant gliomas and GBMs, Gefitinib and Erlotinib are used in several ongoing phase I and II clinical trials (Raizer, 2005). In general, only small subsets of patients are responsive to Gefitinib or Erlotinib monotherapy (Rich et al., 2004;Mellinghoff et al., 2005).

However, it is possible that combined therapy using EGFR inhibitors in conjunction with other inhibitors, radiotherapy and/or chemotherapy will improve patient outcome. For example, several pieces of evidence suggest that inhibition of both EGFR and the Akt pathway inhibits the growth of gliomas (Mellinghoff et al., 2005;Goudar et al., 2005).

Another RTK target is PDGFR, which is frequently mutated in secondary GBM. The PDGFR inhibitor used in current clinical trials is Imatinib mesylate (ST157, Gleevec), which has been proven effective in GBM cell lines (Kilic et al., 2000). Results from the phase II study indicated that Imatinib mesylate has limited clinical benefit (Kesari et al., 2005) and increases the risk of intratumoral hemorrhage (Wen and Kesari, 2004;Reardon et al., 2005). Although PDGFR doesn't get as much attention as EGFR, this target is possibly as important as EGFR. That is because PDGFR and EGFR have similar pathways in GBMs and their mutations in GBMs are mutually exclusive (Kleihues and Cavenee, 2000). Thus, if inhibition of RTKs is critical for treatment, then PDGFR inhibitors are needed in the patients with PDGFR but not EGFR mutations.

Other than the RTKs themselves, downstream signals of the RTK pathway can also be targeted for drug tests and one of those generating interest is mTOR (the mammalian target of rapamycin). mTOR expression is mediated by the RTK-PI3K-Akt pathway, and regulates protein synthesis (Burnett et al., 1998). Several inhibitors of mTOR have been used in

clinical trials and result in modest benefits (Kesari et al., 2005). In one study using a mouse model, treatment with the mTOR inhibitor CCI-779 resulted in apoptosis in a subset of tumor cells (Hu et al., 2005). All of these results suggest the potential use of mTOR inhibitors on patients with cancers involving RTK-PI3K-Akt pathway. Inhibitors are available for multiple points in the RTK-FT-Ras-raf-mek-Erk pathway. Some of them are already in clinical trials, such as FT (farnesyl transferase) and Raf inhibitors. Inhibitors for Ras and Mek are available, but they have not been evaluated in humans. The inhibitors targeting the RTK/VEGFR pathways, together with protein degradation and histone deacetylase are summarized in Figure 3.

1.5.2 Gene therapy

In addition to using small molecular inhibitors, gene therapy is another attractive treatment that has been tested in malignant gliomas for many years. In this strategy, a gene carried by a virus is delivered to the brain either by stereotactic intratumoral injection or intraoperative injection into the tumor cavity. The most commonly used viruses are adenovirus and retrovirus. Compared with retrovirus, which affects proliferating cells only, adenovirus transduces both proliferating and quiescent cells, thus offering higher transduction efficiency. The strategies used in gene therapy include: delivery of suicide genes to kill the tumor cells; delivery of tumor suppressor genes; delivery of a gene to promote apoptosis or an anti-angiogenesis gene; delivery of a rapid replicating virus vector to compete for DNA consumption in the proliferating tumor cells; delivery of drugs to tumor cells using high-affinity ligands; delivery of a gene to enhance the immune response; and delivery of antisense oligonuleotides (Pulkkanen and Yla-Herttuala, 2005). Gene therapy has proved safe and effective with very good outcomes in a small portion of patients (Wen and

Kesari, 2004). However, the low transduction efficiency of virus limits its further uses. Based on the fact that neural stem cells are responsive to and migrate into glioma areas, it is suggested that using neural stem cell-guided gene therapy could be one of the ways to increase the efficiency of gene therapy (Kanzawa et al., 2003).

1.5.3 Immunotherapy

Immunotherapy is a relatively less well-developed therapy that introduces a monoclonal antibody to the tumor. The targeted antigen is usually specific to or highly expressed in tumors. Most often, the antibody can be radio- labeled or conjugated to a toxin that helps damage the tumor cells. For example, Tenascin, an extracellular matrix glycoprotein, monoclonal antibody is labeled with ^{131}I and used in clinical trials to delay tumor growth in malignant gliomas patients (Cokgor et al., 2000). Alternatively, the antibody itself is used to disrupt the function of the targeted antigen, which needs to be in the cell surface, such as the monoclonal antibody to EGFR (Yang et al., 1999). Using vaccination strategies is another intriguing option in immunotherapy (Yang et al., 2003).

Figure 3. Summary of targeted molecular inhibitor therapy in malignant gliomas.

Multiple molecules can be targets for drug tests, as indicated by arrows in the genetic pathways of human gliomas. Those molecules are in pathways mainly related to signal transduction. At the upstream end of the pathway, EGFR, PDGFR and VEGFR are some of the most interesting targets involving both inhibitor and antibody tests in clinical trials. Two main pathways downstream of growth factor receptors are Ras-Raf-Mek-Erk and PI3K-Akt-mTOR; the latter is also counter controlled by PTEN. To disable the Ras pathway, an inhibitor to farnesyl transferase is used, which interrupts the activation of Ras from receptor tyrosine kinase, or an inhibitor to downstream raf. To disable the Akt pathway, an inhibitor of mTOR downstream of Akt is used. Other inhibitors are related to the regulation of cell activity at the broader level of protein degradation and gene expression, such as inhibitors to proteasome and HDAC (histone deacetylase).

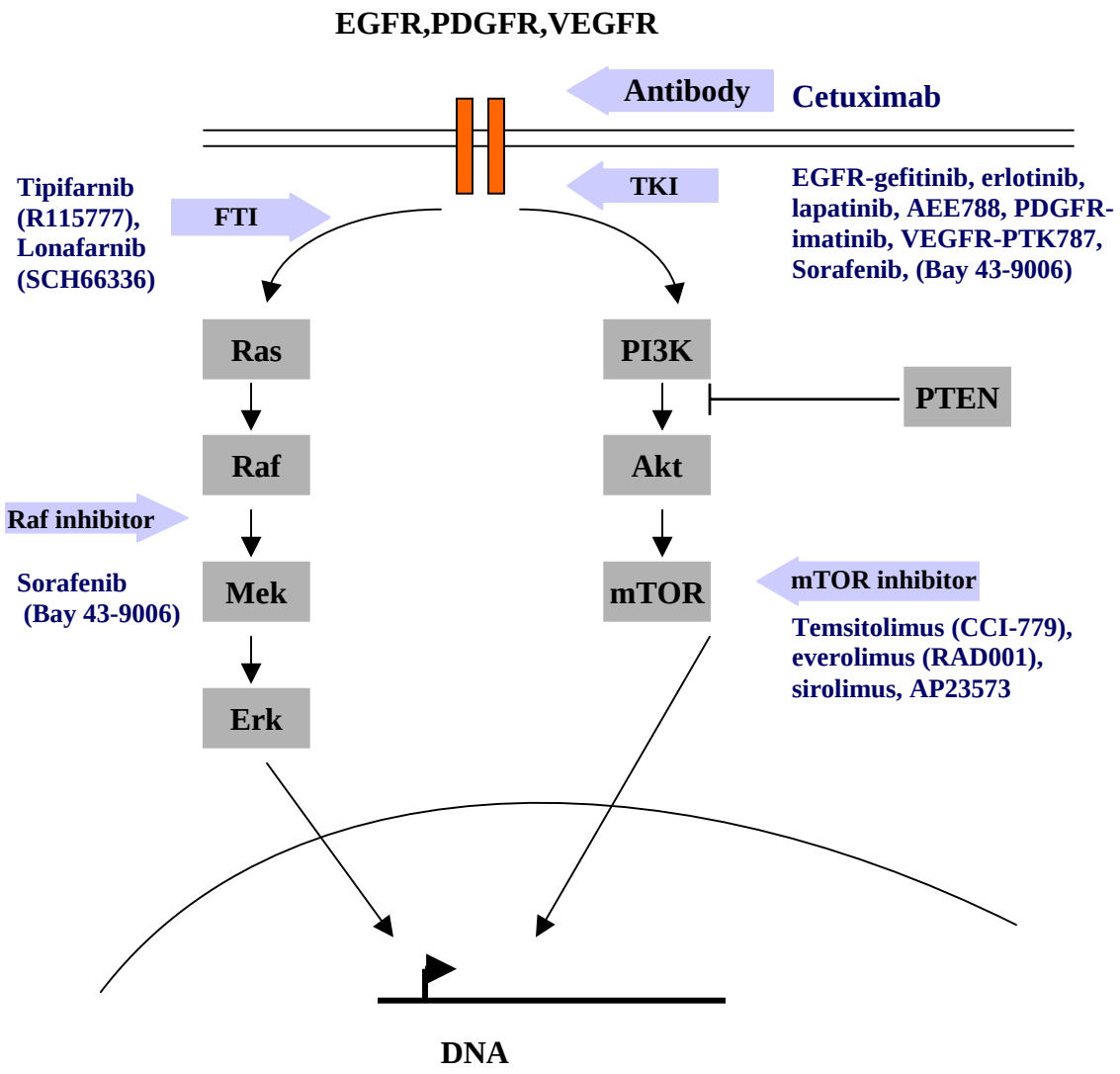

Apadted from Kesari et al., 2005

CHAPTER TWO

ROLES OF K-Ras IN THE ETIOLOGY OF GLIOBLASTOMA:

PART 1 (TUMORIGENESIS)

EGFR, which activates the Ras-ERK pathway in high-grade gliomas, is frequently amplified or overexpressed in glioblastoma multiforme (GBM), especially in primary GBM. To generate a mouse model simulating this change in human GBMs, we transferred a constitutively activated K-Ras mutant allele (K-Ras^{G12D}) at its endogenous expression level to astrocytic lineage cells by introducing a GFAP-Cre allele to floxed stop floxed K-Ras^{G12D} knock-in mice. As a result, some mutant mice (8.3%) developed brain tumors resembling human primary GBMs, in a location adjacent to rostral SVZ (sub ventricular zone). These results indicate that mutant K-Ras at its physiological level, possibly targeting precursor populations in the SVZ (described in Chapter 3), was sufficient to initiate *de novo* glioblastoma formation. Brain tumor formation was accelerated in mice with a p53+/- background, in which the remaining p53 allele was lost (LOH). However, those tumors had characteristics of primitive neuroectodermal tumors (PNET), and had both glial and neuronal differentiation with almost no necrosis.

Introduction

Gliomas, including astrocytoma and the less common oligodendroglioma, are the most common malignant primary brain tumors in humans (Kleihues and Cavenee, 2000). Grade IV gliomas, also known as glioblastoma multiforme (GBM), account for about 50% of gliomas and usually occur in adults after middle age (CBTRUS, 2006). The prognosis for GBM patients is very poor because GBM is highly malignant and incurable by currently available treatments. Thus, we are interested in generating mouse models of GBM to promote better understanding of this disease and to pave the way for new therapeutic tests.

Our lab has generated a grade III astrocytoma mouse model by using transgenic T_{121}, a truncated large T antigen of SV40, which disrupts Rb pathway by inhibiting Rb as well as its family members p107/130 (Xiao et al., 2002). However, since grade III astrocytoma doesn't progress to GBM, we were interested in determining what secondary mutation(s) is required for the transition to highly malignant GBM. The Ras-ERK pathway is one of the most interesting candidates, since the activation of this pathway was not detected in this model, despite the fact it was frequently up- regulated in human GBM (Guha et al., 1997). Moreover, the Ras-ERK pathway is related to the later stage of gliomas, since it was found up-regulated in high-grade gliomas, (Guha et al., 1997) and mutations in Ras are always associated with the GBM phenotype in mouse models (Ding et al., 2001; Holland et al., 2000). Before testing if Ras contributes to the tumor progression in our TgT_{121} model, we first examined the role of Ras alone in astrocytoma formation.

In a previous astrocytoma mouse model, H-Ras overexpression predisposed astrocytes to different grades of astrocytoma, in a dose-dependent fashion (Ding et al., 2001): higher levels of transgenic mutant H-Ras elicited GBM formation while lower levels leaded to grade II/III

astrocytoma. This suggests that the dose of oncogene could affect the role of this gene in tumorigenesis, such that overexpression of the oncogene, especially in the case of multiple copies of transgene, doesn't reflect the real situation found in humans. To avoid or minimize this artificial effect, we used a K-Ras^{G12D} knock-in mouse, in which a stop element flanked with loxP sites is in front of the mutant gene (Jackson et al, 2001). The K-Ras^{G12D} mice were crossed to a GFAP-Cre (glial fibrillary acidic protein) mouse line. Upon Cre expression in astrocytes, the stop element was removed, and then K-Ras^{G12D} was expressed under the control of its endogenous promoter. Thus, K-Ras^{G12D} was introduced at its physiological level to the astrocytic lineage cells, including astrocytes, neurons and neural precursors. This chapter focuses on the tumorigenesis caused by this mutant K-Ras allele. The specific cell types susceptible to tumorigenesis will be stated in Chapter 3.

Results

Introduction of an endogenous level of K-Ras^{G12D} to astrocytic cells

To generate an astrocytoma mouse model simulating an abnormal Ras pathway in humans, we used a conditional loxP-stop-LoxP K-Ras^{G12D} knock-in mouse (Jackson et al., 2001) (Fig. 4A). In the conditional K-Ras^{G12D} knock-in mouse, a mutation was introduced in the exon 1 of the K-Ras gene, which changed the twelfth amino acid, from Gly to Asp. As a result, the function of GTPase was disabled in the K-Ras^{G12D} protein and made it a dominant positive mutant. However, the K-Ras^{G12D} gene is only expressed upon Cre mediated recombination of the stop element that is flanked by LoxP sites upstream of this gene. To restrict K-Ras^{G12D} expression in astrocytes, we introduced Cre specifically to astrocytes by using a GFAP-Cre transgenic mouse line (Zhuo et al., 2001) (Fig. 4A). In this line, Cre

expression is under the control of a 2.2kb human glial fibrillary acidic protein (hGFAP) promoter, which is turned on in mature astrocytes. However, unexpectedly, recent studies show that the hGFAP promoter is also expressed in stem cells (radial glial cells) in development (Zhuo et al., 2001). Using a Rosa/26 reporter mouse line (Dr. McCarthy; Soriano, 1999), we have shown that the reporter protein is expressed as early as E12.5 in the telencephalon, medulla and spinal cord (Fig4B). These structures contain stem cells, which develop into both astrocytic and neuronal populations in adults.

To confirm deletion of the stop element in adult astrocytes and neurons, we used the Rosa/26 reporter to do β-gal immunohistochemistry (IHC) staining in the adult brain cortex, which turned out to be positive (Fig4C). β-gal is a protein expressed in the reporter mouse when loxP sites were recombined. Since the Rosa/26 reporter mouse can't express β-gal in astrocytes, the positive cells were mainly neurons (Casper and McCarthy, 2006). To test if deletion occurred in astrocytes, we did IHC staining for Cre, which was driven by the GFAP promoter in adult astrocytes, and confirmed that it was expressed (Fig 4C).

Therefore, in our mouse model, the endogenous K-Ras promoter controls the expression of mutant K-Ras^{G12D} allele in GFAP expressed/expressing cells, including mature astrocytes and neurons. In addition, K-Ras^{G12D} can potentially be expressed in adult neural stem cells in the sub ventricular zone (SVZ), as it is known now that those cells express GFAP protein (data from reporter line not shown here; Doetsch et al., 1999).

Glioblastoma in the front brain

K-Ras$^{+/G12D}$;GFAP-Cre$^{+/-}$ mice developed both a brain and a skin phenotype (latter not described here). The majority of K-Ras$^{+/G12D}$;GFAP-Cre$^{+/-}$ mice were sacrificed due to the presence of skin tumors (data not shown), but some mice died from hydrocephalus at a

Figure 4. Targeting K-Ras^{G12D} to astrocytic lineage cells at its physiological expression level.

A: Schematic drawing of gene constructs for the K-Ras^{G12D} knock-in mouse and the GFAP-Cre transgenic line. The upper panel is a diagram of the K-Ras^{G12D} mutant fragment. In Exon1, a mutation resulting in the change of amino acids from G to D at the 12th residue is introduced. A stop element flanked with LoxP sites is upstream of Exon1 so that the mutant protein cannot be produced until Cre recombinase is introduced. In the knock-in mouse, K-Ras^{G12D} expression is under the control of the K-Ras endogenous promoter. The lower panel shows the construct used to generate the transgenic Cre line. Cre expression is under the control of a 2.2kb human GFAP (glial fibrillary acidic protein) promoter (Zhuo et al., 2001). B: A Rosa26 reporter mouse strain (B6; 129S4-Gt(ROSA) 26Sortm1Sor) was used to test efficiency of deletion of the stop element. In this reporter line, positive lacZ staining (blue) will indicate that loxP sites were recombined. The upper panel shows 12.5 day embryos with the genotype of RosaStop$^{+/m}$;K-Ras$^{+/G12D}$;GFAP-Cre$^{+/-}$. The lower panel shows a negative control (without RosaStop^{m}). LacZ staining shows that deletion began as early as embryonic day 12.5 and occurred mainly in the telencephalon, medulla and spinal cord. C: Cre and β-Gal (Beta-galactosidase) IHC (immunohistochemistry) staining confirmed that embryonic deletion of LoxP sites resulted in the removal of the stop element in both glial and neuronal populations in the adult. The upper panel shows the cortex area in a RosaStop$^{+/m}$;K-Ras$^{+/G12D}$;GFAP-Cre$^{+/-}$ brain. The lower panel shows negative controls from RosaStop$^{+/m}$;K-Ras$^{+/G12D}$;GFAP-Cre$^{-/-}$ mice. The left panel shows β-Gal staining and the right panel shows Cre staining. Positive staining is brown and the counter stain is blue. Scale bar in each image in C is 20μm.

A.

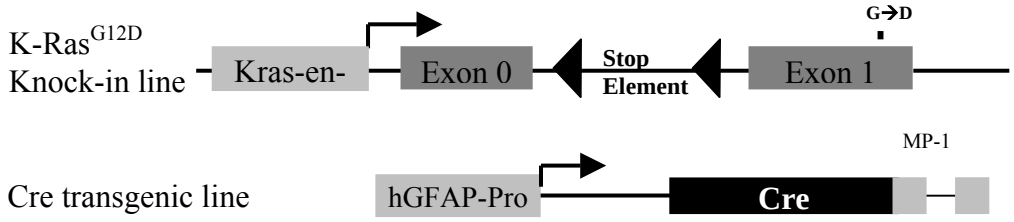
K-Ras^{G12D}
Knock-in line
Kras-en-
Exon 0
Stop
Element
G→D
Exon 1
Cre transgenic line
hGFAP-Pro
Cre
MP-1

B. E12.5

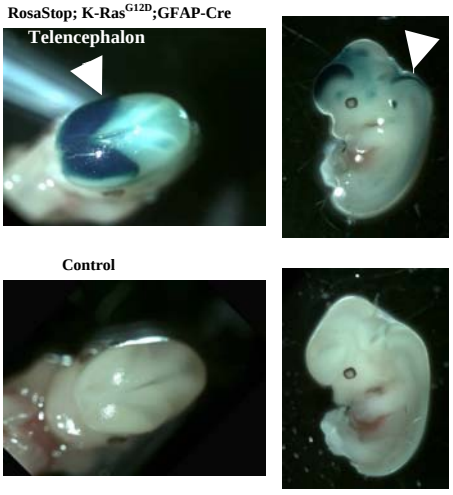
RosaStop; K-Ras^{G12D};GFAP-Cre
Telencephalon
Control

C.

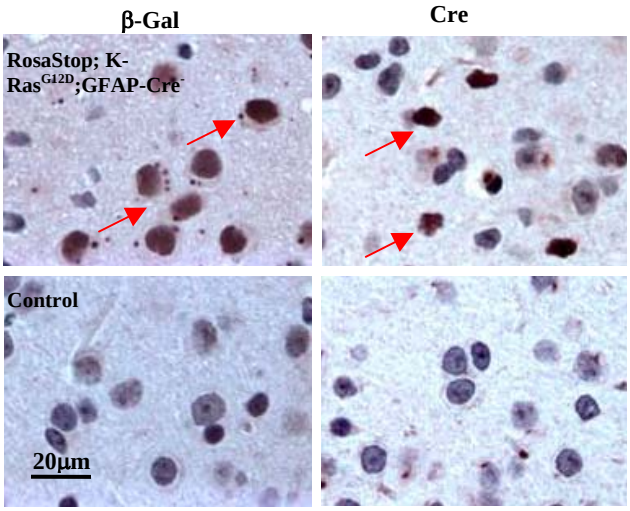
β-Gal
Cre
RosaStop; K-Ras^{G12D};GFAP-Cre
Control
20μm

young age and the remaining mice died from brain tumors or seizure at about 7 months of age. In 8.3% of the K-Ras$^{+/G12D}$;GFAP-Cre$^{+/-}$ mice older than 5.5 months (Table 3, Fig. 8), solid brain tumors developed in 5.5-8 months in the junction between the olfactory bulb and the sub ventricular zone (SVZ) (Fig. 5A), or in the hypothalamus/thalamus (data not shown). The brain tumors were very aggressive; the volume of the tumor dramatically increased in one week. The brain tumor had features resembling human glioblastoma, such as pseudopallisading necrosis and angiogenesis (Fig. 5; Table 3). One of the solid brain tumors that developed in this system was similar to gliosarcoma, a subtype of human glioblastoma multiforme (Kleihues and Cavenee, 2000). Most of these tumor cells appeared to have a spindle and fibrosarcoma-like morphology, and in addition, some cells were immuno-reactive to GFAP indicating an astrocytic origin.

IHC staining of p-ERK, a downstream signal of Ras, was positive in the majority of tumor cells, indicating that the Ras-ERK pathway was activated, thus providing evidence of K-Ras^{G12D} expression as an oncogenic event related to tumorigenesis (Fig. 6A). In those tumors, cells were heterogeneous and only a sub-set of them were immuno reactive to GFAP as indicated by IHC staining (Fig 6B, 6C), which is similar to human GBMs. Furthermore, pseudopallisading cells surrounding a necrotic center were intensely stained by GFAP IHC (data not shown), which also resembles human GBMs. 95% of human GBMs are immuno-reactive to nestin protein, a marker for neural precursors. By performing nestin IHC staining we found that almost all tumor cells were positive for this marker of precursor cells. This also indicated that the tumor cells were in a stage of de-differentiation or un-differentiation. IHC staining of synaptophysin, a marker for neuronal differentiation was negative in those

tumors (Fig. 7D; table 3), confirming that they were glioblastomas. In conclusion, all of the evidence here strongly suggests that these tumors can be categorized as glioblastomas.

Glioblastomas developed in this model are possibly primary GBMs

As discussed in the introduction, glioblastoma multiforme can develop from low-grade astrocytoma after 5-10 years latency (secondary GBM), or can develop *de novo*, (primary GBM). These two types of GBM are indistinguishable in tumor histology, and the only difference is diagnosis history. In our mouse model, the brains of 9 mice sacrificed at terminal stage (7 months), were analyzed. The brain abnormalities included an expanded population in the SVZ precursor cell niche, an expanded corpus callosum and a smaller hippocampus (Table 2). However, no neoplastic lesions were observed (Fig 11). The abnormal areas were well organized, suggesting a developmental defect rather than a tumorigenic effect. Since no low-grade gliomas were identified, GBMs developed in this model were similar to human primary GBMs. Interestingly, this is the first spontaneously arising mouse model of primary GBM, in which the tumors developed without the early detection of neoplastic lesions indicative of lower grade gliomas.

Figure 5. Tumors developed in the frontal brain of adult mice

Solid brain tumors arose in K-Ras^{G12D};GFAP-Cre mice (A). Tumors usually developed in the junction between the front brain and the olfactory bulb as shown by arrows. B is a normal brain control. H&E sections show the tumor at low magnification (C). Staining shows abundant angiogenesis and necrosis. The olfactory bulb morphology was normal. Representative images of necrosis and angiogenesis from H&E sections are shown in D and E. Arrows point to necrosis and vessels. The pseudopallisading appearance of cells around the necrosis center is noticeable.

Scale bar in C is 500μm and scale bar in D and E is 50μm.

Abbreviations: T-tumor; O-olfactory bulb; C-cortex.

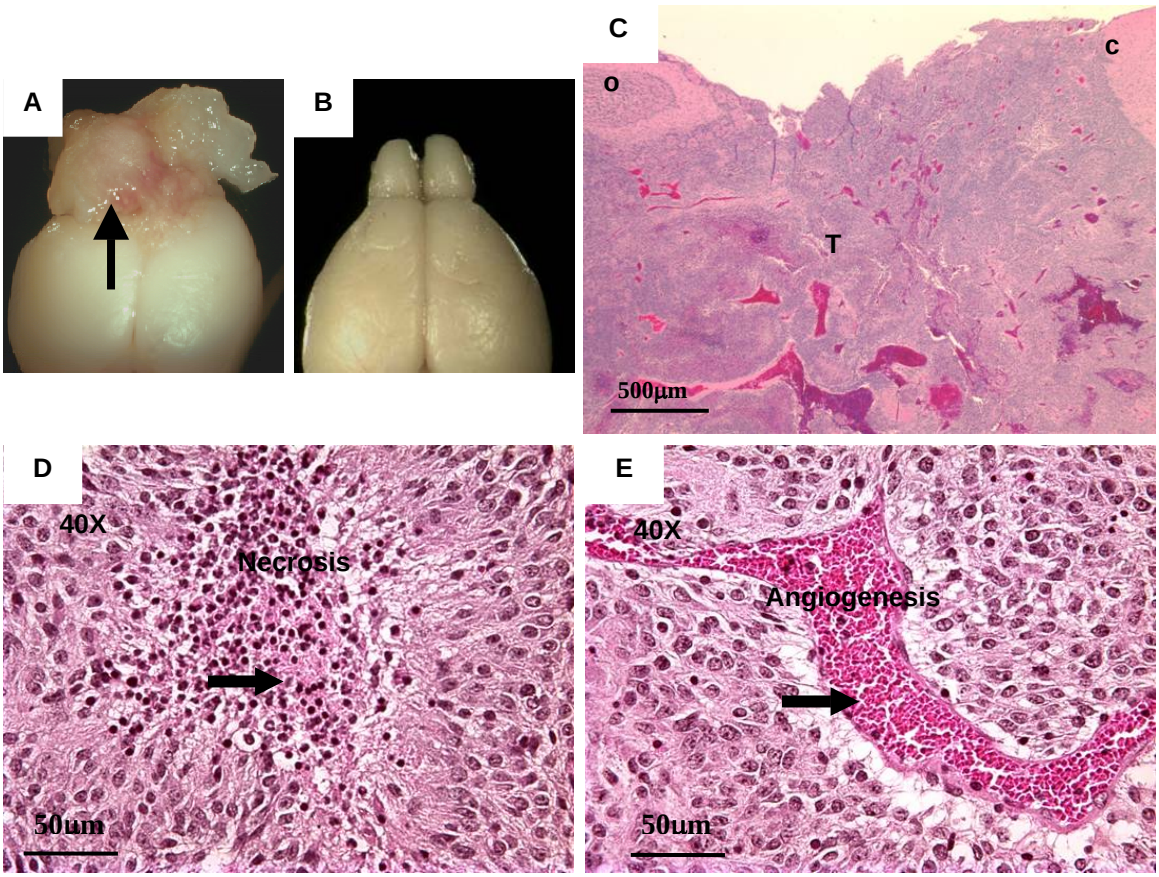
A
B
C
c
o
T
500µm
D
40X
Necrosis
50um
E
40X
Angiogenesis
50um

Figure 6. Characterization of brain tumors in K-Ras^{G12D};GFAP-Cre mice

p-ERK IHC staining indicates that the K-Ras/ERK pathway was activated in K-Ras^{G12D};GFAP-Cre tumors (A and B). Positive staining is brown and counter staining is in blue.

GFAP staining indicates that the tumors contained an astrocytic population (C and D). Positive GFAP staining is blue and counter staining is red.

Nestin staining indicates that tumors contained a dedifferentiated or undifferentiated neural precursor population (E and F). Positive staining is brown and counter staining is blue. Images in the right panel are magnifications from the boxed areas in images in the left panels. Arrows point to the cells with positive staining. Scale bar in A, C and E is 500um and scale bar in B, D and F is 50um.

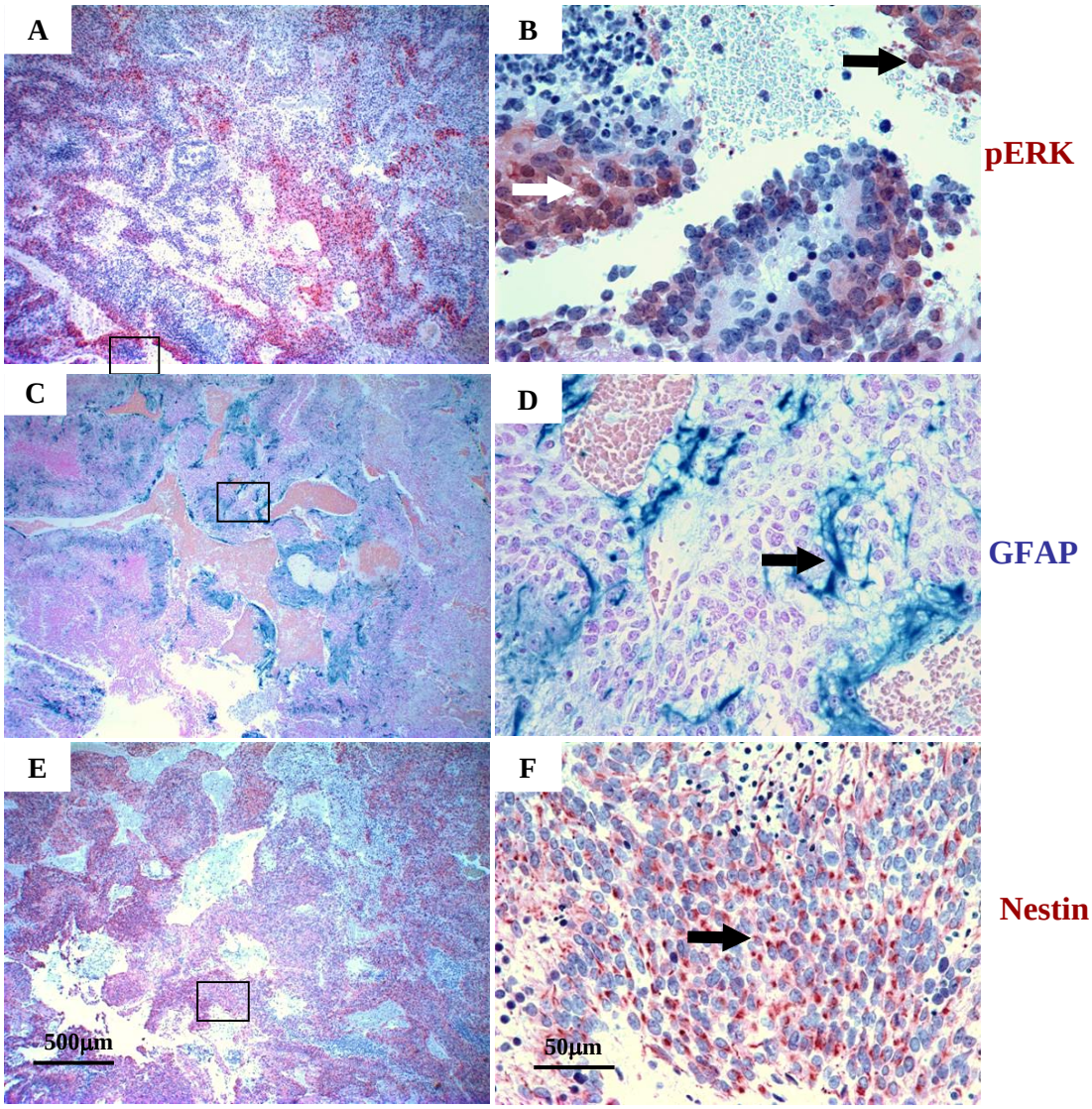
A
B
pERK
C
D
GFAP
E
F
Nestin
500μm
50μm

Table 2. Abnormalities in mice more than 5 mon old.

Abnormal Rostral SVZ (SVZa), RMS, SVZ	Thicker Corpus callosum (CC)	Smaller Hippocampus
100% (9/9)	100% (9/9)	100% (9/9)

p53 deficiency contributed to the acceleration of tumorigenesis, but changed the tumor classification from GBM to PNET

Loss of function mutations of p53 are a common event in human secondary glioblastoma. Although p53 itself is rarely mutated in primary glioblastoma, its antagonist MDM2, which tags p53 protein for degradation, is amplified in more than 50% of primary GBMs. Thus, we asked if p53 deficiency contributed to the progression of tumorigenesis in this mouse model. We generated K-Ras$^{+/G12D}$;GFAP-Cre$^{+/-}$;p53$^{+/-}$ mice by doing triple crosses. As shown by the survival curve in Fig. 8A, tumorigenesis was greatly accelerated in the p53$^{+/-}$ background. At the same time, the frequency of tumors is much higher in the p53$^{+/-}$ background (Table 3). Similar to K-Ras$^{+/G12D}$;GFAP-Cre$^{+/-}$ tumors, tumors on a K-Ras$^{+/G12D}$;GFAP-Cre$^{+/-}$;p53$^{+/-}$ background were highly vascular (Fig. 7A, 7B) and a portion of the tumor cells showed astrocytic differentiation (Table2). Tumors in K-Ras$^{+/G12D}$;GFAP-Cre$^{+/-}$ mice with p53 wild type were different than tumor cells in mice with a p53$^{+/-}$ background. The cells from mice with p53+/- looked primitive and undifferentiated as shown in Fig 7A. IHC staining of neural cell markers showed that the tumors contain both astrocytic and neuronal cells (Fig. 7E, F and Table 3), suggesting that they are primitive neuroectodermal tumors (PNETs) instead of GBMs. Consistent with human GBM and PNET, necrotic centers were abundant in the tumors of K-Ras$^{+/G12D}$;GFAP-Cre$^{+/-}$ mice, but hardly seen in the tumors of K-Ras$^{+/G12D}$;GFAP-Cre$^{+/-}$;p53$^{+/-}$ mice (Fig. 8B). These results indicate that a lack of p53 did contribute to the tumorigenesis; however, p53 changes the differentiation of tumor cells, which converts the tumor from GBM to PNET. Interestingly, tumor cells were more heterogeneous in the p53$^{+/-}$ background mice. Sometimes the size of tumor cells was increased with abnormal nuclear (Fig 7C) indicating of giant cell

glioblastoma, suggesting that a deficiency of p53 may contribute to such a phenotype in human GBM.

p53 loss in tumors in $p53^{+/-}$ background

Although tumorigenesis was accelerated in mice with a $p53^{+/-}$ background, it is not clear whether p53 protein is functional in tumors due to the existence of a wild type allele of p53. To test this, we examined if p53 was expressed in tumors by performing p53 IHC staining in tumors with $p53^{+/+}$ and $p53^{+/-}$ backgrounds (Fig. 9A, 9B). We found that p53 was not expressed in tumors with a $p53^{+/-}$ background indicating that the tumor suppressor functions of p53 were abrogated. In contrast, p53 was expressed throughout the whole GBM tumor in $Kras^{+/G12D}$;GFAP-$Cre^{+/-}$ mice. Interestingly, especially higher level of p53 protein expression were observed in pseudopallisading cells surrounding the necrotic center compared to other region. Correlation of increased p53 expression and the necrotic center suggests the possible involvement of p53 in necrotic genesis. This may explain the absence of necrosis in tumors with $p53^{+/-}$ background.

To test if lack of p53 expression in PNET is caused by loss of the remaining wild- type allele of the p53 gene, we performed PCR analysis of the wild type and knockout alleles of p53 from samples extracted from either the tumor area or surrounding normal brain tissue. As shown in Fig. 9C, there was barely detectable p53 wild type allele in the tumor area, whereas p53 was present in the normal tissue. This result suggests that loss of heterozygosity (LOH) of p53 occurred in tumor cells and these were selectively expanded in PNET tumors.

Figure 7. Characterization of tumors in mice with a $p53^{+/-}$ background.

H&E sections from multiple tumors in K-$Ras^{+/G12D}$;GFAP-$Cre^{+/-}$;$p53^{+/-}$ mice were analyzed (A-C). In a portion of the tumors, cells were round with a dense nucleus and not much cytoplasm, suggesting that the cells are primitive (A). In some tumors, cells were around fine vessels (B), similar to a structure called a rosette, which is usually seen in human PNET. Multinucleated giant cells were observed in some tumors (C).

Synaptophysin IHC staining showed neuronal differentiation in K-$Ras^{+/G12D}$;GFAP-$Cre^{+/-}$;$p53^{+/-}$ tumors (E), but not K-$Ras^{+/G12D}$;GFAP-$Cre^{+/-}$ (D). Positive staining is brown. Counter staining is shown in blue.

NeuN IHC staining detected mature neurons (F). Brown color is positive staining, blue color is counter staining.

Scale bar in A, B, C and F is 100μm and scale bar in D and E 300μm.

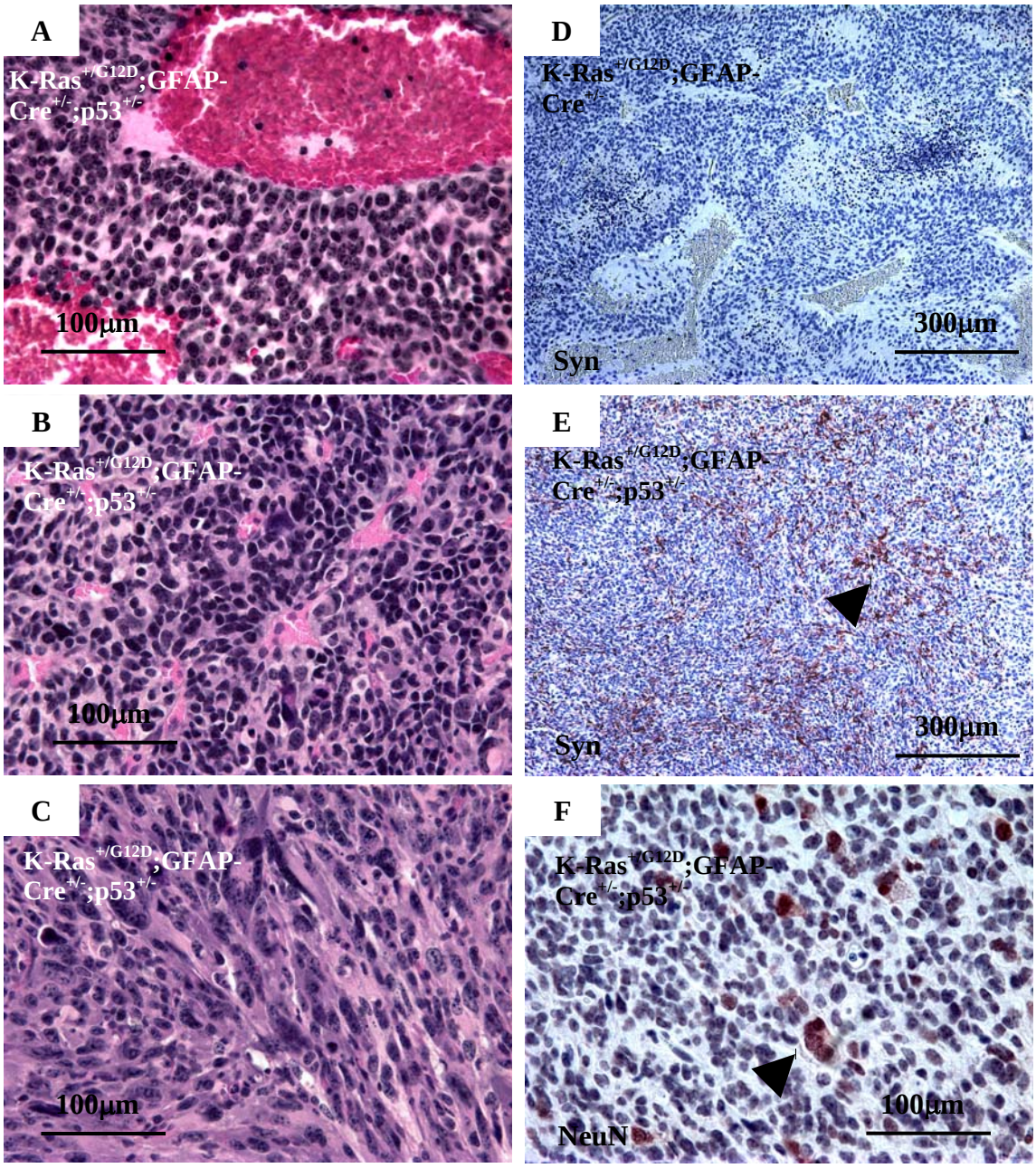
A
K-Ras+/G12D;GFAP-Cre+/-;p53+/-
100μm
B
K-Ras+/G12D;GFAP-Cre+/-;p53+/-
100μm
C
K-Ras+/G12D;GFAP-Cre+/-;p53+/-
100μm
D
K-Ras+/G12D;GFAP-Cre+/-
Syn
300μm
E
K-Ras+/G12D;GFAP-Cre+/-;p53+/-
Syn
300μm
F
K-Ras+/G12D;GFAP-Cre+/-;p53+/-
NeuN
100μm

Figure 8. Tumor growth was accelerated in the $p53^{+/-}$ background mice.

Brain tumor survival curves of K-$Ras^{+/G12D}$;GFAP-$Cre^{+/-}$ mice (in red) and K-$Ras^{+/G12D}$;GFAP-$Cre^{+/-}$;$p53^{+/-}$ (in green) are shown in panel A.

The bar graph summarizes the number of necrotic centers in the tumors (B). Numbers were obtained by counting the total number of necrotic centers in one section, from the middle layer of tumors of similar sizes. The presence of necrotic centers were a typical phenotype in K-$Ras^{+/G12D}$;GFAP-$Cre^{+/-}$ mice, while this was rarely observed in K-$Ras^{+/G12D}$;GFAP-$Cre^{+/-}$;$p53^{+/-}$ mice. p= 0.0009.

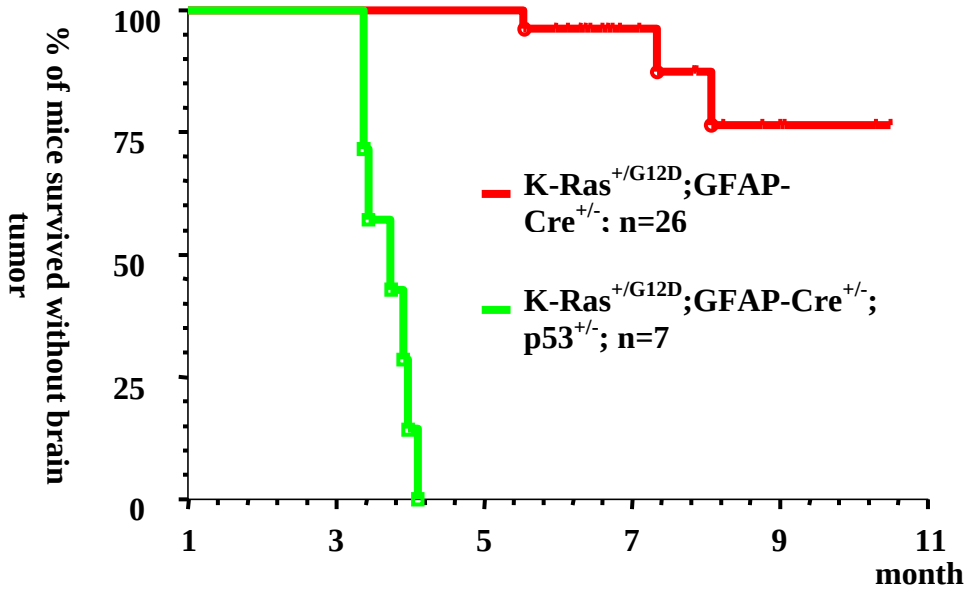
% of mice survived without brain tumor
100
75
50
25
0
1
3
5
7
9
11
month
K-Ras+/G12D;GFAP-Cre+/-: n=26
K-Ras+/G12D;GFAP-Cre+/-; p53+/-; n=7

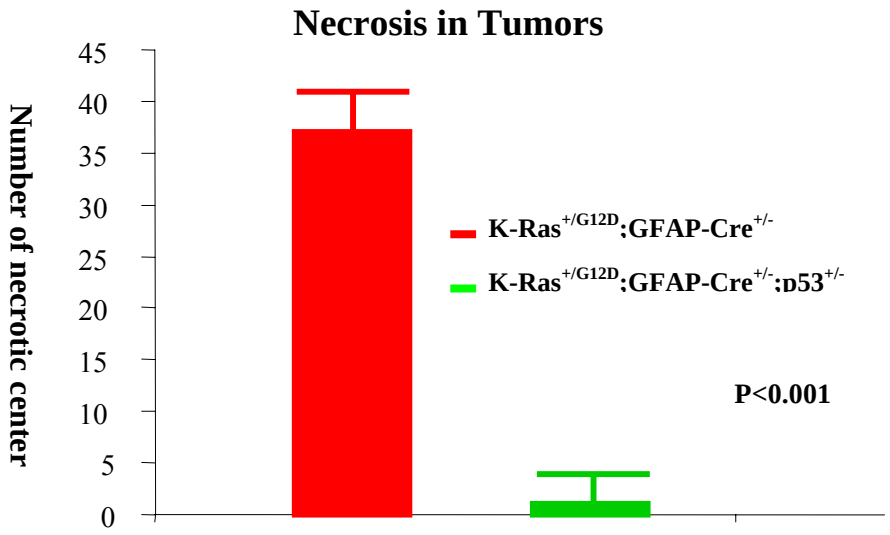
Necrosis in Tumors
Number of necrotic center
45
40
35
30
25
20
15
10
5
0
K-Ras+/G12D;GFAP-Cre+/-
K-Ras+/G12D;GFAP-Cre+/-;p53+/-
P<0.001

Table 3. Tumor frequency and marker study in tumor with/without p53.

	$Ras^{+/G12D}$;GFAP-$Cre^{+/-}$	$Ras^{+/G12D}$;GFAP-$Cre^{+/-}$, $p53^{+/-}$
Tumors	**8.57%(3/35[1];GBM[2])**	**100%(7/7[1];PNET[3])**
Nestin	++++	++++
GFAP	+~++	+++
S100	++	+++
Synaptophysin	--	+~+++
NeuN	--	--~+

1. **Only includes mice after initial onset of tumors (greater than 5 months of age); mice younger than 5 months of age will not included due to incidence of skin tumors and hydrocephalus.**
2. **GBM: glioblastoma multiforme.**
3. **PNET: primitive neuroectodermal tumors.**

Figure 9. LOH of p53 in brain tumors with a $p53^{+/-}$ background.

IHC staining of p53 was performed in tumors with genotypes of K-$Ras^{+/G12D}$;GFAP-$Cre^{+/-}$ (A) and K-$Ras^{+/G12D}$;GFAP-$Cre^{+/-}$;$p53^{+/-}$ (B). Positive staining was identified in the K-$Ras^{+/G12D}$;GFAP-$Cre^{+/-}$ tumor, as indicated by the brown color. In contrast, there was no positive staining in K-$Ras^{+/G12D}$;GFAP-$Cre^{+/-}$;$p53^{+/-}$ tumors, indicative of no p53 expression. Counter staining is blue.

PCR (polymerase chain reaction) assays show the second allele of the p53 gene was deleted in tumor cells with a $p53^{+/-}$ background (C). DNA was extracted from cells both from the tumor and from a normal brain area from paraffin sections of seven brains. The upper panel is a PCR to test if the wild type allele of the p53 gene is present. The lower panel tests the presence of the knocked-out allele of p53, which was also used as DNA quality control. + is positive control and – is negative control.

Scale bar in A is 50μm.

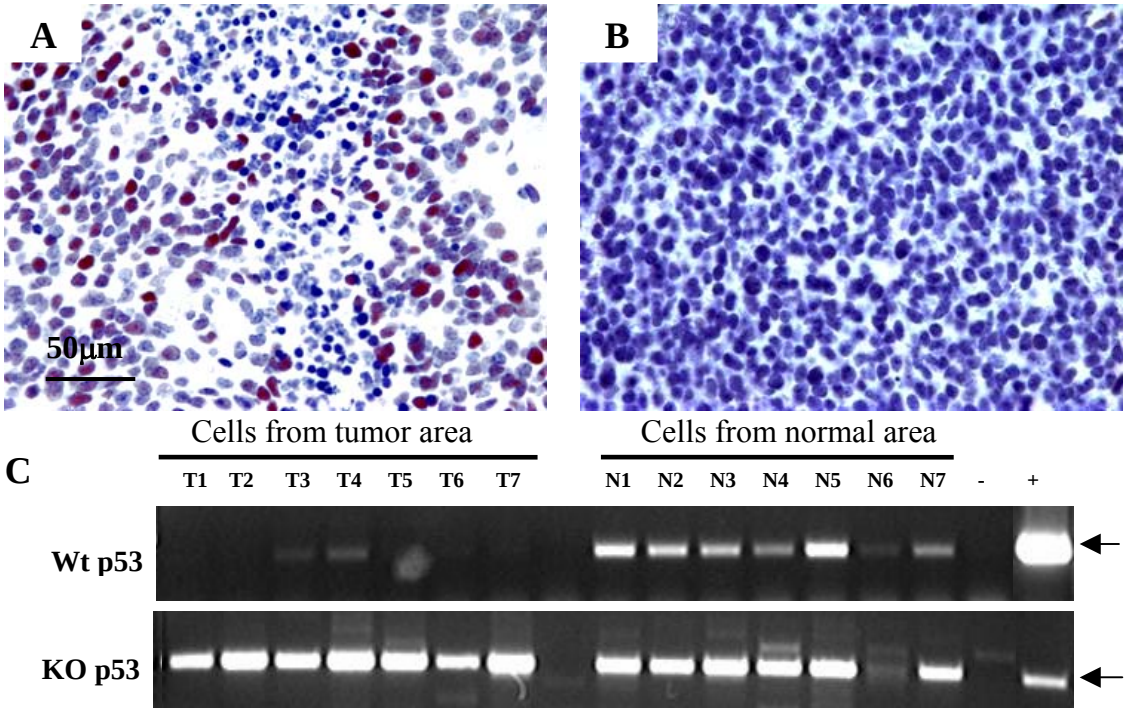
A
50μm
B
C
Cells from tumor area
Cells from normal area
T1 T2 T3 T4 T5 T6 T7
N1 N2 N3 N4 N5 N6 N7 - +
Wt p53
KO p53

Discussions

Endogenous levels of K-Ras^{G12D} predispose brain to GBM formation

This study shows that physiological levels of K-Ras^{G12D} in astrocytic lineage cells leads to brain tumors with many of the characteristics of human primary glioblastoma (Fig 5), providing direct evidence that the K-Ras pathway is involved in GBM formation. However, secondary mutations may be required for the tumorigenesis since it took about 7 months for tumors to develop; the penetrance of tumorigenesis is low (8.3%); and no pre-tumor nodules were identified in most cases. Secondary mutations could be random, supported by the fact that every tumor had very different features. For example, in one case, the tumor cells looked like glial cells, while in another case, tumor cells are fibrosarcoma-like. It could be that different second or third mutations occurred in these two cases. The differences in tumor morphology shown here could also reflect the heterogeneous nature of the tumor, which resembles human GBMs. However, to draw a definitive conclusion, further analysis of this model is needed.

Since K-Ras^{G12D} is under the control of its endogenous promoter, functional activation of this mutant requires the transcriptional activation of the K-Ras gene. Physiological levels of K-Ras^{G12D} in the brain are able to initiate GBM, suggesting that the K-Ras gene is activated in certain cells, which are prone to tumorigenesis. This cell-of-origin question will be discussed in Chapter 3.

Using constitutively active Ras mutants to generate astrocytoma or GBM mouse models has resulted in different phenotypes. It has been shown that overexpression of one copy of ^{V12}H-Ras causes grade II or grade III astrocytoma formation and multiple copies of ^{V12}H-Ras leads to a GBM like lesion (Ding et al., 2001). In another study, K-Ras^{G12D} itself could not

elicit glial genesis when targeted to either mature astrocytes or precursor cells; however, K-Ras^{G12D} combined with Akt caused GBM formation when targeted to precursors (Holland et al., 2000). Our model shows that physiological levels of K-Ras^{G12D} by itself were sufficient for GBM formation. These conflicting results could be due to different Ras mutants/isoforms or targeting these mutations to different cell populations. For example, the same K-Ras^{G12D} was used in Holland's model and ours; however, our model showed that a single mutation of K-Ras^{G12D} was sufficient for GBM formation, while K-Ras^{G12D} required Akt to initiate GBM in Holland's model (Holland et al., 2000). One of the reasons for this conflicting data is possibly the targeted cell. Virus was used in Holland's model to transfer K-Ras^{G12D}, therefore a smaller population of cells may have been affected by the mutant allele.

p53 loss and PNET formation

Our work shows that physiological levels of K-Ras^{G12D} predisposed brain to primary GBM. Surprisingly, a p53 deficiency in this model changed the classification of the tumor from GBM to PNET. In humans, except for being mutated in early stage of GBM, p53 mutation is also related to PNET. Our result is consistent with a recent reported GBM mouse model (Zhu et al., 2005), in which Nf1 (a RasGTPase activating protein, GAP) and p53 were mutated in brain, resulting in tumorigenesis with both glial and neuronal differentiation. Generating mouse models of GBM, which accurately simulate the genetic changes of GBM in humans, could be important. Point mutations in p53 are frequently found in the early stage of secondary GBM, but not in primary GBMs. Since MDM2 is frequently mutated in primary GBMs and is in the same pathway as p53, we assumed that a p53 mutation could substitute for an MDM2 mutation in primary GBMs. However, our result demonstrating that p53 loss changes the type of tumors elicited by physiological levels of K-Ras^{G12D}, suggests that this

may not be true. Furthermore, though p53 mutations and EGFR mutations are common in human GBMs, they are mutually exclusive, indicating a unique underlying mechanism of p53 pathway inactivation for tumor evolution.

In this model, the p53 mutation is introduced into every cell, thus targeting a broader spectrum of cells than those with the K-Ras^{G12D} mutation. Recent work by Hill et al. showed that disruption of the Rb pathway in prostate epithelium induces both autonomous p53 loss in epithelium and non-autonomous p53 loss in stromal cells. A similar scenario could occur here in glial tumor cells, which would subsequently cause p53 loss in the neuronal population and transform them. Once neuronal cells or precursors are transformed, they evolve with glial tumor cells, forming a tumor mass including both glial and neuronal cells. An alternative possibility could be that p53 loss affects cell differentiation or different cells were targeted.

Materials and methods

Genetic engineered mouse breeding. To target the mutant K-Ras allele specially in astrocytes, K-Ras^{G12D} conditional knock-in mice (from Dr. Tyler Jack's lab) were crossed to GFAP-Cre mice (from Dr. Ken D McCarthy's lab). To generate K-Ras$^{+/G12D}$;GFAP-Cre$^{+/-}$;p53$^{+/-}$ mice (p53 mice originally from Jackson labs), K-Ras$^{+/G12D}$;p53$^{+/-}$ mice were generated first, then mated to GFAP-Cre$^{+/-}$ mice, because K-Ras$^{+/G12D}$;GFAP-Cre$^{+/-}$ mice can't nurse offspring well. K-Ras$^{+/G12D}$;GFAP-Cre$^{+/-}$;Rosa/26$^{+/m}$ were generated by mating Rosa/26$^{+/m}$;GFAP-Cre$^{+/-}$ mice to K-Ras$^{+/G12D}$. For K-Ras$^{+/G12D}$ mutant allele genotyping, primers are 5' – AGC TAG CCA CCA TGG CTT GAG TAA GTC TGC A – 3' and 5' – CCT TTA CAA GCG CAC GCA GAC TGT AGA – 3'. PCR condition is 94^{o}C 3min, 35

cycles of 94°C 30sec, 60°C 1min 30sec and 72°C 5min, and then 72°C 5min. For GFAP-Cre genotyping, primers are 5' – TGA TGA GGT TCG CAA GAA CC – 3' and 5' – CCA TGA GTG AAC GAA CCT GG – 3'. PCR condition is 94°C 1'30'', 35 cycles of 94°C 30sec, 59°C 1min and 72°C 5min, and then 72°C 5min. For p53 knock out allele PCR, primer sets were 5' – TCC TCG TGC TTT ACG GTA TC – 3' and 5' – TAT ACT CAG AGC CGG CCT – 3'. PCR condition is 94°C 3min, 35 cycles of 94°C 1min, 60°C 2min and 72°C 2min, and then 72°C 5min. For Rosa/26+/m mutant allele genotyping, primers are 5' – AAA GTC GCT CTG AGT TGT TAT– 3' and 5' – GCG AAG AGT TTG TCC TCA ACC– 3'. PCR condition is 94°C 2min, 35 cycles of 94°C 30sec, 60°C 30secn and 72°C 30sec, and then 72°C 3min.

Histology and immunohistochemistry.

Tissue processing and H&E. Mice were euthanized in a CO_2 chamber. Brain tissue was removed and fixed in 10% formalin for 20hr- 24hr, then stored in 70% EtOH. Fixed tissues were paraffin embedded and sectioned at 5μM. Hematoxylin and eosin staining was performed as previously described (Symonds, Krall et al., 1994).

Single staining procedure. Paraffin sections were deparaffinized with Histo-clear and rehydrated with ethanol/H_2O, followed by a PBS wash. For antigen retrieval, sections were treated with citrate buffer by microwave heating for 2min at high power and 7min at power 2, and then were cooled to room temperature. Depending on the antibodies, slides were pre-treated with trypsin or trilogy or not pre-treated. Slides were washed twice with double-distilled water for 5min then quenched in 5% H_2O_2 with ddH_2O for 5 min. After washing, the slides were blocked with 5% goat serum/ PBS-T (0.1MPBS, 0.5% Tween 20) for 30min at room temperature. Primary antibody was diluted in 5% serum/ PBS-T and the slides were

incubated at room temperature for 1hr or at 4°C over night depending on which antibodies were used. Slides were washed and incubated with a 1:333 dilution of secondary antibody in 2% serum/ PBS-T for 30 min. After washing, the slides were incubated with Vectors Vectastain elite AB solution, and the color developed using Vector's NovaRED substrate kit. Slides were counter stained using Vector's hematoxylin for 2min, rinsed briefly in double-distilled water, and then rinsed in Li_2CO_3 for 1-3 seconds. After washing, the slides were dehydrated and mounted. A few samples were stained using Vector's ABC-AP substrate kit instead of Vector's NovaRED substrate kit and counter stained with Nuclear Fast Red for 12 min at room temperature without the quenching step.

Primary antibodies used were: GFAP(Z0334, DAKO rabbit at 1:100); NeuN (Chemicon mouse at 1:500);Cre (69050-3 Novagen, rabbit at 1:6000); phosphor-Erk1,2$^{Thr202/Tyr204}$ (9101, cell signaling, rabbit at 1:50); Syn (A0010 Dako, rabbit at 1:50); β-gal(anti-b-galactosidase, A-11132 molecular Probes; rabbit at 1:500); p53(NCL-p53-CM5p Novo, rabbit at 1:750).

LacZ staining. Staged embryos (including E12.5), newborn pups or adult tissue were collected and washed with cold 0.1M PBS, then fixed in 4%PFA/0.1M PBS at 4°C with shaking for 30min for embryos and 24h for the rest. Samples were then washed in 0.1M PBS, 3 X 20'. Fresh LacZ staining solution (1mg/ml X-gal, 5mM K_3FE, 5mM K_4FE, 2mM $MgCL_2$, 0.02% NP40, 0.01% Na Deoxicholate in 0.1M PBS) was added. E12.5 embryos were incubated at 37°C (or RT with longer incubation time) overnight; other samples were incubated at room temperature and checked every 2h for staining status. The staining reaction was stopped by rinsing three times in PBS for 20 min each and the samples were stored in 70% EtOH. For embryos, tails were cut and used for genotyping PCR.

p53 LOH by PCR. To extract DNA, targeted cells in the tumor area or in the normal region were scratched using an 18-gauge needle under a dissection microscope. A fresh needle was used for each scratch. 50ul extraction solution A (25mM NaOH/0.2mM EDTA) was added, and samples were incubated at 65°C for about 20hr. 50ul solution B (40mM Tris-HCl) was then added, mixed well, and spun for 2 min and the supernatant kept for PCR. The PCR to detect the p53 knockout allele was performed as above. For the p53 wild-type allele PCR, primers were 5' – ACA GCG TGG TGG TAC CTT AT – 3' and 5' – TAT ACT CAG AGC CGG CCT – 3'. PCR condition was 94^{o}C 3min, 35 cycles of 94^{o}C 1min, 60^{o}C 2min and 72^{o}C 2min, and then 72^{o}C 5min.

CHAPTER THREE

ROLES OF K-Ras IN THE ETIOLOGY OF GLIOBLASTOMA:

PART 2 (CELL OF ORIGIN)

In chapter two, we presented a mouse model in which activation of K-Ras^{G12D} is under the control of its endogenous promoter in astrocytic lineage cells, including astrocytes, neurons and neural precursors. Although mixed populations of cells were involved in glioblastoma genesis, this model offers a system to understand the cell-of-origin of GBM, since specific cells susceptible to tumorigenesis can be identified in the pre-tumor stage. When the brain was examined at sub terminal stages, we observed an abnormal cell population consisting of neural precursors accumulating around the anterior sub-Ventricular Zone (SVZa) stem cell niche that belongs to type C precursors, which was absent in the control. Ras-ERK pathway activation was detected in the region of SVZa. In addition, both astrocytes and neurons were less susceptible to tumorigenesis than precursors, based on the fact that the expanded astrocytes were well organized and quiescent and the neurons were not much different from those in control. Thus, our results suggest that SVZ precursors, possibly type C cells, could be the original targets for primary GBM formation.

Introduction

The cell-of-origin in GBM has been an intriguing topic in the field of GBM study (Sanai et al., 2005;Holland, 2001;Gutmann et al., 2006). Since secondary GBM can be developed from grade II/III astrocytoma, it is suggested that mature astrocytes are the original targeted cells (Kleihues and Cavenee, 2000). On the other hand, since the majority of GBM cells are nestin immuno-reactive, which is characteristic of neural precursors, and they are heterogeneous, it has also been suggested that GBM can originate from neural precursors (Kleihues and Cavenee, 2000;Maher et al., 2001). The latter theory is possibly more applicable to primary GBM, as no early stage astrocytoma is observed.

Current mouse models usually use either hGFAP (human GFAP) or nestin promoters to restrict the range of cells for targeted genetic mutations (Weissenberger et al., 1997;Holland et al., 2000;Ding et al., 2001;Xiao et al., 2002). At the same time, these promoters were used to provide clues as to whether GBM develops from astrocytes (GFAP promoter), or precursors (nestin promoter). However, recent progress in neurology suggests that the expression spectrum of these promoters is more complicated than was previously understood.

Although GFAP is a marker for mature astrocytes, studies have shown that hGFAP promoter also directs gene expression in neural stem cells, either in the developmental stage (Campbell and Gotz, 2002;Malatesta et al., 2000;Malatesta et al., 2003;Zhuo et al., 2001) or in the adult (Doetsch et al., 1997;Doetsch et al., 1999). In the embryonic stage, GFAP is expressed in radial glial cells, which are a dominant glial population, and serve as precursor cells that differentiate into both neurons and astrocytes (Campbell and Gotz, 2002). In the adult stage, GFAP is also expressed in neural stem cells, which accounts for a very small portion of brain (Doetsch et al., 1997).

Nestin is a neural precursor marker, nevertheless it is not astrocyte specific. In adult brain, there is a stem cell niche residing in the sub-ventricular zone, which continually generates neuronal cells destinated to the olfactory bulb through a route called the Rostral Migratory Stream (RMS) (Doetsch et al., 1997). This stem cell niche is composed of three types of precursors that express nestin. They are SVZ astrocytes (also named type B stem cells), type C transit amplifying immature precursors and type A neuroblasts (McKay, 1997;Alvarez-Buylla and Garcia-Verdugo, 2002). Usually, type B stem cells differentiate into type C transit amplifying immature precursors and then further differentiate into type A neuroblasts (Fig. 13). Among them, the neuroblast is a precursor of neurons. Therefore, a nestin promoter will direct mutated gene expression in multiple types of precursors, including astrocytic and neuronal precursors, and can't be used to determine which precursor is the origin of GBM.

To better understand how neural precursors or mature astrocytes are subjected to GBM genesis, a new system is needed. Unexpectedly, the mouse model generated here provides some clues about which cell type(s) are prone to tumorigenesis when physiological levels of K-Ras^{G12D} are introduced.

Results

Brain abnormalities caused by endogenous level of K-Ras^{G12D}

To examine the global effect caused by K-Ras^{G12D}, 9 mice dissected before the terminal stage were analyzed and evaluated the morphological changes in the brain by H&E sections (Fig. 11). The terminal stage was defined as about 7 months in age, because all mice died from seizures or brain tumors by that age. Primary abnormalities in the brain include a

thicker corpus callosum, an expanded cell population in SVZa/ RMS/SVZ region and a smaller hippocampus. The penetrance of abnormality is 100%, which is also summarized in Table 1 in Chapter 2. As addressed in Chapter 2, K-Ras^{G12D} can potentially be activated in mature astrocytes and neurons. Thus, we examined whether both astrocytic and neuronal populations were affected by overactivated K-Ras pathway. For this purpose, we used GFAP IHC staining to label astrocytes and used NeuN IHC staining to label neurons. Astrocytic populations were expanded dramatically in the corpus callosum and RMS/SVZa (Fig. 12), but not in the hippocampus (Fig. 12B; staining data not shown). In contrast, the neuronal population was not changed in the whole brain (Fig. 12C). This result suggests that astrocytes were affected by K-Ras^{G12D} actvation but not neurons.

Since no neoplastic lesion was observed and the abnormal regions were well organized with a structure similar to the control, it is possible that the observed changes were caused by abnormal brain development. To test this, PCNA IHC staining was performed to mark proliferating cells, to see if there are actively proliferating cells in those expanded cell populations in the adult. No proliferation was observed in either the corpus callosum or hippocampus, indicating that the expanded astrocyte population was quiescent in these areas confirming that the abnormal populations were expanded in the developmental stage. For the SVZ cells, which are active in normal mice, the number of proliferating cells was increased in the mutant brain (Fig. 11E). Again, since the structure of that region was well organized and similar to normal brain, this increase is possibly due to the expansion of the whole population rather than the transformation of the cells. Interestingly, proliferating cells were restricted to the stem cell niche since positive cells were rarely observed outside the niche (data not shown).

Figure 10. Neural stem cell niche in the SVZ area.

Box on the left shows the structure of the whole brain, in which the sub ventricular zone (SVZ) and stem cell niche are highlighted by a yellow dashed-line circle. The SVZ is a region contiguous to the lateral ventricle (LV) and the dark line in the SVZ is the stem cell niche in the anterior SVZ (rostral SVZ, SVZa). Cell components inside the stem cell niche are illustrated on the right. Three types of precursor cells reside in the SVZ: type B stem cells/SVZ astrocytes (blue), type C transit amplifying immature precursors (green), and type A neuroblasts (red). Type B stem cells differentiate into type C transit amplifying precursors, which further differentiate into type A neuroblasts (Doetsch et al., 1999). Type A neuroblasts then form a chain that is wrapped by astrocytes and travel all the way to the olfactory bulb, where these cells differentiate into mature neurons.

O-olfactory bulb, H-hippocampus, CB-cerebellum, SVZ-sub-ventricle zone, LV-lateral ventricle

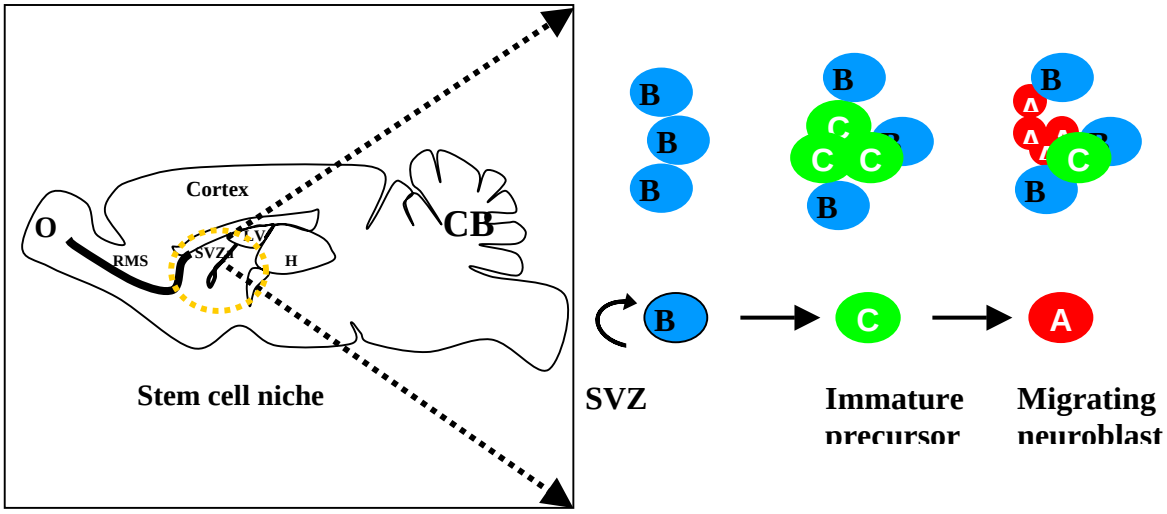

(Adapted from Doetsch F, et al, 1999)

Abnormal precursors around the neural precursor niche

Since the neural stem cell niche was the only active proliferating population among the three abnormal regions and tumors developed in a contiguous area, this region was further examined. Analysis of mice at 2 weeks, 1.5 months and 7 months of age showed that the stem cell niche shrinks as mice age. However, the degree of shrinkage is much smaller in the mutant brain (Fig. 13). To further analyze this area, nestin IHC staining was performed to study precursor populations in this area. Strikingly, an abnormal precursor population was identified outside the stem cell niche in the K-Ras$^{+/G12D}$;GFAP-Cre$^{+/-}$ mice (A and C), while in the normal brain, nestin positive cells are restricted to the neural precursor niche (B and D).

SVZ precursors include three different types: type B stem cell which are also SVZ astrocytes, type C transit-amplifying neuronal precursors and type A neuroblast cells. Here, a marker study is used to determine which type of precursor the abnormal cells outside stem cell niche are. Three precursors can be distinguished by specific cell markers: type B cells are both nestin- and GFAP-positive; and type C cells are nestin-positive only; type A cells are both nestin- and Tuj1-positive (Garcia-Verdugo et al., 1998). Double staining of nestin/GFAP and nestin/Tuj1 were performed on brain sections containing the RMS/SVZ layer. The abnormal precursors were nestin positive with no overlap with GFAP or Tuj1 staining, indicating that these abnormal precursors are type C cells (Fig. 14E-H). Interestingly, multiple pre-tumor nodules that contain similar abnormal precursors were observed in the nearby stem cell niche (Fig. 15), suggesting a correlation of abnormal precursors with tumorigenesis.

Ras downstream signals of p-ERK are activated in the stem cell niche

According to the previous study, EGF-EGFR signal is related to the maintenance of the stem cell compartment (Doetsch et al., 2002). As proposed in Fig. 16G, in a normal situation, type B stem cells don't express EGFR, but they will express it once activated; type C cells always express EGFR owing to active proliferation (Doetsch et al., 2002). p-ERK, a well-established downstream signal of Ras, was used here to teat if the Ras pathway was activated in these precursors. The level of IHC staining is stronger in mutant brains than in controls based on the number of positive staining cells and the strength of the positive stain, consistent with the possibility that K-Ras pathway is over activated in the mutant. p-ERK positive staining was not found in neuroblasts according to the double staining of p-ERK and Tuj1 (marker for neuroblast) (Fig. 16). Thus, this system has shown the activation of Ras-ERK pathway in type C and/or type B cells. This is similar to the pattern of EGF-EGFR expression in cells of the SVZ, where EGF-EGFR is expressed in type C transit amplifying cells, activated type B stem cells, but not in type A neuroblasts (Doetsch et al., 2002). Furthermore, abnormal type C precursors distributed outside the stem cell niche, which is consistent with the proposal that (expansion or increase of the) EGF-EGFR signal will cause type C cells to reprogram and migrate out of the niche (Doetsch et al., 2002). Since abnormal type C cells were not observed in other regions of the brain, it is unlikely that they are vestiges of developmental precursors that are distributed everywhere in the brain.

Figure 11. Abnormal regions in the brain of K-Ras^{G12D} before terminal stage.

The abnormalities include an expanded population in the stem cell niche, a larger corpus callusom and a smaller hippocampus. Panels A and B are brain sections from K-Ras$^{+/G12D}$;GFAP-Cre$^{+/-}$ mice at about 7 months. Panels C and D are comparable brain sections from a control mouse (Ras$^{+/G12D}$ without Cre). The corpus callosom (CC) is highlighted by the black line. The cell population in the dark area, as pointed to by arrows, is precursors in the RMS, SVZ and SVZa. H indicates the area of the hippocampus.

Panel E is the summarized data of PCNA (define) IHC staining, which marks proliferating cells. The red bar indicates cell numbers from K-Ras$^{+/G12D}$;GFAP-Cre$^{+/-}$ and the black bar indicates cell numbers from normal brains .

Abbreviations: RMS-rostral migratory stream; SVZ-sub-ventricular zone; SVZa-rostral or anterior sub ventricular zone; CC-corpus callosom; H-hippocampus.

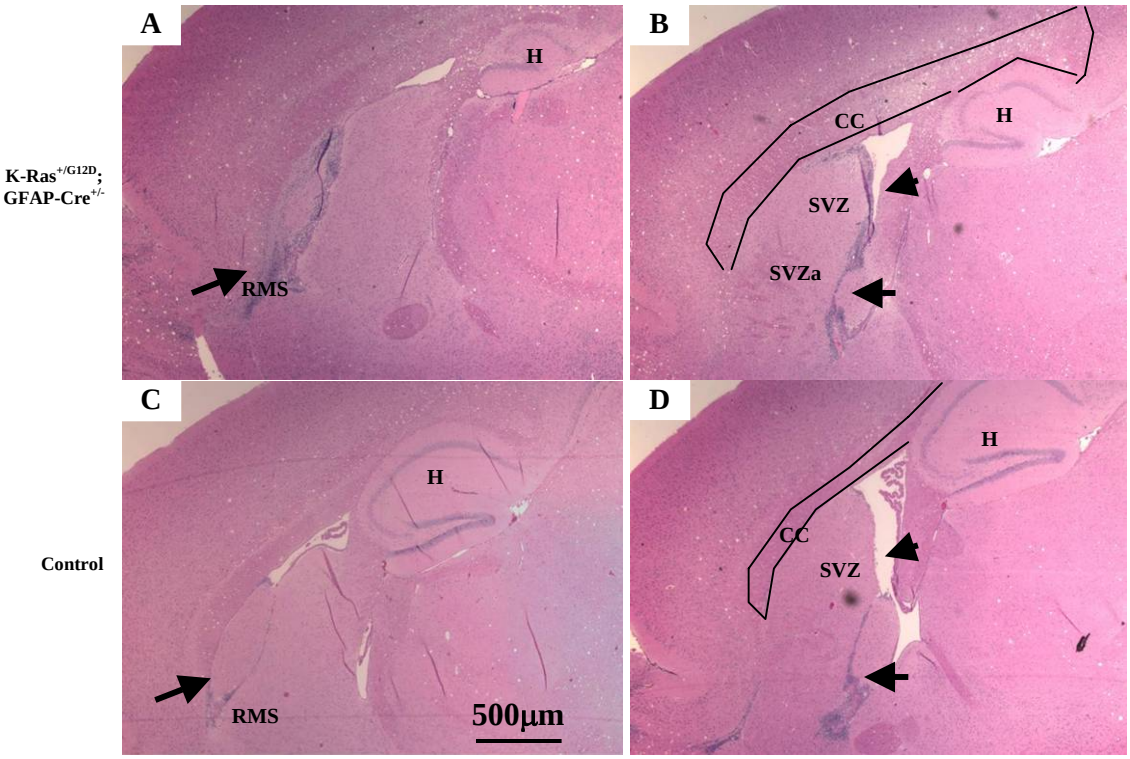
A
B
C
D
H
CC
SVZ
SVZa
RMS
500µm
K-Ras+/G12D; GFAP-Cre+/-
Control

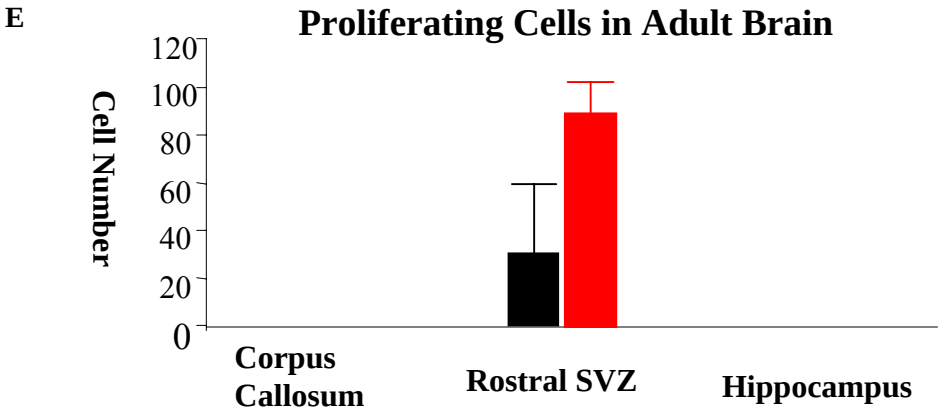
E
Proliferating Cells in Adult Brain
Cell Number
120
100
80
60
40
20
0
Corpus Callosum
Rostral SVZ
Hippocampus

Figure 12. The number of astrocytes but not of neurons is increased in abnormal regions.

Two major cell populations in the brain, neurons and astrocytes, were examined by marker staining (A). The genotype of the mutant is K-Ras$^{+/G12D}$;GFAP-Cre$^{+/-}$ and the control is K-Ras$^{+/G12D}$ or GFAP-Cre$^{+/-}$. Green staining is GFAP indicating astrocytes, and red staining is NeuN indicating neurons. The staining shows that the actrocytic cell population was expanded, while the neuronal population was similar to the control in the area of corpus callosum and RMS/SVZa. The structure and organization of the expanded population of astrocytes in the mutant brains were similar to control. The bar chart summarizes the quantification of astrocytes (B) and neurons (C), in which cortex neurons were counted as representative population for neurons.

Abbreviation: RMS-rostral migration stream; SVZa-rostral or anterior sub ventricular zone; CC-corpus callosom.

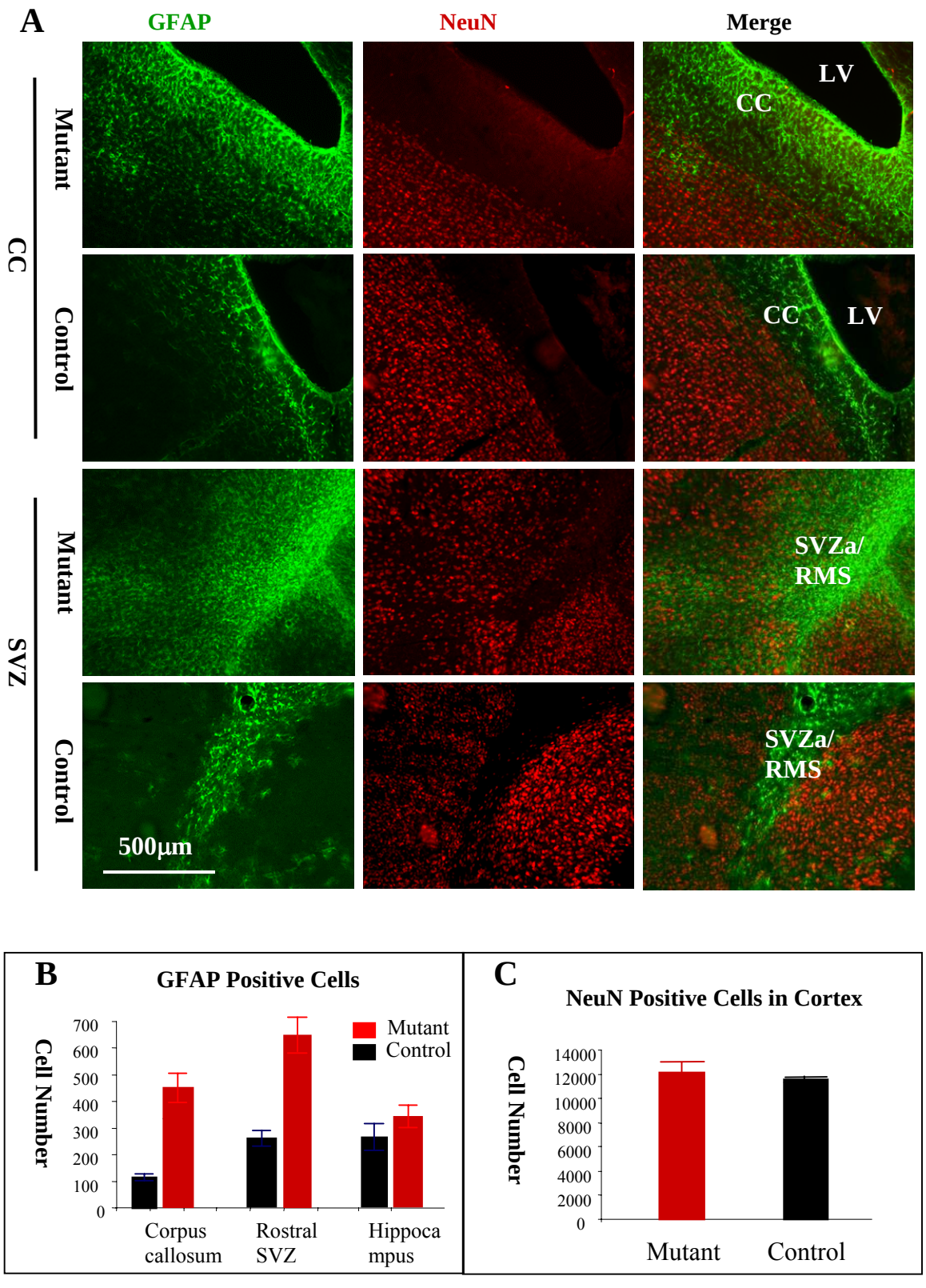
A
GFAP
NeuN
Merge
CC
SVZ
Mutant
Control
Mutant
Control
LV
CC
CC
LV
SVZa/
RMS
SVZa/
RMS
500µm
B
GFAP Positive Cells
Cell Number
700
600
500
400
300
200
100
0
Mutant
Control
Corpus
callosum
Rostral
SVZ
Hippoca
mpus
C
NeuN Positive Cells in Cortex
Cell Number
14000
12000
10000
8000
6000
4000
2000
0
Mutant
Control

Figure 13. Morphology changes in the SVZ area when K-Ras^{G12D} mice were aged.

H&E sections show the stem cell niche (dark cell population in the section as pointed by arrows) from two weeks (A and B), 1.5 months (C and D) and 7 months (E and F) brains. Niche stem cells (dark populations) were found to be no different between the mutated (A) and the control (B) brains at 2 weeks of age. However, this area shrank at the age of 1.5 months old in normal mice (D), and further shrank at the age of 7 months. However, in the mutant mice, the shrinkage was not as severe as in the control (B and D).

Abbreviation: SVZ-sub-ventricular zone

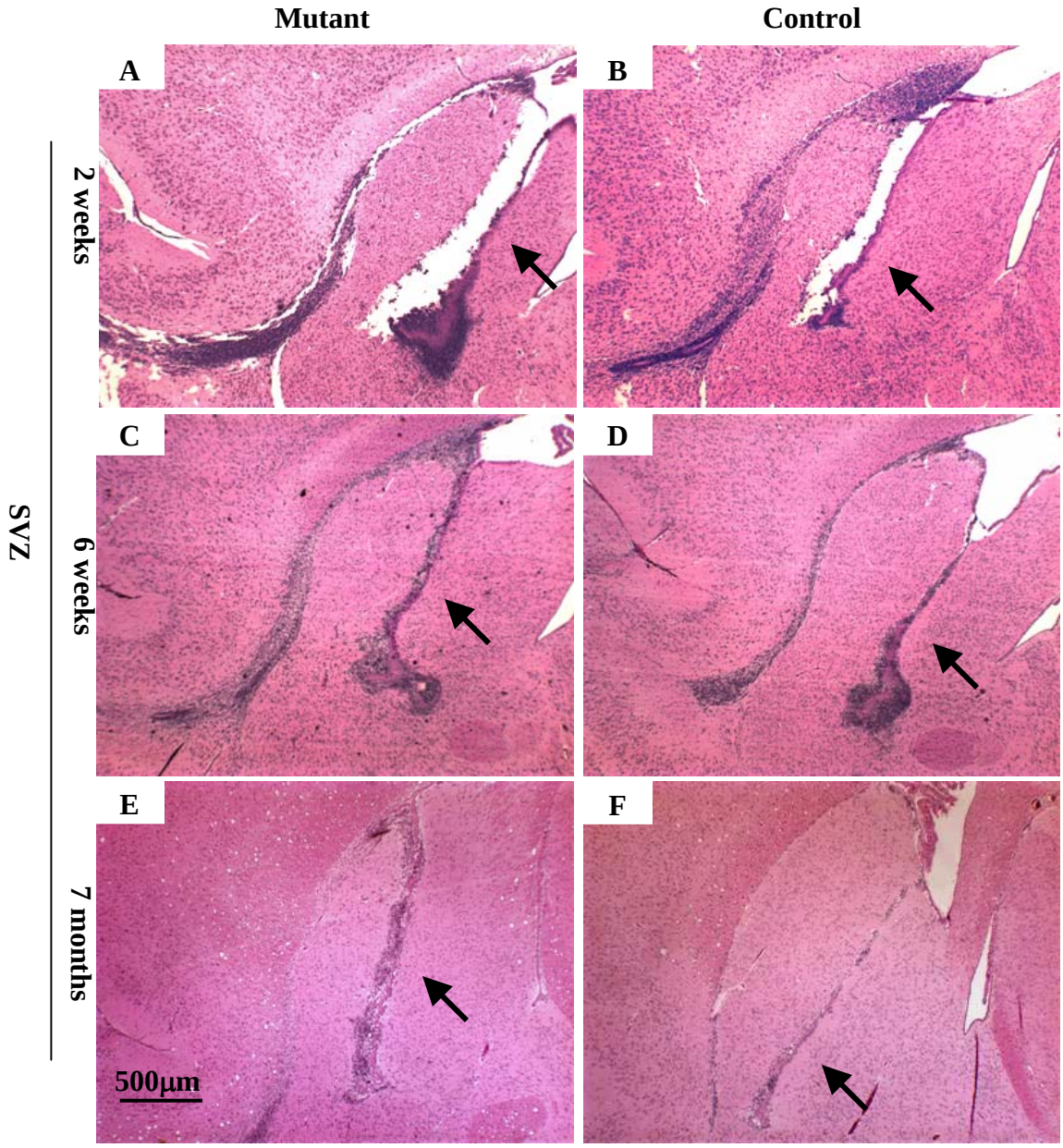
Mutant
Control
A
B
C
D
E
F
2 weeks
6 weeks
7 months
SVZ
500µm

Figure 14. Abnormal precursor population outside the stem cell niche.

The SVZ area was analyzed by nestin IHC staining for the precursor population. A-D is nestin IHC staining. An abnormal cell population was identified outside the stem cell niche (dark area) in the K-Ras$^{+/G12D}$;GFAP-Cre$^{+/-}$ mouse (A and C). In the control, precursors were restricted to the stem cell niche (B and D). Brown is positive staining for nestin and blue is the counter stain.

Panel E-H show double staining to examine the specific type of precursors, including double staining of Nestin/GFAP to show stem cells, and Nestin/Tuj1 to show neuroblasts. No overlap was identified for either Nestin/GFAP double staining (E) or Nestin/Tuj1 double staining (G), featuring type C precursors. Nestin staining is green; GFAP and Tuj1 are red. E and H are the normal controls.

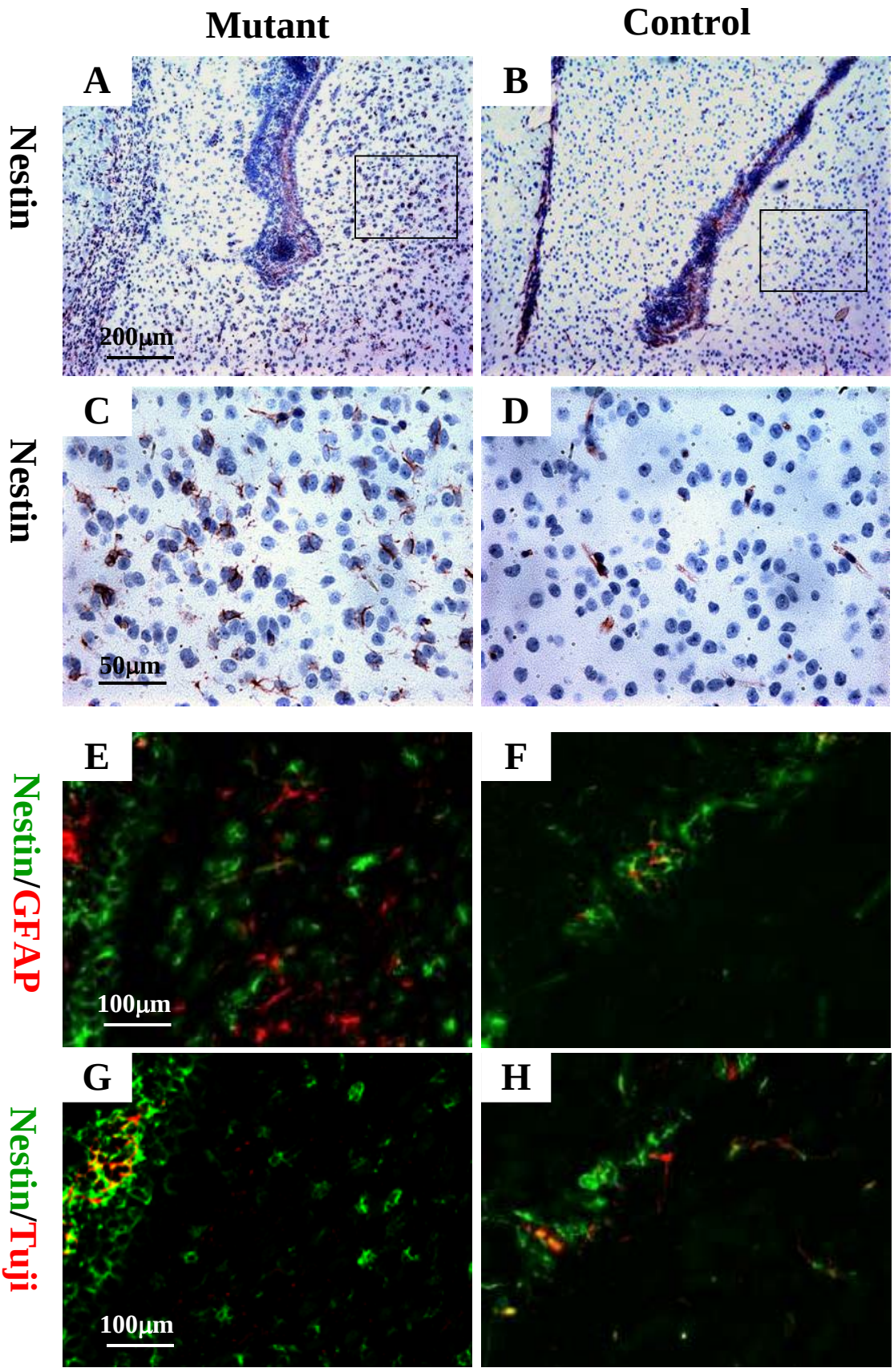
Mutant
Control
A
B
Nestin
200μm
C
D
Nestin
50μm
E
F
Nestin/GFAP
100μm
G
H
Nestin/Tuji
100μm

Figure 15. Pre-tumor nodules in the brain of K-Ras^{G12D} mice.

This figure shows a representative picture of a pre-tumor nodule from K-Ras$^{+/G12D}$; GFAP-Cre$^{+/-}$ mice. Nestin staining (A and B) and Nestin/GFAP double staining (C) indicate that the pre-tumor nodule cells are similar to the abnormal precursors outside the stem cell niche. A blue circle highlights the area of the nodule, and B is a magnification of the boxed area in A.

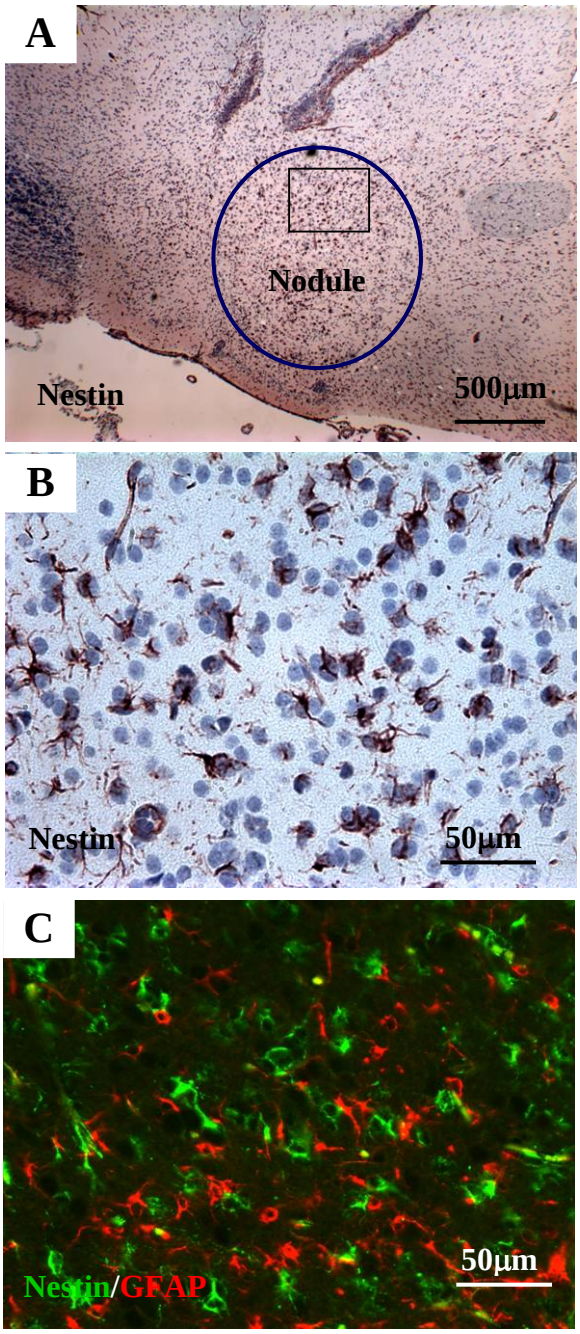
A
Nodule
Nestin
500μm
B
Nestin
50μm
C
Nestin/GFAP
50μm

Figure 16. p-ERK activation in precursors.

Positive IHC staining of p-ERK (pointed to by arrows) was observed in the stem cell niche precursors, both in K-Ras$^{+/G12D}$;GFAP-Cre$^{+/-}$ mice (B) and in control (A). The positive p-ERK stain is brown and the counter stain is blue. The p-ERK positive cells have a morphology resembling type C (or type B) precursors, unlike type A neuroblasts, which have an elongated and condensed nucleus as highlighted by 'A' in the figure. C is an H&E section from a similar area showing morphology of the cells. Double staining of p-ERK (green) and Tuj1 (red) showed no overlap of stains (F), confirming that the p-ERK positive cells are not neuroblasts. E is lower power view of p-ERK single staining and D is a control without primary antibody.

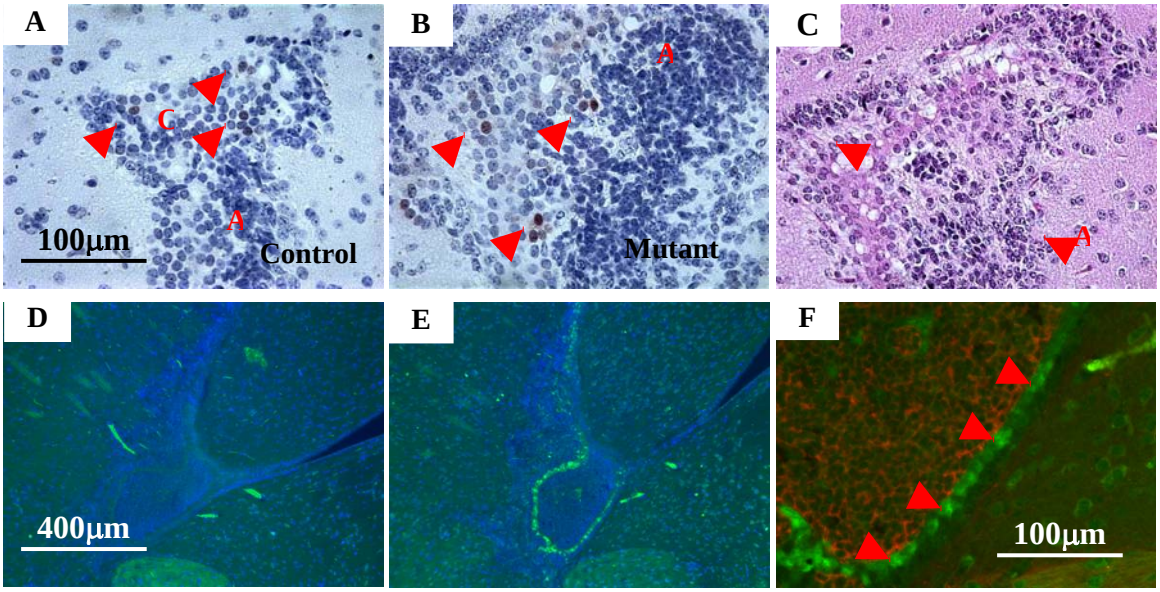
A
C
A
100μm
Control
B
A
Mutant
C
A
D
400μm
E
F
100μm

Discussions

The Cell of origin of primary glioblastoma

In this study, we show evidence for the first time that physiological levels of K-Ras^{G12D} initiate the tumorigenesis of primary glioblastoma without earlier detection of low-grade gliomas. Our model is different from other models of secondary GBM, in which mutations were usually introduced into astrocytes using the GFAP promoter (Ding et al., 2001;Xiao et al., 2002;). The mutation in our system was under the control of its endogenous promoter and expressed in a broader cell population in the brain. Thus, the original cells susceptible to transformation could be different from the models using GFAP or nestin prompters. Indeed, we have identified abnormal type C precursors outside the stem cell niche, which are transit amplifying type C cells and could be the cell of origin of GBM. Three abnormal populations were observed in the brain with mutant K-Ras^{G12D}, including hippocampus astrocytes, corpus callosum astrocytes and stem cell niche precursors. Among them, hippocampus astrocytes and corpus callosum astrocytes were unlikely to be subjected to transformation, since they are quiescent in the adult stage and no tumor or neoplastic lesions were observed in those regions. Except for abnormal type C precursors, the entire cell population in the stem cell niche was expanded and could potentially be transformed, thus arguing that type C precursors are the cell of origin of GBM. However, several observations support the hypothesis that abnormal type C cells but not precursors in the stem cell niche are targeted for tumorigenesis. First, although the precursor population in the niche was expanded, the cell morphology and niche structure were similar to those in the normal brain. Second, pre-tumor nodules were composed of abnormal type C cells and were in a location independent

of the stem cell niche. Third, portions of cells in the stem cell niche are neuroblasts, while no neuronal differentiation was found in the GBM tumors.

Type C precursors are EGF responsive cells in the precursor niche. A recent report from Doetsch et al. showed that prolonged exposure of type C cells to EGF interrupts their neuronal differentiation and endows them with the ability to migrate (Doetsch et al., 2002). Comparatively, stronger activation of K-Ras/ERK signal was present in type C cells or type B cells (Fig. 16). Thus, the possible scenario (Fig. 17) of the tumorigenesis occurring here could be that in the stem cell niche, overactivated K-Ras reprograms type C cells, which are then able to migrate out of niche. Once those cells travel out of the niche, they lose the EGF stimulation, which is restricted to the stem cell niche, and become quiescent. If there is a secondary stimulation, either from the microenvironment or from a second mutation inside the cells, the type C cells are then transformed. It is likely that once those abnormal neural precursors are transformed, they progress to GBM aggressively in a short time because of the high plasticity of precursors, which explains the evolution of primary glioblastoma without an early clinical history. In contrast, transformed mature astrocytes in low grade astrocytoma may need a longer period of time to gain not only proliferation but also de-differentiation or trans-differentiation abilities that lead to a phenotype of secondary GBM.

Primary GBM: its association with EGFR/K-Ras pathway and neural precursors

Receptor tyrosine kinase (RTK) pathways, including EGFR and PDGFR, are frequently mutated in human GBM (Kleihues and Cavenee, 2000). Interestingly, to a certain degree EGFR is specific to primary GBM while PDGFR is specific to secondary GBM, suggesting a distinctive etiology despite similar pathways being disrupted in the two GBMs. It is not clear how the PDGFR mutation contributes to secondary GBM formation, but this study indicates

that EGFR pathway activation in precursors could be a predetermining factor for primary GBM formation. In our model, overactivation of K-Ras pathway, possibly from the EGFR signal, resulted in the abnormal type C precursors appearing outside the stem cell niche. Thus, it seems that type C precursors are sensitive to changes in the EGFR/Ras signal and susceptible to reprogramming. In another sense, the type C precursors is a "weakest target", prone to transformation when the EGFR/Ras signal is maladjusted. Though no direct evidence is available as yet, type C cells seem to be related to primary GBM in this model. Type C cells are highly plastic, since they are actively proliferating and differentiating. It is possible that type C cells gain epigenetic modifications or signal activation facilitating their proliferation and differentiation (Cheng et al., 2005). Similar genetic or epigenetic changes could be needed for tumorigenesis. Thus, once type C cells are transformed, they could evolve into GBM so quickly that an early neoplastic lesion would be difficult to detect. For the tumor developed from but tumor formation could require additional mutations to transform a quiescent mature astrocyte into a tumorigenic cell and further evolve.

In recent years, the hypothesis that stem cells in the brain could be the cell of origin of glioblastoma has garnered huge amounts of attention (Sanai et al., 2005). The majority of glioblastomas in humans are primary GBMs (Kleihues and Cavenee, 2000;Ohgaki et al., 2004;). However, although it is realized that genetic mutations are different in primary and secondary GBMs (Kleihues and Cavenee, 2000;Ohgaki et al., 2004), determining the cell of origin of these cancers is still an unexplored field, and could be critical for treatment (Sanai et al., 2005). Unlike secondary GBM, which was generated numerous GEM mouse models, the mechanisms of primary GBM formation have been less reported, possibly due to a lack of mouse models. Our data show for the first time that type C precursors are related to primary

GBM formation. Although no direct evidence proves the evolution from type C cell to primary GBM, if this hypothesis is true, it will have a profound impact on elucidating the etiology of primary GBM.

Figure 17. Model of tumorigenesis.

One of the possible mechanisms for how tumors are evolved in this model is that normally, the precursors are restricted to the stem cell niche. The K-Ras pathway is activated in the precursor population, possibly via EGF-EGFR signal. However, when the K-Ras pathway is constitutively activated, type C cells are reprogrammed and migrate out of the stem cell compartment. Subsequently, secondary mutations occur in these abnormal populations, resulting in the transformation of cells, which further evolve into primary GBM in a relatively short period of time.

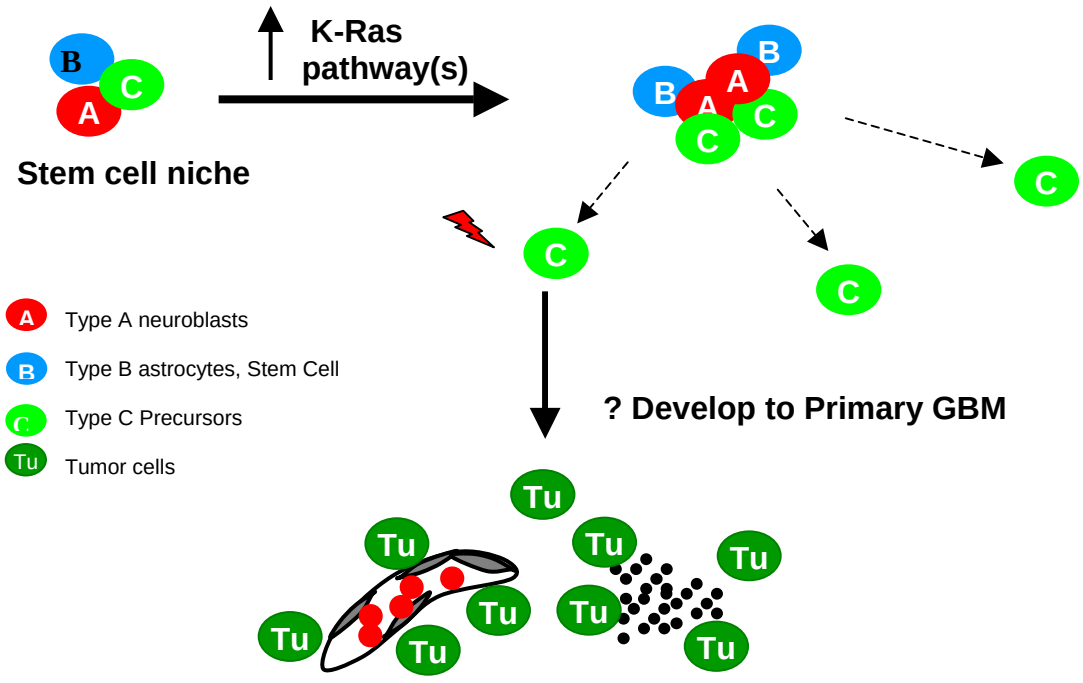
K-Ras
pathway(s)
Stem cell niche
? Develop to Primary GBM
Type A neuroblasts
Type B astrocytes, Stem Cell
Type C Precursors
Tumor cells

Materials and methods

Histology of brain and step sections. Dissection of mouse and brain processing was same as described in chapter two. To check the abnormality of whole brain, paraffin embedded brain was step sectioned, so that different layers of brain can be analyzed. One section from each step was stain with hematoxylin and eosin for histology.

Single staining procedure. Detail is as described in chapter two. Primary antibodies used were: GFAP(Z0334, DAKO rabbit at 1:100); NeuN (Chemicon mouse at 1:500);GFAP (556330 BD, mouse at 1:1000); Tuj1 (anti-β-tubulin type III Covance, mouse at 1:500). Cre (69050-3 Novagen, rabbit at 1:6000); phosphor-Erk1,2$^{Thr202/Tyr204}$ (9101, cell signaling, rabbit at 1:50); PCNA(SC-7907, Santa Cruz, rabbit at 1:100).

Immunofluorescence double staining procedure. After de-paraffin, sections were pretreated with citrate buffer as above. After washing twice with PBS, slides were blocked in 5% goat serum/ PBS-T for 30min in room temperature. Added first primary rabbit antibody diluted in 5% goat serum/ PBS-T and incubated in 4°C over night. In second day, washed slides in PBS-T 3 times and 5 min each. Blocked slides again in 5% goat serum/ PBS-T for 30min in room temperature. Added second primary mouse antibody diluted in 5% goat serum/ PBS-T and incubated in 4°C over night. In third day, wash slides in PBS-T 3 times and 5 min each. Added ALEXA FLUOR 488 goat anti rabbit and ALEXA FLUOR 543 goat anti mouse secondary antibody (Molecular Probes) in 5% goat serum/ PBS-T to slides and incubated slides at 4°C for 45min. Wash 3X PBS/Tween 20, 5~10min each time, and washed with water at last. Counter stained and mounted slides with vector's VectaShield Hardset with DAPI. Primary antibodies used were: GFAP(Z0334, DAKO rabbit at 1:100); NeuN

(Chemicon mouse at 1:500);GFAP (556330 BD, mouse at 1:1000); Tuj1 (anti-β-tubulin type III Covance, mouse at 1:500).

CHAPTER FOUR

INDUCIBLE MODELS OF SPONTANEOUS HIGH-GRADE ASTROCYTOMAS PROVIDE MECHANISTIC INSIGHT AND AVENUES FOR PRELINICAL DEVELOPMENT

There is currently no effective therapy for high-grade astrocytomas. Studies in accurate and accessible preclinical animal models are required to both understand these diseases and to facilitate development of diagnostic tests and therapies. We have developed an inducible model of glioblastoma (GBM) in genetically engineered mice (GEM) that was constructed based on common specific pathways deregulated with high frequency in the human malignancies: disruption of the pRb pathway, K-Ras activation and Pten inactivation. GEM were engineered such that these events are inducible (alone or in combination) specifically in adult astrocytes. Induction is elicited by activation of CreERtam, expressed from the human GFAP promoter, after intraperitoneal 4OH-tamoxifen (4-OHT) injection. With high penetrance and reproducible timing, the combination of all three events induces tumors that possess all common histological features of human GBM, including high mitotic indexes, angiogenesis, pseudo palisading tumor cells and necrosis. Furthermore, analysis of event combinations provides insight into disease etiology. For example, without Pten inactivation, pRb inactivation and K-Ras activation predispose to high-grade astrocytic tumors that lack the necrotic phenotype characteristic of GBM. Neither activation of K-Ras nor inactivation

of Pten alone produces detectable pathology, and thus are involved in tumor progression. In contrast, inactivation of pRb function initiates disease that does not progress to high-grade tumors. Because of their inducibility, high-penetrance and molecular and histological similarity to human high-grade astrocytomas, these models are ideal for both further mechanistic analyses and for preclinical studies, including the validation of potential drug targets and diagnostic and therapeutic development.

Introduction

High-grade astrocytomas are the most common human malignant primary brain tumor, and there is currently no effective treatment for these devastating diseases (CBTRUS, 2006). While the standard of care generally involves surgery, radiation and chemotherapy, these treatments are largely palliative as these cancers are among the most lethal and resistant. Post-treatment survival of patients with glioblastoma multiforme (GBM), the most malignant astrocytoma (WHO grade IV), is an average of 9-12 months; with anaplastic astrocytoma (AA; WHO grade III), 2-3 years (Kleihues and Cavenee, 2000; Maher et al., 2001).

GBMs have characteristics of highly proliferative and invasive tumor cells of variable marker specificities, extensive angiogenesis and pseudo palisading necrosis. AAs and GBMs frequently harbor aberrations in cell-cycle regulatory factors, pRb (20-30%), INK4a/ARF (33-68%) or CDK4 (10-15%), amplification or overexpression of the epidermal growth factor receptor (EGFR) (~40% or ~60%), or overexpression of platelet derived growth factor receptor (PDGFR) (60%), and chromosome 10 loss (69%) including Pten tumor suppressor gene locus, and mutation of Pten gene (24%) (Henson et al., 1994;Ueki et al., 1996; Kleihues and Cavenee, 2000; Ohgaki et al., 2004). Although not generally mutated, K-Ras is activated in many tumors at about 40-50% (Friday and Adjei, 2005), likely a result of EGFR/PDGFR activation. GBMs present *de novo* or arise subsequent to lower grade tumors (Kleihues and Cavenee, 2000). While differences in the frequency and spectrum of genetic aberrations between the two groups have been noted, in neither case is the etiology understood. Furthermore, the complexity of the brain and the critical roles of the tumor microenvironment in disease etiology preclude an understanding based solely on studies of human tumor samples. Accurate and accessible preclinical astrocytoma models are essential

for both understanding the underlying mechanisms of disease etiology and for preclinical therapeutic and diagnostic assessment and discovery. For effectiveness in preclinical studies, such models should reflect the molecular and biological characteristics of the human diseases, develop disease predictably with high penetrance, and require minimal expertise for disease induction.

Recent studies have utilized genetically engineered mice (GEM) to model and study astrocytoma with significant success. The results have contributed to our knowledge of basic mechanisms and provide the foundation for further model development. While the existing models have been fruitful, there are still significant impediments to their broad use in preclinical discovery. Here, we report the development and characterization of inducible GEM models that exhibited a multi-step progression of high-grade astrocytoma when harboring most common mutations of human GBM.

Results

Astrocytoma initiation by T_{121}

In a previous study, we reported a mouse model of grade III astrocytoma by disruption of Rb pathway in astrocytes through using a T_{121} that was driven by human glial fibrillary acidic protein (GFAP) transcriptional regulatory fragment (Xiao et al, 2002). T_{121} is a truncated SV40 T antigen and inhibits pRb as well as its family members p107 and p130 (Kleihues and Cavenee, 2000), thus fully disabling pRb's function due to redundancy/compensation of p107/p130 to pRb (Listernick et al., 1999). However, since GFAP promoter expresses as early as E11.5 and thereafter, its application in astrocytoma modeling always resulted in developmental defects such as hydrocephalus and expansion of

sub ventricular zone (Xiao et al, 2002;Ding et al., 2001;Weissenberger et al., 1997). To circumvent early induction of T_{121}, a GFAP-CreER^{TM} mouse was used, in which the function of Cre can be activated by IP injection of 4-OHT at an arbitrary time point (Fig. 18) (McCarthy K, unpublished).

To introduce three oncogenic events, including interruptions of Rb, Ras and Pten pathways, a Cre conditional T_{121} transgenic line, a conditional K-Ras^{G12D} knock-in line (Jackson et al, 2001) and a conditional Pten knockout line were used (Suzuki et al, 2001) (Fig. 18). For each case, the conditional allele is activated when Cre recombinase is introduced. For T_{121}, GFAP promoter controls its expression directly. For K-Ras^{G12D} and Pten loss, their activities were directed by endogenous promoters but restricted to astrocytic cells because the Cre used here was under the control of GFAP promoter (Fig. 18)

In this study, 4-OHT was injected into 3 months old mice, when three events were restricted to mature astrocytes (Fig. 18, lower panel) (McCarthy K, unpublished) and possibly in neural stem cells (Doetsch et al., 1997;Doetsch et al., 1999). To confirm that the loxP sites were recombined by Cre enzyme, DNAs were extracted from multiple brain paraffin sections for PCR detection (Fig. 19). The mutant K-Ras^{G12D} allele generated a larger band product after the stop element was removed and a smaller band product for K-Ras wild type allele. The wild type band is stronger than the mutant band, because both astrocytes and neurons were harbored for PCR and stop element was removed only in astrocytes but not in neurons.

To test if oncogenic events were activated after 4-OHT treatments, T_{121} expression and p-ERK levels were analyzed by IHC staining in the brains of mice 2 weeks post injection (Fig. 20). In this stage, there was no difference in the level of cellularity (Fig. 24) and T_{121}

expression between $T_{121}^{+/-}$ and $T_{121}^{+/-}$;K-Ras^{G12D} brain, indicating the Ras pathway didn't contribute to tumorigenesis in the very early stage. T_{121} positive cells were always cluster together indicating they may proliferate from some targeted astrocytes due to the disruption of Rb pathway (CBTRUS, 2006);(Kleihues and Cavenee, 2000;Maher et al., 2001). p-ERK was detected in both $T_{121}^{+/-}$;K-Ras^{G12D} and $T_{121}^{+/-}$ brain (Fig. 20m). However, p-ERK was hardly detected in K-Ras^{G12D} brain (Fig. 20m), which is as same as in the control, suggesting that endogenous level of K-Ras^{G12D} alone is not oncogenic and the activation of K-Ras pathway is possibly depending on the T_{121} disruption of the Rb pathway (Peeper et al., 1997).

To confirm the expression of T_{121} is in adult astrocytes, T_{121} (red) was double stained with GFAP (green) (Fig. 20 d-g) in the brain sections 2 weeks post 4-OHT. Because GFAP is a cytoplasmic protein and T_{121} is localized to both the cytoplasm and the nucleus, they couldn't be decided to be in the same cells, though they had some yellow overlap in the cytoplasm. To further confirm this result double staining T_{121} with S100, a nuclear protein and glial cell marker was performed (Fig. 20 h-k).

In the mice with T_{121} mutation only (*TgG(ΔZ)* ^{Tam} T_{121}), the IP injection of 4-OHT recapitulated the grade III astrocytoma developed in the $TgG(\Delta Z)T_{121}$ model (Fig. 22a) (Xiao A, 2002). As predicted, expanded population in sub ventricular zone observed in $TgG(\Delta Z)T_{121}$ model, which may be caused by the expression of T_{121} in developmental stage, didn't not appear in this new system. $TgG(\Delta Z^{Tam})T_{121}$ mice lived up to more than one year post 4-OHT injection without the observation of tumor mass in brain (Fig. 21a, 22a, 24). In either mice with single mutation of K-Ras^{G12D} or Pten$^{-/-}$, no obvious brain lesion was observed (data not shown). Thus, among the three oncogenic events, only T_{121} can initiate astrocytoma genesis; on their own, over activated K-Ras pathway at physiological levels

(Fig. 21a) or Pten loss were not sufficient to initiate tumorigenesis (data not shown here) (Fraser et al., 2004).

Acceleration of astrocytoma genesis with K-Ras^{G12D} mutation

Interestingly, when mutations of T_{121} and K-Ras^{G12D} were co-presenting, brain tumor development was dramatically accelerated (Fig. 21b, Fig. 24), such that the solid tumor bulb could be visually identified (Fig. 23d). The locations of brain tumor are variable, including front brain, thalamus, brain stem, and optical nerve, which reflect the broader induction of oncogenic events in astrocytes.

To determine if over activated Ras pathway played a role in the astrocytoma progression, resulting in the progression of the grade III astrocytoma to GBM, tumor masses with combined mutations of T_{121} and K-Ras^{G12D} were characterized. Brain tumor cells in T_{121};K-Ras^{G12D} mice looked poorly differentiated and tumors were packed by cells without much cytoplasm (Fig. 22b). However, large portions of tumor cells were immuno-reactive to GFAP (Fig. 23a) indicating a glial origin. Staining of the neuronal differentiation marker synaptophysin is negative and staining for the neural precursor marker nestin is positive indicating the GBM characteristics of tumors (Fig. 23b, 23c). Furthermore, angiogenesis was a consistent phenotype in solid tumors as exemplified by the big vessels in the H&E sections (Fig. 22b), whole brain image (Fig. 23d) or 3D view of vessel network generated based on MRA data (Fig. 23e, 23f), indicating the GBM-like feature of the tumors. The fact that intensive angiogenesis occurred in the brain tumor with combined mutations of T_{121};K-Ras^{G12D} but not with single mutation of T_{121} suggests the important role of Ras pathway in the angiogenesis observed in GBM, which may be a critical factor for the solid tumor formation.

To test how the over activated K-Ras pathway cooperated with T_{121} mutation in astrocytoma progression, brains from mice 2weeks, 2 months and 4 months post 4-OHT treatment were analyzed. After 2 weeks, there were small clusters of tumor cells distributed around the brain in either T_{121} or T_{121};K-Ras^{G12D} brains (Fig. 24). It is interesting that there was no difference in the cellularity (Fig. 24), T_{121} level (Fig. 20b, 20c), or apoptosis/proliferation level (data not shown) between T_{121} and T_{121};K-Ras^{G12D} at this stage. This suggests that physiological level of K-Ras^{G12D} didn't contribute to the tumorigenesis initiated by T_{121} in the very early stage, though there was some activated signal of K-Ras pathway as indicated by p-ERK IHC (Fig. 20l, 20m). However, after 2 months, there was increased cellularity in both T_{121} and T_{121};K-Ras^{G12D} brains. At this stage, surprisingly, there already were peri-nuclear and peri-vascular satellites (red and blue arrows in Fig. 24), especially in the brain with the combined mutations of T_{121} and K-Ras^{G12D}, consistent with a grade III astrocytoma. Moreover, as compared to the 2 week's time course, increased cellularity was much more severe in the brain with combined mutations of T_{121} and K-Ras^{G12D} than T_{121} single mutation at 2 months time course. This indicates that K-Ras pathway have been adequately activated (supported by p-ERK and p-Akt staining and data not shown here) and accelerates tumorigenesis at this stage. After 4 months post 4-OHT treatment, the tumorigenesis was further accelerated in the T_{121};K-Ras^{G12D} brain. Cell clusters with very high cell density distributed as patchy pattern in the brain and there was solid tumor formation in some locations, possibly developed from those clusters. In contrast, tumor cells were equally distributed in T_{121} single mutation brain without big cluster of tumor cells.

In the previous studies, disruption of Rb pathway by T_{121} always resulted in increased levels of proliferation and apoptosis in several mouse models including astrocytoma (Xiao et

al., 2002;Simin et al., 2004;Hill et al., 2005a). To test if overactivated K-Ras pathway has impact on those two events related to T_{121}, the levels of apoptosis and proliferation in the brains were examined. We compared proliferating cells and apoptotic cells with T_{121} expressing cells, instead of total cells in the field. There was no obvious change in the level of proliferation (Fig. 25) despite the fact that K-Ras can signal to a mitogenic pathway (Pruitt and Der, 2001). This suggests that, in term of proliferation, K-Ras^{G12D} is upstream of Rb pathway, which controls the G1 to S transition in cell cycle, such that overactivated K-Ras pathway couldn't further loosen the control of cell proliferation when T_{121} was expressed. Interestingly, there was some apoptosis in the T_{121};K-Ras^{G12D} brain, but the level is significantly decreased at about 42% compared with T_{121} brain ($p=0.028$). This indicates that K-Ras^{G12D} could signal to some anti-apoptotic pathway without completely blocking the apoptotic pathway of tumor cells. Thus, the partial inhibition of apoptosis by K-Ras^{G12D,} could be one of the reasons contributing to the higher cellularity in the T_{121};K-Ras^{G12D} brain. It is also possible that the transformed tumor cells in the T_{121};K-Ras^{G12D} brain obtain the ability to growth independently of T_{121} or both T_{121} and K-Ras^{G12D} that also could contribute to the progression of tumorigenesis.

Contribution of Pten$^{-/-}$ to further GBM evolution

Necrosis, a hallmark feature of GBM, was not present in tumors with combined mutations of T_{121} and K-Ras^{G12D}. Necrosis appears in most human GBM cases although it is not a criterion for the diagnosis of GBM (WHO). Interestingly, in this study, when Pten$^{+/-}$ or Pten$^{-/-}$ mutation was added to the mutations of T_{121} and K-Ras^{G12D}, not only angiogenesis but also necrosis, especially with pseudopallisading cells around the necrotic center, were exhibited in tumors (Fig. 22b). Few studies have addressed the relationship of gene mutations

with GBM morphologies and this is the first direct evidence showing that Pten loss is related to the necrotic center formation. However, whether the disruptions of Rb and overactivated K-Ras pathway were required for the function of Pten in necrosis is not known. VEGF levels are usually up-regulated in the progression of astrocytoma and are dramatically high in the necrotic regions in human GBM due to the angiogenic response caused by hypoxic stress (WHO). A similar feature was observed in this model as VEGF in-situ experiment indicated a high level of VEGF mRNA surrounding the necrotic center (Fig. 23g).

Histologically, the tumor cells were more glial-like in a more loose structure in the T_{121};K-Ras^{G12D} ;Pten$^{-/-}$ than in T_{121};K-Ras^{G12D} background; this was also found in some area in the T_{121};K-Ras^{G12D} ;Pten$^{+/-}$ background possibly due to some transition of genetic mutations occurred in this background. Same as the tumors developed in the T_{121};K-Ras^{G12D} background, marker studies in these groups of tumor also suggested that they belong to GBMs (Fig. 23a-c).

When Pten$^{+/-}$ was added to the combined mutations of T_{121} and K-Ras^{G12D}, majority mice developed solid brain tumors in the front brain with median survival time of 4.3 months, which is close to that of T_{121};K-Ras^{G12D} mice(Fig. 21c). However, when Pten alleles were lost, the median onset of tumors was accelerated from 4.73 months to 2.17 months (Fig. 24, 21c). Mice died from brain tumor or other causes (Fig. 21), when solid brain tumors were sorted out, there were significant accelerations of tumorigenesis in T_{121};K-Ras^{G12D} ;Pten$^{+/-}$ (T_{50}=4.01 months) and T_{121};K-Ras^{G12D} ;Pten$^{-/-}$ (T_{50}=1.13 months) backgrounds compared with T_{121};K-Ras^{G12D} ;Pten$^{+/+}$ background (T_{50}=4.83 months) ($p < 0.05$ in both cases, T test) (Fig. 21d).

Examination of the histology showed that a higher cellularity was observed in T121;K-Ras^{G12D} ;Pten$^{-/-}$ mice than in T_{121} and T_{121};K-Ras^{G12D} mice two weeks post 4-OHT injection/treatment (Fig. 24), suggesting Pten's involvement in the early stages of tumorigenesis. 2 months after 4-OHT injection, cellularity further increased in T_{121};K-Ras^{G12D} ;Pten$^{-/-}$ mice, where either a big tumor mass or pre-tumor nodule was observed, while similar lesions appeared about 4 months post 4-OHT treatment in T_{121};K-Ras^{G12D} mice. The analysis of proliferation and apoptosis showed that apoptosis level was further decreased in the T_{121};K-Ras^{G12D} ;Pten$^{-/-}$ mice compared with T_{121};K-Ras^{G12D} mice. These results indicate that the Pten pathway is not completely overlapped with K-Ras pathway and is important for the tumor progression.

Figure 18. Schematic illustration of the strategy to induce oncogenic events in adult astrocytes.

Multiple oncogenic events were inducible by using three conditional mouse strains (upper panel), including GFAP-floxed stop-T_{121} (*$TgGZT_{121}$*), floxed stop K-Ras^{G12D} knock-in (*$K\text{-}Ras^{+/lslG12D}$*) and floxed exon4/exon5 Pten knock out (*$Pten^{+/fl}$*). Triangles represent loxP sites and "stop" with arrows point to stop signals in the genes. In *$TgGZT_{121}$* conditional transgenic allele, T_{121} expression is under the control of GFAP promoter when stop signals were removed by the recombination of loxP sites by Cre. In *$K\text{-}Ras^{+/lslG12D}$* allele, $K\text{-}Ras^{G12D}$ mutant expression is under the control of K-Ras endogenous promoter when Cre removed floxed-stop. Cre mediated expression of Exons 4 and 5 resulted in loss of a stable Pten protein. To temporally induce the oncogenic events, GFAP-CreER was used, in which Cre activity was activated by IP injections of 4-OHT. A Cre recombinase would induce recombination, thus causing adult astrocytes to harbor three separate mutations: expression of T_{121}, constitutively activated K-Ras, and loss of one Pten allele (lower panel).

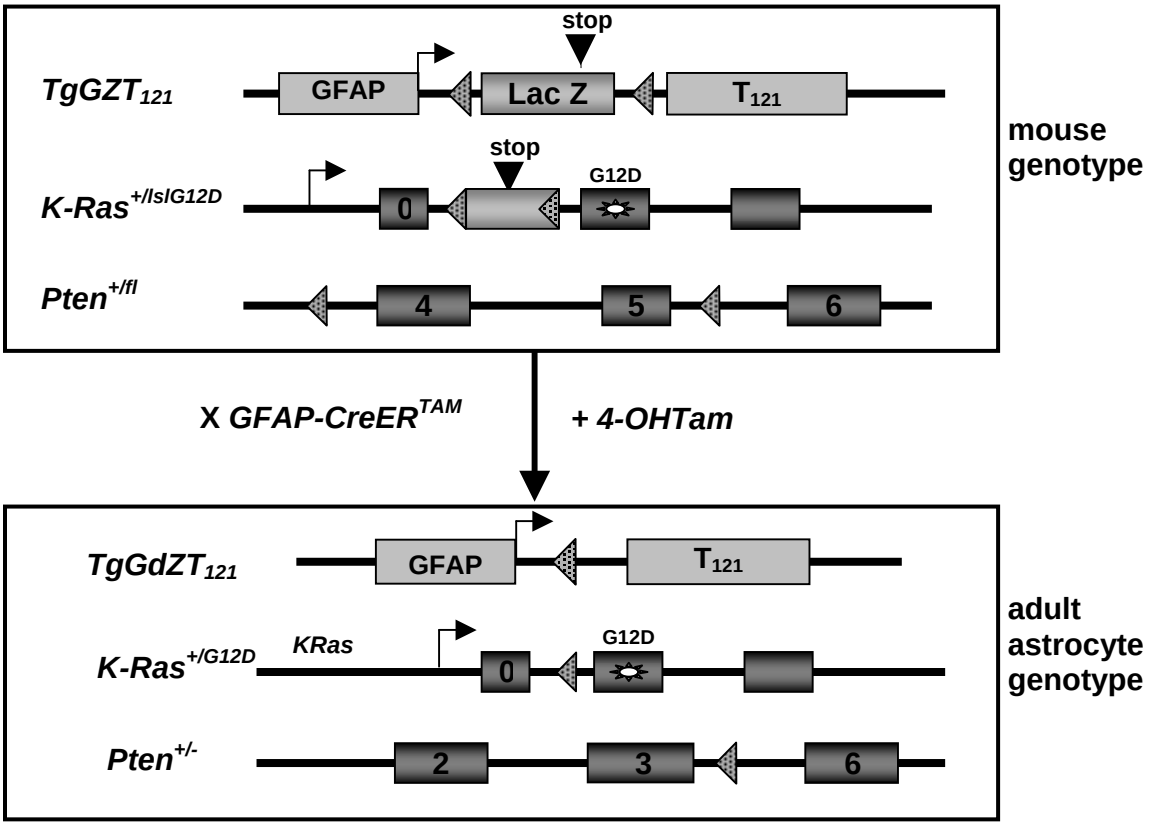
stop
TgGZT121
GFAP
Lac Z
T121
mouse genotype
stop
G12D
K-Ras+/lslG12D
0
Pten+/fl
4
5
6
X GFAP-CreERTAM
+ 4-OHTam
TgGdZT121
GFAP
T121
adult astrocyte genotype
KRas
G12D
K-Ras+/G12D
0
Pten+/-
2
3
6

Figure 19. Recombination of loxP sites after 4-OHT treatment.

DNA was extracted from paraffin sections from T_{121};K-Ras^{G12D} mouse brain two months after 4-OHT treatment. PCR analysis shows that stop elements in GZT_{121} transgenic and K-Ras^{G12D} knock-in alleles were deleted after 4-OHT injection/exposure. The positive control for T_{121} was from tail DNA of a $GdZT_{121}$ mouse that had a broader deletion of stop element. The positive control for K-Ras^{G12D} was from a tumor developed in K-Ras^{G12D};GFAP-Cre mouse. Negative controls were from a wild type mouse.

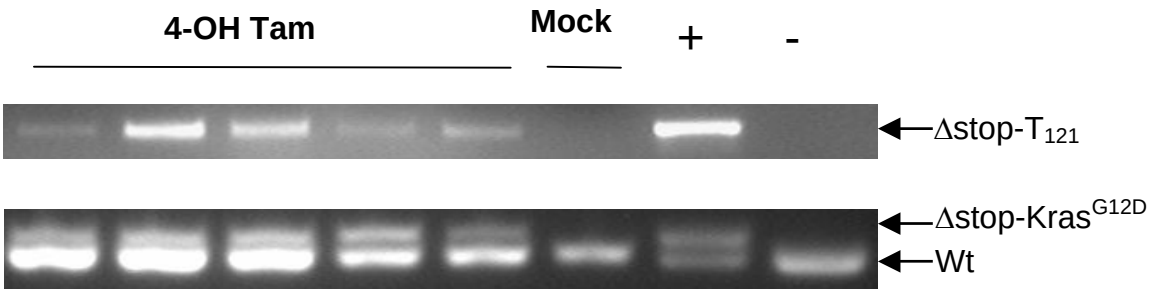
4-OH Tam
Mock
+
-
Δstop-T121
Δstop-KrasG12D
Wt

Figure 20. Induction of oncogenic events in adult astrocytes.

Paraffin brain sections from mouse culled two weeks post-4OHT injections were used for IHC analysis to confirm induction of T_{121} and K-Ras pathway in astrocytes. T_{121} staining shows indistinctive positive stain (brown with blue counter staining) level and pattern in T_{121};$Kras^{G12D}$ (b) and T_{121} (c) brains. In the brain without 4-OHT treatment, T_{121} is not expressed (a). T_{121} expression is specific to astrocytes as shown by double staining of GFAP /T_{121} (d-g) and GFAP/S100 (h-k). GFAP and S100 staining is in green and T_{121} staining is in red. DAPi staining for nuclei is blue. p-ERK, a downstream signal of K-Ras, was activated in cortex of T_{121};$Kras^{G12D}$ and T_{121} (l-m), With a similar level (m). However, there is no expression of p-ERK in the cortex in controls including K-Ras^{G12D} (m). The insets provide further detail; the cellular shapes and relationships to adjacent neurons are all consistent with the immunopositive cells being astrocytes.

Wt: wild type; R: K-Ras^{G12D}; T: T_{121}

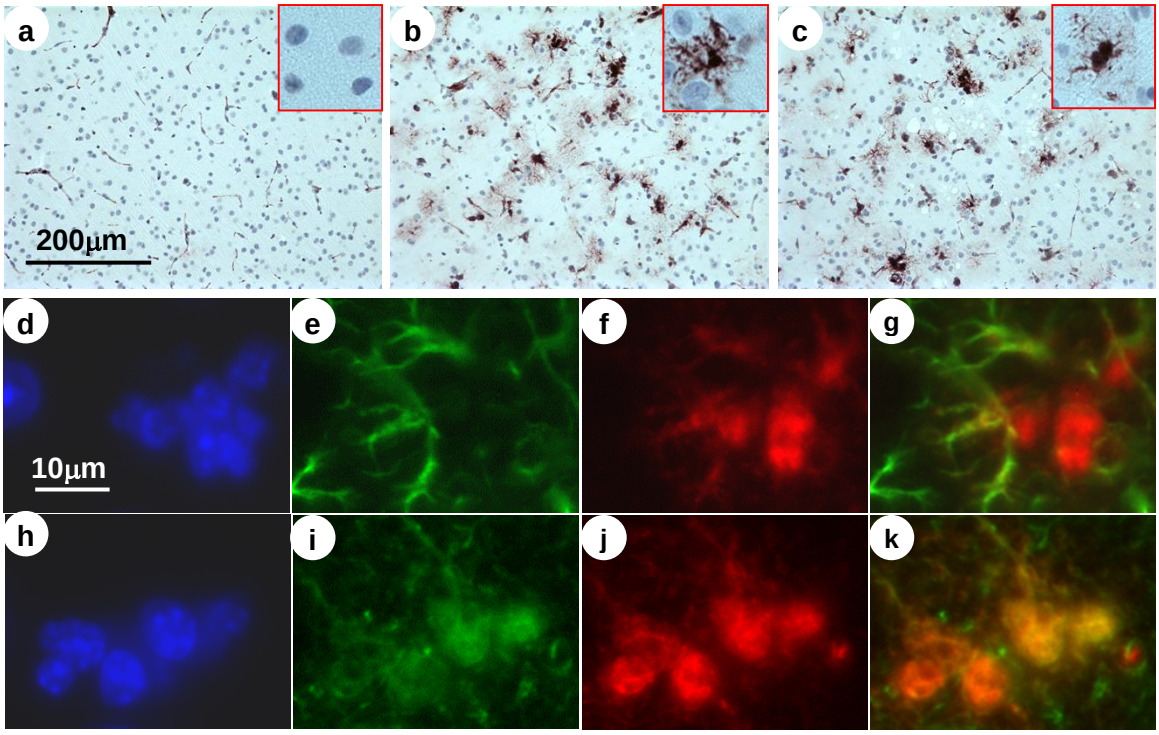
a
b
c
200µm
d
e
f
g
10µm
h
i
j
k

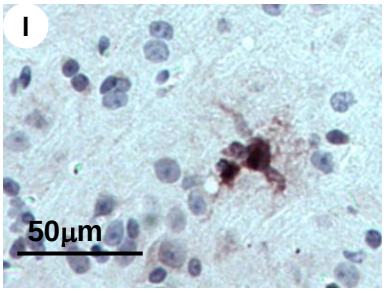
l
50µm

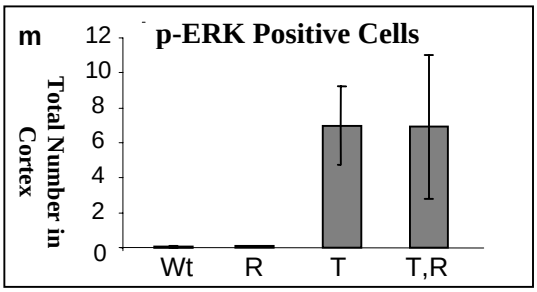
m
p-ERK Positive Cells
Total Number in Cortex
12
10
8
6
4
2
0
Wt
R
T
T,R

Figure 21. Incidence and onset time of tumors in different genetic background.

Death events in different cohort of mice were summarized by Kaplan-Meier survival curves. The times in the curves are months after 4-OHT injections. Individual mouse was indicated as dot in different color according to the tumor type. Tumors are including brain tumor mass (BM, red dot), skin tumor mass (SM, yellow dot), thymus lymphoma (TL, green dot). The dead causes of portion of mice are not determined (ND, dot in blue) or sac for old age (small point in flat line). In cohorts of the single mutation of T_{121} (mean live time is 16.57 months, n=7) or K-Ras^{G12D} (T_{50}=12.27 months, n=11), no solid brain tumor mass was observed though there were skin tumor and thymus lymphoma in portion of mice with K-Ras^{G12D} mutation (A). Survival of combined mutations of T_{121} and K-Ras^{G12D} (T_{50}=4.73 months, n=11) was shown in red line (B); genotypes with $T_{121}^{+/-}$; K-Ras$^{+/G12D}$; Pten$^{+/-}$ (T_{50}=4.3 months, n=13) and $T_{121}^{+/-}$; K-Ras$^{+/G12D}$; Pten$^{-/-}$ (T_{50}=2.17 months, n=10) were shown in purple and gold lines (C). When only brain tumors were sorted out, there was obvious acceleration of tumorigenesis in $T_{121}^{+/-}$; K-Ras$^{+/G12D}$; Pten$^{-/-}$ (T_{50}=1.13 months, n=2) compared with $T_{121}^{+/-}$; K-Ras$^{+/G12D}$; Pten$^{+/-}$ (T_{50}=4.01 months, n=6) and $T_{121}^{+/-}$ and K-Ras$^{+/G12D}$ (T_{50}=4.83 months, n=8).

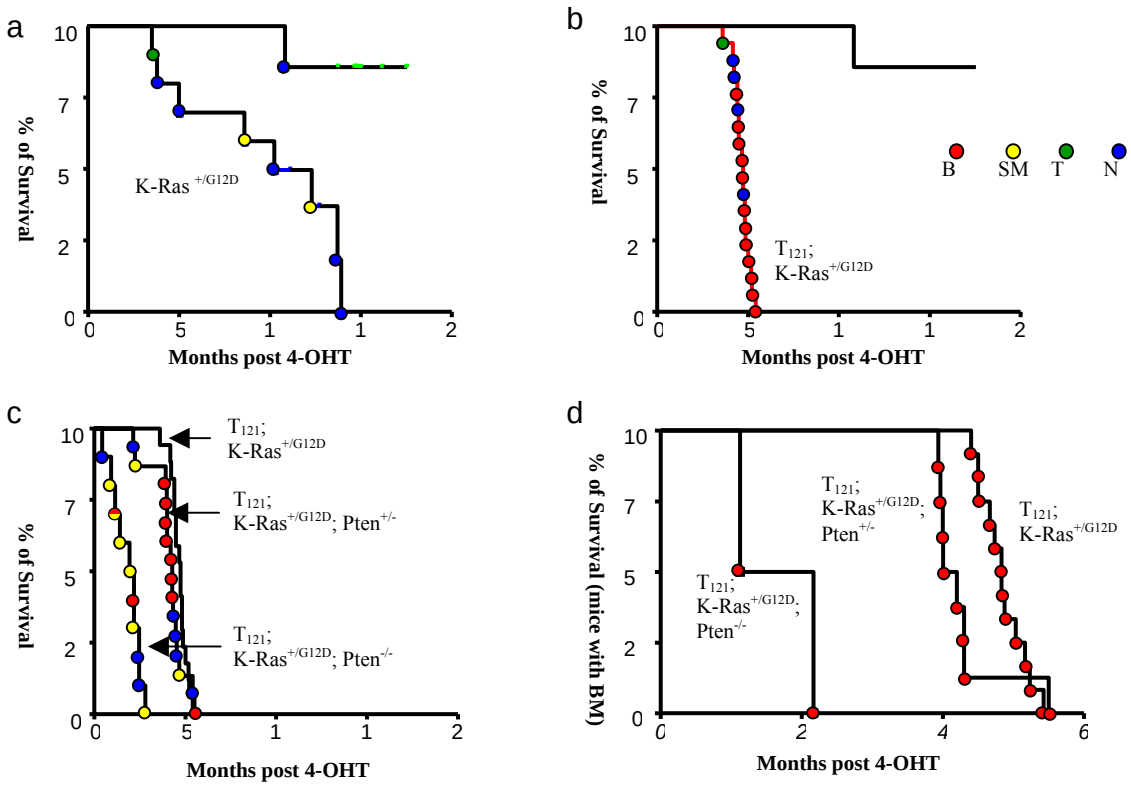
a
% of Survival
K-Ras +/G12D
Months post 4-OHT
b
% of Survival
B
SM
T
N
T121;
K-Ras+/G12D
Months post 4-OHT
c
% of Survival
T121;
K-Ras+/G12D
T121;
K-Ras+/G12D; Pten+/-
T121;
K-Ras+/G12D; Pten-/-
Months post 4-OHT
d
% of Survival (mice with BM)
T121;
K-Ras+/G12D;
Pten-/-
T121;
K-Ras+/G12D;
Pten+/-
T121;
K-Ras+/G12D
Months post 4-OHT

Figure 22. Progression of astrocytoma in different genetic backgrounds.

4a, H&E staining showed increased cellularity in the T_{121} brain (bottom panel) about one year post 4-OHT treatment, compared with normal control (top panel). Note the diffuse infiltration of the cerebral cortex by anaplastic-appearing astrocytoma cells. 4b, solid tumor masses developed in T_{121};K-Ras^{G12D} brains; these tumors displayed extensive vascular development in the form of an extensive vasculature, but no necrosis was observed. When Pten loss was added to those mutations, solid tumors featuring both angiogenesis and necrosis developed. Black arrows and "N" designate foci of necrosis. Tumor cells were poorly differentiated with the combined T_{121} and K-Ras^{G12D} mutations. While when Pten$^{+/-}$ or Pten$^{-/-}$ mutation was added to T_{121} and K-Ras^{G12D} mutations, some tumor cells had a more glial appearance, with more visible eosinophilic cytoplasm and some background fibrillarity,

a.

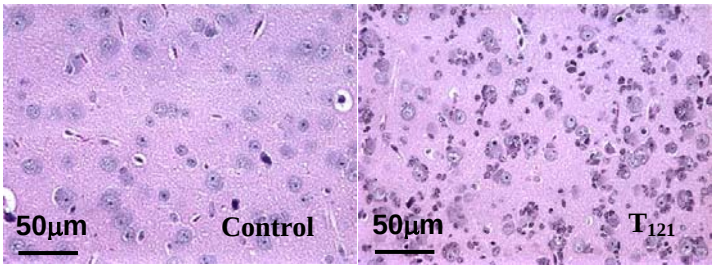
50µm
Control
50µm
T121

b.

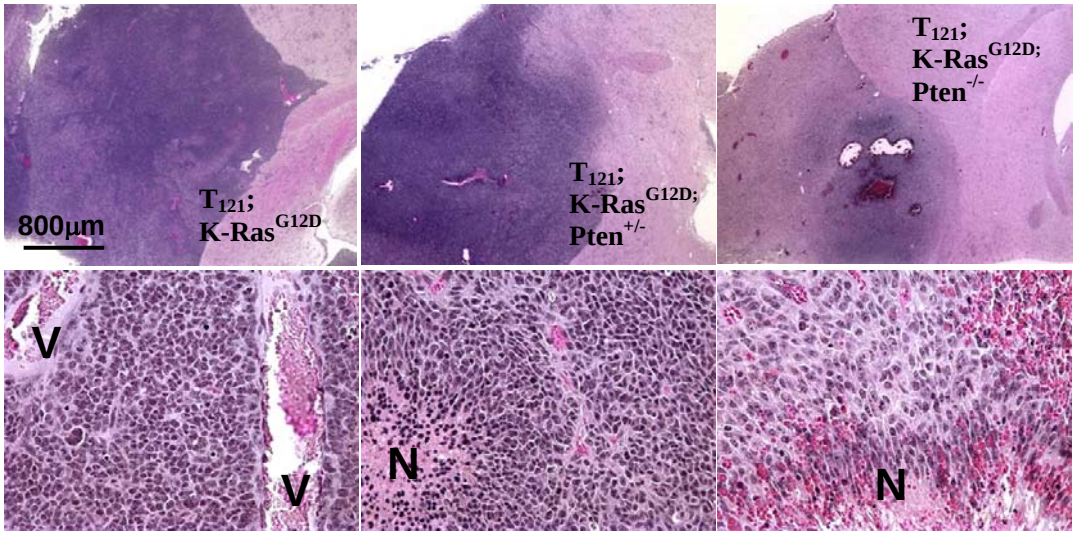
800µm
T121; K-RasG12D
T121; K-RasG12D; Pten+/-
T121; K-RasG12D; Pten-/-
V
V
N
N

Figure 23. Solid tumor mass featuring characteristics of human GBM.

a-c: Representative immunohistochemistry demonstrating the glial nature of the tumors: GFAP shows conspicuous staining of cell cytoplasm, including perikarya and processes (a); nestin is expressed (b); tumor cells are negative for synaptophysin (c).

d, macroscopic picture of a solid tumor (red arrow) in the frontal lobe (control on left; T_{121};K-Ras^{G12D};Pten$^{+/-}$ on right). The red color of the tumor shows considerable vascularity. e-f, panel e is MRA image of a brain tumor located in the brain stem/cerebellum of a T_{121},K-Ras^{G12D} mouse. Red arrow points to the tumor as shown by white area in the T1 MRA image. Solid tumors are highly vascular as exemplified by the 3D view of vessel distributions out (blue) of and inside (red, gold, yellow, and cyan lines) the tumor bulb (f). g-h: Necrosis, including with perinecrotic palisades of tumor cells, was a common feature (left panel, highlighted by blue dash line) in tumors from T_{121};K-Ras^{G12D};Pten$^{+/-}$ or T_{121};K-Ras^{G12D};Pten$^{-/-}$ mice. VEGF expression, as shown by in-situ hybridization, was upregulated in the palisading cells around necrotic foci, as is seen in human glioblastomas.

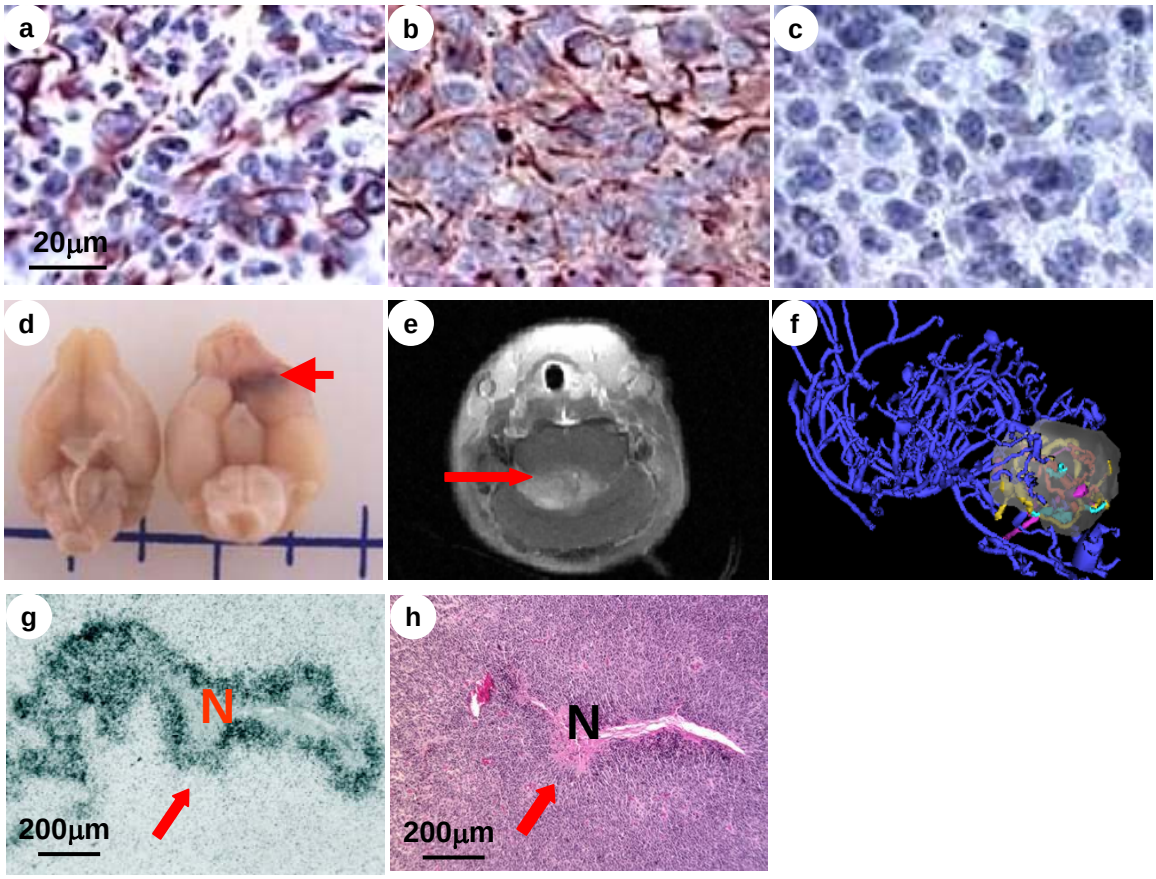
a
20μm
b
c
d
e
f
g
N
200μm
h
N
200μm

Figure 24. Contribution of different genetic changes to the astrocytoma progression.

H&E staining of brain sections from mice 2 weeks, 2 months and 4 months post-4-OHT treatment were used for time course analysis (a.). In image a, panels from left to right are the representative brains of controls, T_{121}, T_{121};K-Ras^{G12D} , and T_{121};K-Ras^{G12D};Pten$^{-/-}$. All images were from similar fields in the cortex of brain. Controls include GFAP-CreER treated with 4-OHT or T_{121};K-Ras^{G12D} treated with vehicle. Brains in K-Ras^{G12D} mice were similar to controls (data not shown). There was slight increased cellularity (green arrows) in T_{121} and T_{121};K-Ras^{G12D} mice two weeks after 4-OHT treatment. The cellularity in T_{121};K-Ras^{G12D};Pten$^{-/-}$ is higher than T_{121} or T_{121};K-Ras^{G12D} at 2 weeks and 2 months post-4-OHT. Red arrows point to perineuronal satellitosis and blue arrows points to perivascular satellitosis.

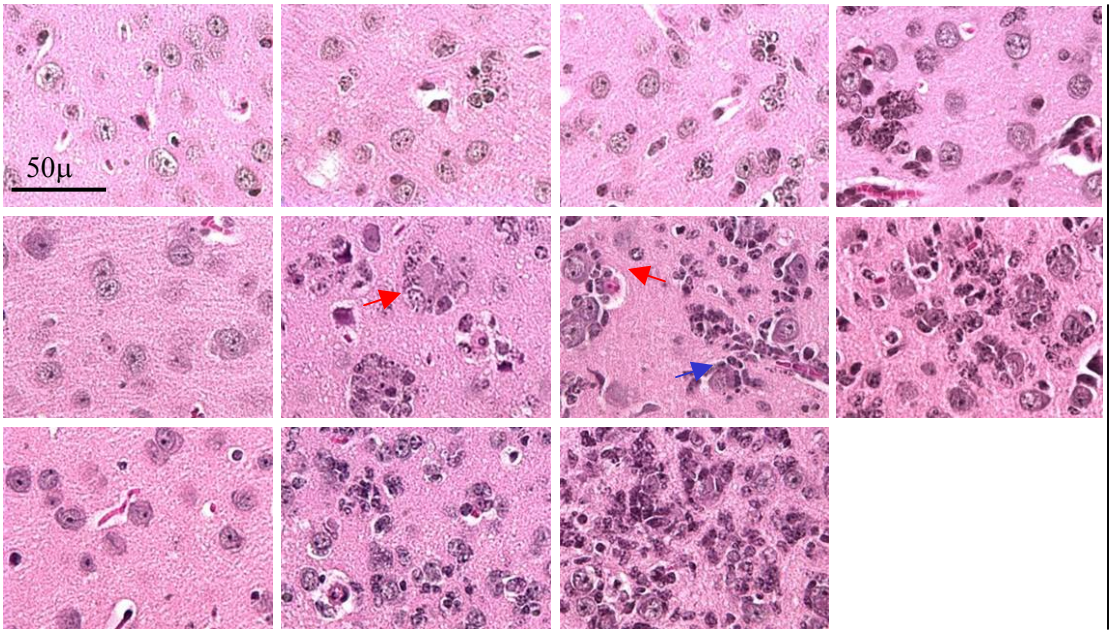
50μ
2 weeks
2 months
4 months
Control
T121
T121; K-RasG12D
T121; K-RasG12D; Pten-/-

Figure 25. Contribution of different genetic changes to proliferation and apoptosis.

Quantification of proliferating cells and apoptotic cells versus T_{121} expressing cells are from mice 2 months after 4-OHT treatment. Related apoptosis and proliferation data of 2 weeks were similar between T_{121} and T_{121};K-Ras^{G12D} (data not shown here). When T_{121};K-Ras^{G12D} brains were compared with T_{121} brains, proliferation rates increased about 22% (P value =0.395). Apoptosis was significantly decreased by 42% (P value=0.028). Three mice were used to generate each bar. When T_{121};K-Ras^{G12D};Pten$^{-/-}$ brain was compared with T_{121};K-Ras^{G12D} brain, proliferation rate increased about 10%, but this is not statistical significant (p=0.5422). Apoptosis level was greatly decreased about 40% and it is statistical significantly (p=0.074).

T=T_{121}; R=K-Ras^{G12D}; P=Pten; Wt=wild type.

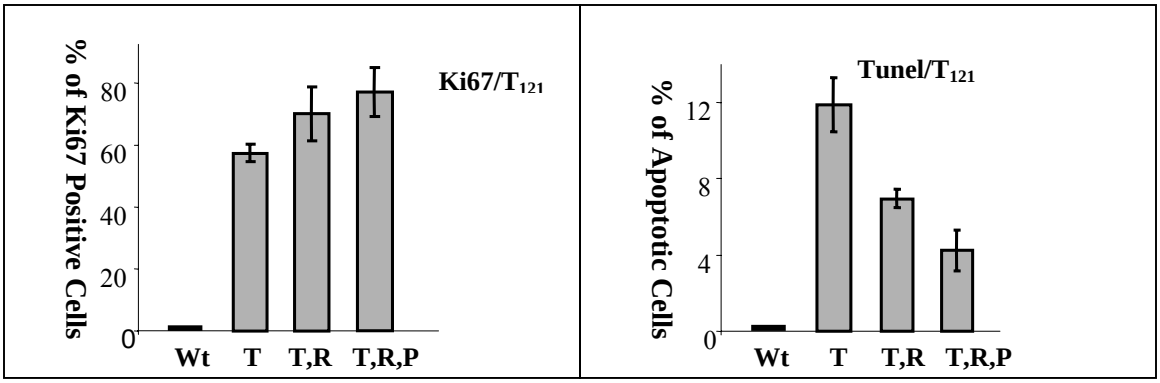
% of Ki67 Positive Cells
80
60
40
20
0
Ki67/T121
Wt
T
T,R
T,R,P
% of Apoptotic Cells
12
8
4
0
Tunel/T121
Wt
T
T,R
T,R,P

Discussions

Evade developmental defects by adulthood induction of tumor genes

In currently available astrocytoma models, the GFAP promoter is largely used to direct gene mutations in astrocytes either by straight transgenic technique or conditional induction mediated by GFAP-Cre. However, GFAP expresses as early as E11.5 in the radial glial cells, which are neural stem cells and can differentiate into both astrocytes and neurons. Thus, it is not known if the neuronal population is affected and also subjected to tumorigenesis using this strategy. Although neuronal differentiation was observed in some models (Zhu et al 2005; Zhang et al unpublished), it is not know that if they were differentiated from neural precursors or if they were transformed from neuroblasts. In addition, mouse models generated using direct GFAP regulation always have brain defects unrelated to tumor formation, such as retarded growth, hydrocephalus and expanded population in the SVZ (Weissenberger et al., 1997; Ding et al., 2001; Xiao et al., 2002). These phenotypes were possibly caused by the interruption of brain development due to the early induction of oncogenic events. As a result, those mice usually are not suitable to cross with other genetically mutated mice.

In this study, we adopted a new strategy to circumvent developmental defects by using a GFAP-CreER mouse. Here, the recombinase function of the CreER chimeric protein is controlled by IP injection of 4-OHT. Thus, we were able to temporally induce the oncogenic events by injection of 4-OHT at about 3 months old. At this stage, the brain is developed and most cells are mature except for a very small portion of neural precursors. Compared with the early induction of T_{121} from embryonic stage, there was no developmental defect of brain, such as hydrocephalus and no abnormal population in the sub ventricular zone (SVZ). Thus,

this system has proved an applicable strategy to evade early induction of tumor genes. Furthermore, this strategy can introduce multiple genetic mutations at the same time without the early death caused by the developmental defects.

In the adult stage, except for mature astrocytes, GFAP also expresses in the neural stem cells that are a small population residing in the sub-ventricular zone. In this model, tumor masses developed in multiple locations, including frontal brain, brain stem, thalamus and optical nerve. And pre-tumor nodule can be identified anywhere in the brain. All of this suggests majority of tumors, if not all, evolved from mature astrocytes.

Multiple mutations are needed for the GBM formation and progression

Genetic studies indicate that the evolution of GBM involves more than one genetic mutation based on the fact that multiple mutations coexist in same GBMs (Kleihues and Cavenee, 2000). Recent work with genetically engineered mouse models suggests that one mutation is not sufficient for GBM formation (Kleihues and Cavenee, 2000). The scenario could be each mutation contributes to certain features of tumor, especially for the progression of low grade to high-grade astrocytoma in secondary GBMs. Thus, it is intriguing to know how various genetic mutations contribute to tumor evolution.

Time course analysis of tumorigenesis shows abnormal cell clusters were observed 2 weeks after 4-OHT introduction in the brain with T_{121} mutation alone (Fig. 20a-c, 24). This suggests that disruption of the Rb pathway can initiate tumorigenesis, ruling out other possibilities such as foregoing mutations are required to initiate tumorigenesis. Other than Rb_f inactivation, neither K-Ras mutation not Pten loss can initiate tumorigenesis of astrocytes, which was consistent with previous reports ((Hermanson et al., 1992); (Ichimura et al., 1998); (Huang et al., 1996). In another astrocytoma mouse model, overexpression of

mutant H-Ras led to different grades of astrocytoma dependent on dose. The possible reasons could be: in this system, mutant K-Ras was under the control of its endogenous promoter, which was not turned on in normal brains; or, if there was expression, mutant K-Ras caused cell cycle arrest instead of cell proliferation (reference).

However, interestingly, tumorigenesis was greatly accelerated when mutant K-Ras was added to pRb_f inactivation. At two months post 4-OHT treatment, peri-nuclear and peri-vascular satellitetosis were present which is indicative of a grade III astrocytoma. Most strikingly, at about 4 months post 4-OHT treatment, solid tumors with GBM characteristics developed. Mutant K-Ras seems to be critical for the formation of a solid tumor, because diffusive astrocytoma developed in both T_{121} and T_{121}; $Pten^{-/-}$ background without progression to a solid tumor. One of the key factors for solid tumor formation could be angiogenesis, as indicated by previous studies, which show that Ras pathways contribute to new vessel formation in the solid tumors (Miyakawa et al., 2000).

Necrosis and angiogenesis are two hallmark features of human GBM. However, necrosis was not observed in the solid tumor with mutations of T_{121};$K\text{-}Ras^{G12D}$. Surprisingly, when $Pten^{+/-}$ or $Pten^{-/-}$ was added to combined mutations of T_{121} and $K\text{-}Ras^{G12D}$, necrosis surrounded with pseudopallisading cells was a typical phenotype. The difference cannot be attributable to the mouse stain effects, since they are in similar backgrounds (see method). Although, Pten loss is likely responsible for the necrosis phenotype, it is not known that if this correlation needs to be in the context of T_{121} or/and $K\text{-}Ras^{G12D}$ mutations. In earlier reports, it is suggested that Ras and Akt pathways collaborate to the necrogenesis, in a way that Ras promotes the cell death, which is achieved through necrosis due to the blockage of apoptosis by Akt. This is possible, since Pten loss did contribute to the reduced apoptosis in

this system and in our earlier report (Fig. 25; Xiao et al., 2006). However, conclusion could not been made since necrosis was also observed in the T_{121};K-Ras^{G12D};Pten$^{+/-}$ background, in which the general level of apoptosis is relatively higher than inT_{121};K-Ras^{G12D};Pten$^{-/-}$ background (data not shown). It is not clear if local LOH of Pten occurs in the necrotic regions. Although the exact mechanism is not known yet, Pten's involvement in the necrogenesis could have significant implication for the clinic, since necrosis is correlated to worse prognosis of patients.

Preclinical uses of the model

Since conventional treatments have little effect on the outcome of malignant glioma patients, it is particularly intriguing to use applicable targeted molecular therapies. The model generated in this study mimicked the most common genetic mutations in human glioblastoma and in turn, mice developed brain tumors with human GBM features. Thus, it offers a very promising system for preclinical drug testing, particularly targeted molecular therapies. Multiple pathways can be tested based on the availability of inhibitors, such as RTK-Ras pathway and Pten-Akt pathway. In recent reports, it is suggested that inhibitors that counteract both EGFR overexpression and Pten loss could result in a positive response of patients (Mellinghoff et al., 2005). Our mouse model offers a system, in which the underlying mechanism can be explored. We also showed the value of MRA studies to monitor tumor growth and malignancy based on the vessel turtuosity (Fig. 23e-f) (Watanabe et al., 1997).

Materials and methods

Experimental mice. GZT_{121} conditional transgenic mice were maintained by crossing to BDF1 mice (Xiao et al, 2002). K-Ras^{G12D} conditional knock-in mice (Jackson et al, 2001), $Pten^{f/f}$ (Suzuki A. et al, 2001) and GFAP-$CreER^{TM}$ (McCarthy K, unpublished) mice were maintained by crossing to B6 mice. The mice with the genotypes of GZT_{121}, K-Ras^{G12D}, and GFAP-$CreER^{TM}$ were at about 83.6% B6 and 12.5% D2 background. The mice with the genotypes of GZT_{121}, K-Ras^{G12D}, $Pten^{f/f}$ and GFAP-CreER were at about 90% B6 and 6% D2 background.

4-OHT treatments. 4-OH Tamoxifen (Sigma) was suspended in 100% ethanol, then mixed with sunflower oil for a final concentration of 1mg 4-OHT per 100ul. 4-OHT was dissolved in 10% ethanol/90% sunflower oil by ultrasound sonification for 5-10 minutes until mixed solution was clear. An intraperiton injection of the fresh solution was administered to 3 months old mice 1mg per day for 5 consecutive days.

Histopathology. Mice were dissected at about 2 weeks, 2 months and the terminal stage or 13months~18months after 4-OHT treatment. Brains including olfactory bulb were removed and fixed in 10% formalin for 20-24 hours before transferred to 70% ethanol. Brains were embedded in paraffin and sectioned with a sagittal orientation at 5um. Hematoxylin and eosin staining were performed as described previously in Chapter 2.

Immunodetection. Paraffin sections were used for immunohistochemistry staining as described (Chen et al, 1992). For antigen retrieval, slides were either boiled in citrate buffer (pH 6.0) for 10 minutes or treated by proteinase K 5-15 minutes. For IHC staining, mouse anti-SV40 T antigen (N-terminal-specific monoclonal Ab2, 1:300 for single staining and 1:100 for double staining, Oncogene, Cambridge, MA) was used; goat anti-Ki67 (1:1500,

polyclonal M-19, Santa Cruz Biotechnology, Santa Cruz, CA) was used; rabbit anti-GFAP (1:500, Z0334, DAKO,) was used; rabbit anti-S100 (1:100, Z0311, DAKO) was used; rabbit anti-Synaptophysin (1:50, A0010, DAKO) was used; rabbit anti-phospho-Akt $^{Ser\ 473}$ (1:50, 9277, Cell signaling) and rabbit anti-phospho-Erk1,2$^{Thr202/Tyr204}$ (1:50, 9101, Cell signaling) were used. To detect the substrate conjugated to secondary antibody, Vector's ABC elite kit and Vector's RovaRED kit was used.

Paraffin sections were used for immunofluorescence double staining. After deparaffinized, rehydrated and antigen retrieval, brain sections were blocked with 5% goat serum in PBS/0.05% Tween 20 first, then incubated with first primary antibody. Sections were washed with PBS/T and blocked with 5% goat serum again before incubated with second primary antibody. Sections were incubated with ALEXA FLUOR 488 goat anti-rabbit and ALEXA FLUOR 543 goat anti-mouse secondary antibody (1:200 for each) at 4^{o}C for 45 minutes. After wash, sections were counter stained and mounted with vector's VectaShield Hardset with DAPI.

PCR for the deletion of stop elements. To prepare DNA, cells were scratched from 5um paraffin embedded, formalin fixed brain sections. The cells were incubated in 30ul of solution A (25mM NaOH/0.2mM EDTA) at 68°C 24h. Then 30ul of solution B (40mM Tris-HCl) was added. The mixed solution was vortexed and centrifuged 10 minutes at 2000rpm. For PCR testing the deletion of LoxP sites in the T_{121} transgenic allele, primers were 5' – TGA TCA GAA CCA TCA TG – 3' and 5' – GTT GAC CAG AGT GGC GTA GG – 3'. PCR condition was 94 ^{o}C 5'; 94 ^{o}C 1', 55 ^{o}C 1', 72 ^{o}C 1' 35 cycles. For PCR testing the deletion of LoxP sites in the K-RasG12D knock-in allele, primers were 5' – GGG TAG GTG TTG GGA TAG CTG – 3' and 5' – TCC GAA TTC AGT GAC TAC AGA TGT ACA GAG

– 3’. PCR condition was 98 ^{o}C 5’; 98 ^{o}C 30’’, 58 ^{o}C 30’’, 72 ^{o}C 30’’ 35 cycles. DNA samples were collected from brain paraffin sections about 2 months after 4-OHT treatment. Primer sets detected the fragments after recombination of loxP sites.

Apoptosis assay. To test the apoptosis level, two weeks post-4-OHT, two months post-4-OHT and terminal tumor paraffin sections were used. Apoptotic cells were labeled by modifying genomic DNA utilizing terminal deoxynucleotidyl transferase (TdT) (TUNEL assay) using ApopTag In Situ Apoptosis Detection Kits (Intergen Company).

Quantification of cells. Five random fields in same area of brain for each sample were taken for cell quantification. For two months brain analysis, adjacent sections were used for Ki67 staining, T_{121} staining and tunel assay. Cell numbers were counted using Image J program (NIH).

CHAPTER FIVE

EGFR PATHWAY ACTIVATION IN THE INDUCIBLE GBM MOUSE MODELS AND FUTURE DIRECTIONS

Chapter 4 reports the generation of a highly penetrant (100%) inducible model of human glioblastoma (GBM) in genetically engineered mice (GEM). Since, to our knowledge, this model is the first fully penetrant and regulatable spontaneous model of GBM, we propose to develop it to use in preclinical testing. Therapy using EGFR inhibitors has been proven effective in human cancers including GBMs. However, the role of EGFR in human GBMs is not clear. Although previous studies have established a signal transduction pathway from EGFR to Ras, it has also been reported that EGFR responds to signals from Ras in cancers, possible due to the activation of EGFR ligands. To test the latter possibility, we examine EGFR signal activation by Ras. In addition, the impact of EGFR loss will be directly tested in this model by breeding mice to a conditional EGFR knock out. If the results prove the involvement of EGFR in GBM formation in this system, we will test EGFR inhibitors for GBM treatment. These results will be confirmed using a Magnetic Resonance Angiography (MRA) vessel analysis technique. At the same time, this model potentially has multiple other uses in mechanistic studies and therapeutic tests.

Introduction

Chapter 4 has described the development of an inducible GEM mouse model of human glioblastoma by targeting common mutations observed in human cases, including disruption of Rb pathway, activation of K-Ras and Pten loss. This model is very promising for further uses in mechanistic studies and therapeutic tests since it is highly penetrant, inducible, and similar to human GBM in regard to genetic changes and morphologies. EGFR is an intriguing target based on two aspects of this receptor. First, EGFR is frequently mutated in human GBMs and this mutation is associated with an abnormal Ras pathway (Guha et al., 1997;Kleihues and Cavenee 2000), however, how they interact with each other in GBMs is not clear. Though EGFR signaling to Ras is a well-established pathway, it has also been suggested that EGFR is not necessarily upstream of Ras in their associations in oncogenic functions (Dlugosz et al., 1997). In contrast, Ras is able to signal to EGFR by inducing the secretion of EGFR ligands (Gangarosa et al., 1997). A recent study showed that EGFR promotes cell survival independent of Ras, but this effect was required for oncogenic transformation by Ras signals in skin tumors (Wagner EF et al., 2000), suggesting Ras is upstream of EGFR and/or there is parallel cooperation of the two molecules. This model can be used to test the multiple possibilities for interaction between EGFR and Ras. Second, clinical trails using EGFR inhibitors have proven their limited benefits in treatment of several human cancers, including glioblastoma (Mellinghoff et al., 2005). If it is proven that the EGFR pathway contributes to GBM formation in our system, we will test EGFR inhibitors in this model.

EGFR is a cell membrane protein containing an extracellular ligand binding domain, a transmembrane domain and an intracellular tyrosine kinase domain with multiple

phosphorylation sites in the C-terminal tail (Singh and Harris, 2005). Upon binding to extracellular ligands, EGFR activates its kinase, which phosphorylates EGFR itself and other downstream signals. In this model, the activation of EGFR to Stat3 (signal transducer and activator of transcription 3), one of its downstream targets, was identified. At the same time, direct involvement of EGFR in GBM formation was tested by crossing the T_{121};K-Ras^{G12D};CreER mice to floxed EGFR knock out mice. This chapter will describe some preliminary data about EGFR pathway activation in our GEM, and the future uses of this model.

Results

EGFR activation after induction of T_{121} and K-Ras^{G12D} by 4-OHT

To test if the EGFR pathway is activated in astrocytes after the induction of oncogenic events, EGFR expression was examined in astrocytoma cells by performing EGFR staining by immunohistochemistry (IHC). Positive staining was observed in the tumor cells of mice with the genotype of T_{121};K-Ras^{G12D} two months after 4-hydroxy-tamoxifen (4-OHT) treatment (Fig. 26). EGFR levels were much lower in T_{121} only tumor cells, which received the same treatment. The staining pattern observed in the brain of a mouse with K-Ras^{G12D} mutation only was similar to the control (Fig. 26 A-F). Since EGFR was not expressed in normal astrocytes, the presence of positive staining in tumor cells suggests that its presence is related to oncogenic events, specifically K-Ras^{G12D} activation. EGFR expression could possibly be related to the microenvironment, as EGFR was not expressed in a tumor located in the brain stem, but was expressed at high levels in a tumor from the frontal brain (Fig. 26G-J).

Since EGFR was expressed in tumor cells, it is interesting to know if EGFR was activated acutely after 4-OHT treatment. Thus, a western blot was performed using antibodies to phosphorylated EGFR (p-EGFR) for multiple sites, including tyrosine 845, 992 and 1045 (Fig. 27). To test the acute effect caused by K-Ras^{G12D} or T_{121}, brains were collected two weeks after 4-OHT treatment. Levels of p-EGFR (Tyr 992) and (Tyr 1068) were found increased in both T_{121} and T_{121};K-Ras^{G12D} brains. However, no obvious difference in p-EGFR levels was observed between T_{121} and T_{121};K-Ras^{G12D} brains, suggesting the increase in EGFR levels is caused by T_{121} but not K-Ras^{G12D} at this stage. This result is consistent with previous observations that K-Ras^{G12D} has no apparent effect on the early stages of tumorigenesis as addressed in Chapter 4.

Then the activations of downstream targets of EGFR were tested, including Ras/ERK, PI3K/Akt as well as STATS pathways (Jorissen et al., 2003). Since ERK or Akt pathway is also downstream of Ras activation independent of EGFR (Campbell and Der, 2004), STATS activation was used as an indicator of EGFR pathway activation. The acute activation of p-STAT3 (Fig. 28A), but not p-STAT5 (data not shown), was observed in T_{121} and T_{121};K-Ras^{G12D} brains two weeks after 4-OHT treatment. Similar to the findings for p-EGFR, no obvious difference was observed between T_{121} and T_{121};K-Ras^{G12D} brains at this stage. Two months after 4-OHT treatment, the overall level of p-STAT3 was too low to examine by IHC. The level of p-STAT3 was higher in T_{121};K-Ras^{G12D} than in T_{121} (Fig. 28B-C), but since the number of tumor cells also increased, the association of K-Ras^{G12D} with p-STAT3 level is inconclusive. In the solid tumor, p-STAT3 was highly activated as indicated by the abundance of IHC staining (Fig. 28D).

To test if activated K-Ras pathway affected the expression of ligands, quantitative RT-PCR was performed to examine their mRNA level (Fig. 29). EGFR has seven ligands: epidermal growth factor (EGF), heparin-binding EGF-like growth factor (HB-EGF), amphiregulin (Areg), transforming growth factor-a (TGFa), epiregulin (Epgn), and betacellulin (Btc) (Harris et al., 2003). Neuregulin-1 (Nrg1), which is a ligand of EGFR family members including Erb2, Erb3 and Erb4 (Falls, 2003), was also tested since it is expressed in glial cells and associated gliomas (Raabe et al., 1998;Westphal et al., 1997; Ritch et al., 2003). There was no significant change in most ligands, except for HB-Egf, which was decreased about 30% in both T_{121} and T_{121};K-Ras^{G12D} brains. Interestingly, the levels of Nrg1 were about 3.5 fold higher ($p=0.0392$) than the control in T_{121} brain and 1.3 fold ($p=0.182$) higher than the control in T_{121};K-Ras^{G12D} brain.

Figure 26. EGFR expression after induction of oncogenic events.

Total EGFR levels were tested by IHC staining of brain sections from mice with various genotypes taken 2 months (B-F) after 4-OHT treatment and in solid tumors (G-J) which developed in T_{121}; K-Ras^{G12D};GFAP-CreER. Some tumors were immunoreactive to EGFR (G and H) and some tumors were not (I and J).

Arrows point to the positive brown staining of EGFR. The blue color is counter staining using hematoxylin. A is a brain section of T_{121}; K-Ras^{G12D};GFAP-CreER without EGFR antibody treatment, used as a control for staining.

Scale bar in A-F is 100μm. Scale bars of panels G-J are as listed.

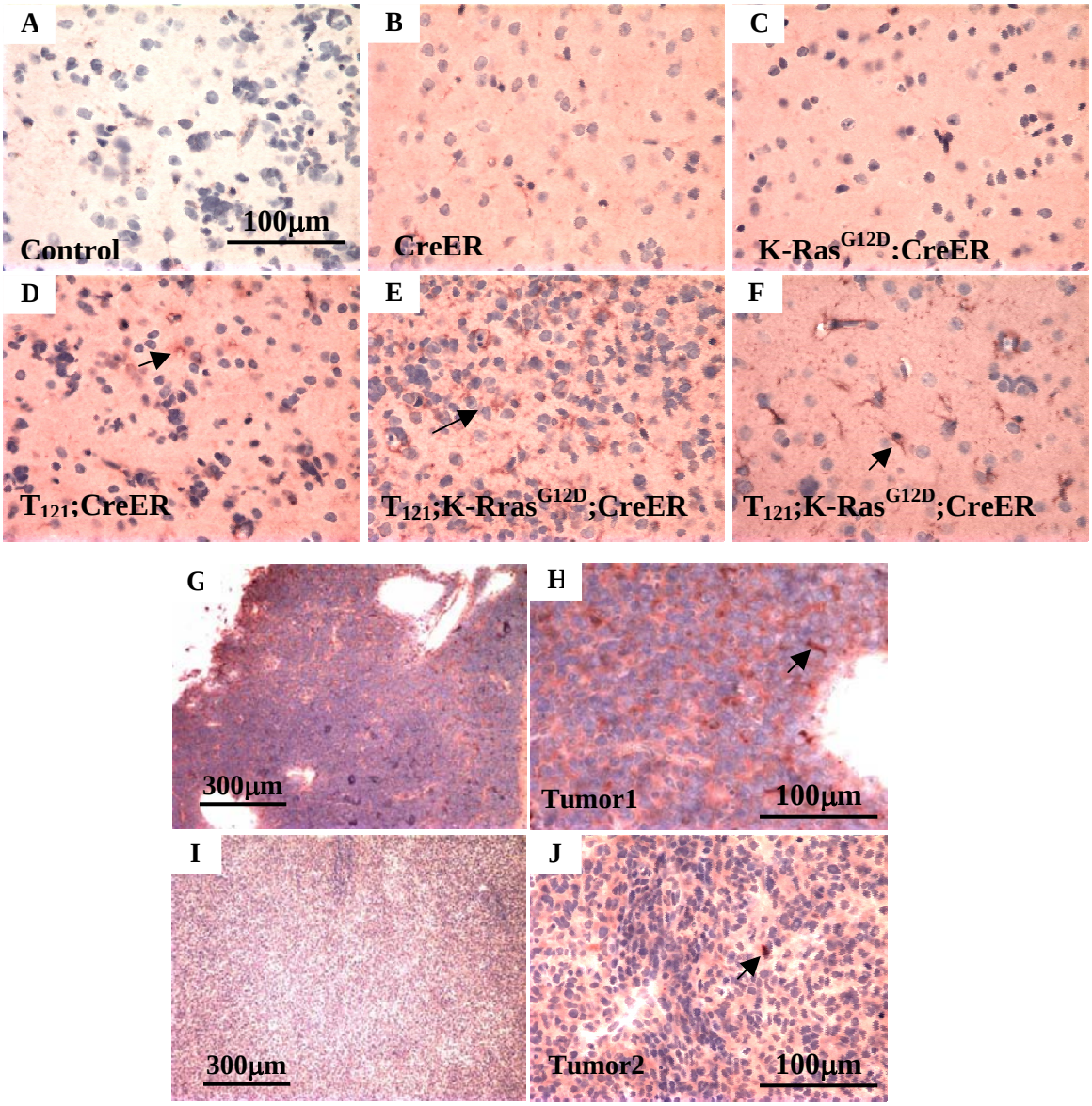
A
100μm
Control
B
CreER
C
K-Ras^{G12D}:CreER
D
T_{121};CreER
E
T_{121};K-Rras^{G12D};CreER
F
T_{121};K-Ras^{G12D};CreER
G
300μm
H
Tumor1
100μm
I
300μm
J
Tumor2
100μm

Figure 27. Activation of EGFR by phosphorylation in multiple sites shortly after 4-OHT treatment.

Levels of total and phosphorylated EGFR were tested by western immunoblot using a brain lysate prepared from mice with various geneotypes taken 2 weeks after 4-OHT injection (A) using EGFR and p-EGFR antibodies (phosphorylated sites in: 845, 992, and 1045). Western immunoblotting to GAPDH, a housekeeping gene, was used as a control for equal loading of proteins. Increased levels of p-EGFR are emphasized by red dashed-line box. This result was confirmed by several repeated experiments using different animals.

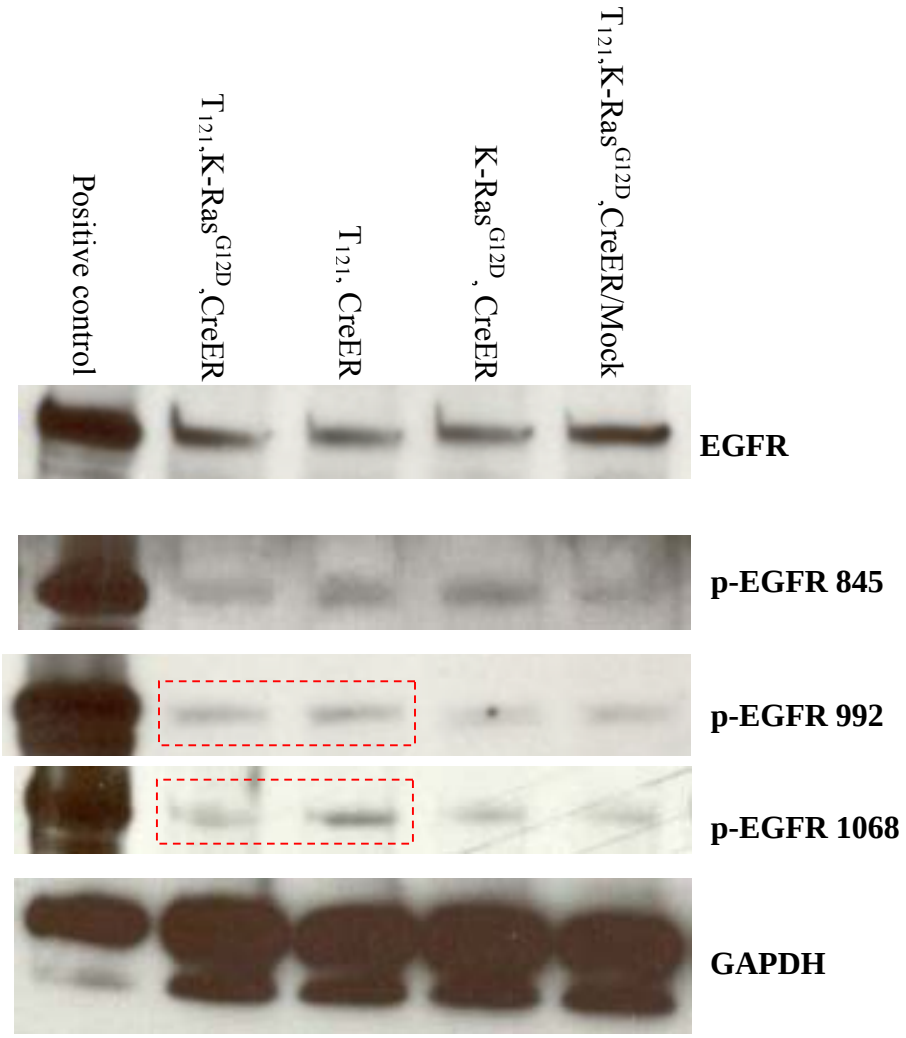
Positive control
T121,K-RasG12D,CreER
T121, CreER
K-RasG12D, CreER
T121,K-RasG12D,CreER/Mock
EGFR
p-EGFR 845
p-EGFR 992
p-EGFR 1068
GAPDH

Figure 28. Activation of p-Stat3 in the short and long term after 4-OHT induction.

p-Stat3 level was tested by western immunoblot with brain lysates taken from mice 2 weeks after 4-OHT injection (A) using a p-Stat 3 antibody (phosphorylated in sites:Tyr705). The GAPDH western blot is used as a control for equal loading of proteins. p-Stat3 IHC staining was performed on brain sections from mice sacrified 2 months after 4-OHT treatment (B,C) and from a solid tumor (D). Weak staining is seen in the tumor cells expressing $T_{121.}$ (B) Staining is slightly stronger in T_{121};K-Ras^{G12D} tumor cells (C). Staining is much stronger in the solid tumors as represented by panel D. Positive control is 293 cells with EGF treatment and negative control is 293 cells without EGF treatment. Scale bar in B-D is 100um.

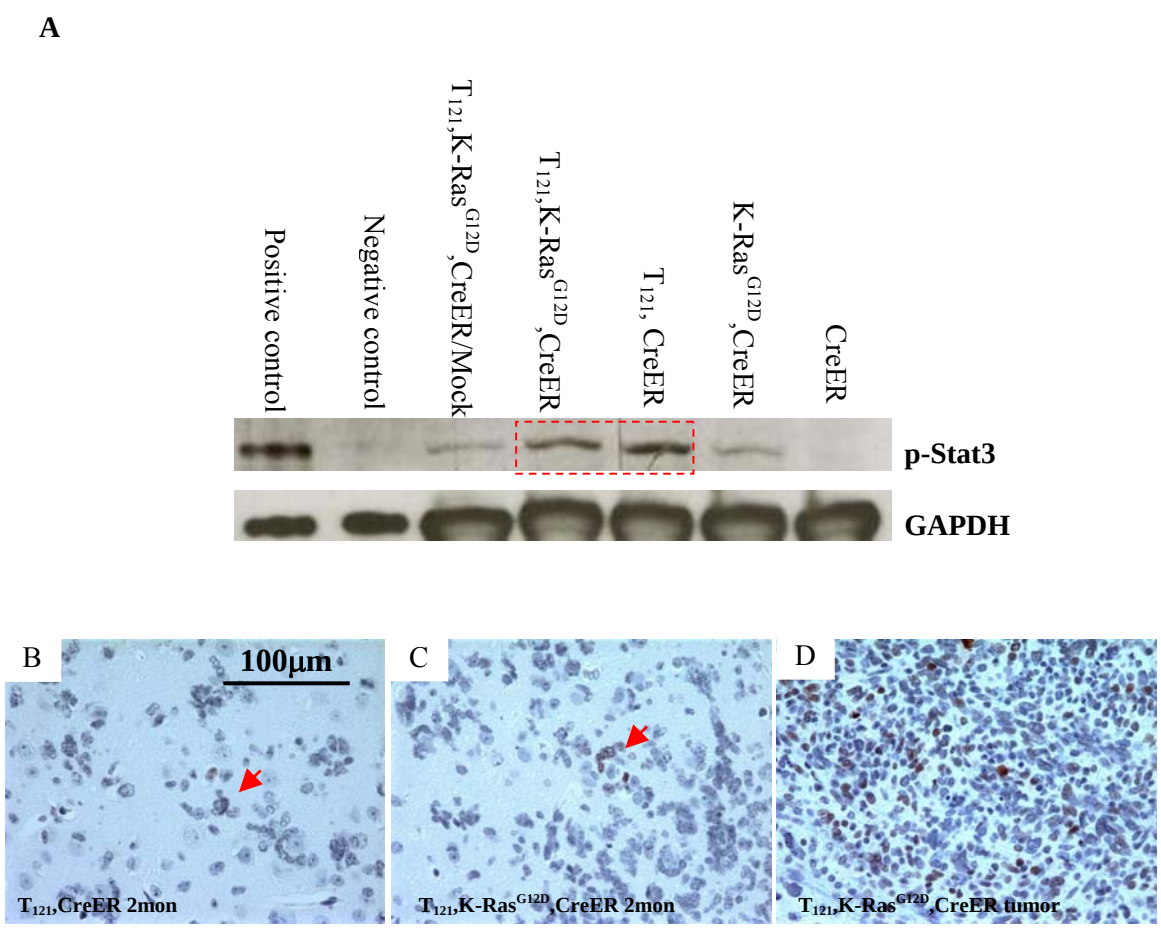
A
Positive control
Negative control
T121,K-RasG12D,CreER/Mock
T121,K-RasG12D,CreER
T121, CreER
K-RasG12D,CreER
CreER
p-Stat3
GAPDH
B
100μm
T121,CreER 2mon
C
T121,K-RasG12D,CreER 2mon
D
T121,K-RasG12D,CreER tumor

Figure 29. Acute activation of the EGF receptor family ligands.

The levels of ligands of EGFR and Nrg1, the latter being the ligand of Erb2, were tested in brains from mice taken two weeks after 4-OHT treatment by quantitative RT-PCR. The control bar was normalized to 1 and the other bars are relative values of experimental samples compared to the control (function: $2^{-(\Delta\Delta G)}$). Three mice in each genotype were used to generate data. Control was from GFAP-CreER and T_{121};K-Ras^{G12D};GFAP-CreER oil treated mice. *: $p<0.001$, **: $p<0.05$, and ***: $p<0.01$

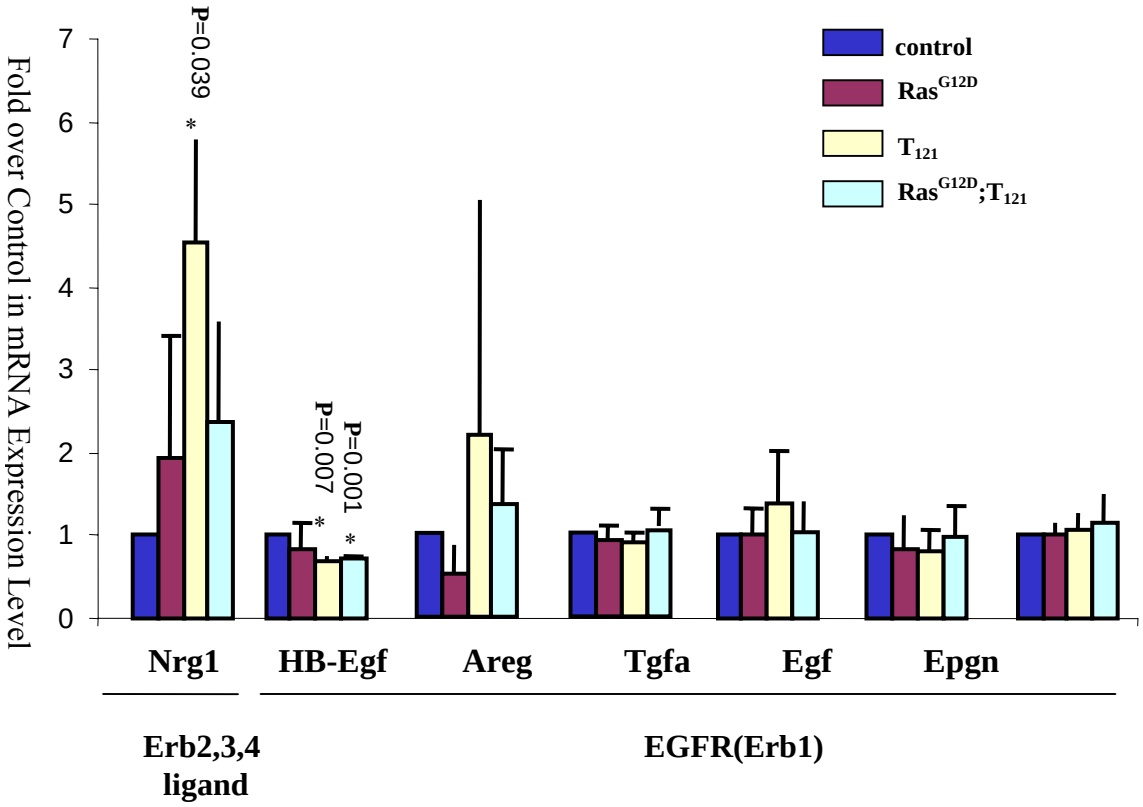
Fold over Control in mRNA Expression Level
7
6
5
4
3
2
1
0
P=0.039
*
P=0.007
*
P=0.001
*
control
Ras^G12D
T121
Ras^G12D;T121
Nrg1
HB-Egf
Areg
Tgfa
Egf
Epgn
Erb2,3,4 ligand
EGFR(Erb1)

Discussions

Our preliminary data suggest that the EGFR pathway is activated in the brain after combined mutations of T_{121} and K-Ras^{G12D} or T_{121} only. However, in brains from mice taken two weeks after 4-OHT treatment, the level of EGFR pathway activation was the same between T_{121} and K-Ras$^{+/G12D}$;T_{121}, suggesting the changes were caused by T_{121} instead of K-Ras$^{+/G12D}$ in early stages. The scenario could be that T_{121} is upstream of K-Ras^{G12D}, and signals through EGFR to activate K-Ras^{G12D}; or T_{121} activates K-Ras^{G12D} directly and thereafter activates EGFR, which is less likely due to the fact that levels of EGFR activation in T_{121} and K-Ras$^{+/G12D}$;T_{121} brains are the same. Alternatively the K-Ras pathway was not completely activated two weeks post 4-OHT treatment, based on the indistinguishable morphology between T_{121} and T_{121};K-Ras$^{+/G12D}$ brains. An analysis of a later stage will be more informative. Since no increased level of EGFR ligands was found in early stages, it will be interesting to elucidate the variation in ligands after K-Ras^{G12D} is fully activated (if this is indeed the case). Thus, more experiments are needed to address the role of K-Ras mutation in the regulation of the EGFR pathway.

Some T_{121};K-Ras$^{+/G12D}$ mice have been crossed to EGFR$^{f/f}$ mice but they have not been fully characterized. Preliminary data indicates that the absence of EGFR did not reduce tumorigenesis dramatically. In a cohort of mice with T_{121};K-Ras$^{+/G12D}$;EGFR$^{f/+}$, solid tumors were observed within 5 months. However, the tumors were much smaller than those found in T_{121};K-Ras$^{+/G12D}$ mice. Moreover, the most frequent location of tumors in T_{121};K-Ras$^{+/G12D}$;EGFR$^{f/+}$ mice was in the cerebellum instead of in the frontal brain as in T_{121};K-Ras$^{+/G12D}$ mice. The onset of tumor formation was usually about 5 months after 4-OHT treatment in T_{121};K-Ras$^{+/G12D}$;EGFR$^{f/+}$ mice, which is a little longer than in T_{121};K-Ras$^{+/G12D}$

mice. Because of difference in genetic backgrounds of mice (T_{121};K-Ras$^{+/G12D}$ is about 86% B6 and T_{121};K-Ras$^{+/G12D}$;EGFR$^{f/+}$ is about 21% B6, 3% D2 and 75% unknown), the timing of tumor formation could be caused by these differences in background strains. For T_{121};K-Ras$^{+/G12D}$;EGFR$^{f/f}$ mice, a collection of samples and their analysis are under way. Two of these mice have died from thymic lymphoma in about 4 months, and the cellularity of the brains was similar to that of T_{121};K-Ras$^{+/G12D}$, but without a big tumor mass. It is possible that EGFR affects tumorigenesis at a later stage, and that this affects the formation of the tumor. More mice have been induced with 4-OHT to initiated tumorigenesis and it will be interesting to discover if EGFR will reduce or delay tumorigenesis.

In this model, if EGFR proves to be involved in tumorigenesis, EGFR inhibitors will be tested to assess their benefit for GBM treatment. Since mono-therapy using EGFR inhibitors has limited benefits to GBM patients (Rich et al., 2004;Mellinghoff et al., 2005), combined therapy of EGFR inhibitors and other treatments could improve the patient responses. Recent clinical trials have reported that the positive impact of EGFR inhibitor on GBM patients is dependent on the presence of both the EGFR mutation (EGFRvIII) and Pten expression (Mellinghoff et al., 2005). Our model provides a good system to test the hypothesis that blockage of both EGFR and Pten pathways is critical for response to treatment, since these two pathways are interrupted in this system. Because tumors developed both with and without Pten loss, in this model can be used to study how EGFR inhibitors contribute to the response of GBM with/without Pten. If EGFR has been proven not to be involved in tumorigenesis in this system, we then can use inhibitors of other components in the Ras pathway, such as raf inhibitors, and do further studies. Overall, this model mimics multiple

common mutations in human GBMs, thus offering several target sites for either drug testing or mechanistic studies.

Materials and methods

Immunohistochemistry. A detailed procedure of immunohistochemistry is described in Chapter 2. Antibodies used were anti-EGFR (1:50, rabbit polyclonal, Cell Signaling), p-Stat3 (1:50, rabbit polyclonal, Cell Signaling). Slides were treated by citrate buffer (pH 6.0) for antigen retrieval.

Western immunoblotting. Brains were harvested from mice 2 weeks after 4-OHT injection. Brain tissue was homogenized in lysis buffer at 4^{o}C. The lysed tissue was rotated for 30 minutes in the cold room, spun at 13,000rpm for 10min. Extracted proteins were heated at 95-100^{o}C for 5 minutes and then loaded on a SDS-PAGE gel (7.5% or 4-20% gradient ready gel, Bio-Rad). Samples were electrophoresed at 100v for 30-60 minutes, and electro-transferred onto nitrocellulose membrane. The membrane was washed with PBS buffer and incubated in blocking buffer (5% milk in PBS-T) for 1 hour. After three washes with PBS-T buffer, the membrane was incubated with primary antibody diluted in 5% BSA/PBS-T buffer with gentle agitation overnight at 4^{o}C. After three washes with PBS-T buffer, membrane was incubated with HRP-conjugated secondary antibody (1:2000) with gentle agitation at room temperature for 1 hour. After three washes with PBS-T buffer, the membrane was incubated with ECL detection reagent for 1 minute, and then exposed to X-ray film. The antibodies used here were anti-EGFR (1:1000, rabbit polyclonal, Cell Signaling), anti-pEGFR^{845} (1:1000, rabbit polyclonal, Cell Signaling), anti-pEGFR^{992} (1:1000, rabbit polyclonal, Cell Signaling), anti-pEGFR^{1068} (1:1000, rabbit polyclonal, Cell signaling), anti-pStat3 (1:1000,

rabbit polyclonal, Cell Signaling) and anti-GAPDH (1:1000, rabbit polyclonal, Novus Biologicals).

Real time RT-PCR. To isolate RNA, liquid N_2 cooled brain tissue was powered in a cooled homogenize. The tissue was transferred to Tri-reagent for 10 minutes until tissue was dissolved. 100µl of BCP was added to the tissue, and the mixture was vortexed and kept at room temperature for 15 minutes. The mixture was spun at 14,000 rpm at 4^{o}C for 15 minutes and 500µl of isopropanol was added. After through mixing, the solution was kept at room temperature for 15 minutes and spun again. Precipitate was washed 3 times with 70% ice-cold ethanol. 40µl of Rnase free water was added and incubated at 56^{o}C for better dissolving. The concentration of RNA was measured and diluted to 0.21µg/µl. Running an agarose gel checked the quality of RNA. For reverse transcription, 9.5µl RNA was added to the RT master mix solution (Invitrogen) and incubated at 37^{o}C for 1 hour. The reaction was stopped at 95^{o}C for 2 minutes and 80µl of water was added to the reaction. To perform real time PCR, 20 ul of the RT reaction (10µl ABSolute QPCR ROX mix (AB gene), 1µl 20x primer mix (Taqman PCR, Applied Biosystems), 5ul H2O and 4 ul cDNA), was prepared in 384-well plate and run in the 7900 real time PCR machine (Applied Biosystems).

REFERENCE LIST

1. Altomare DA, Testa JR (2005) Perturbations of the AKT signaling pathway in human cancer. Oncogene 24:7455-64.

2. Alvarez-Buylla A, Garcia-Verdugo JM (2002) Neurogenesis in adult subventricular zone. J Neurosci 22:629-34.

3. Amatya VJ, Naumann U, Weller M, Ohgaki H (2005) TP53 promoter methylation in human gliomas. Acta Neuropathol (Berl) 110:178-84.

4. Arbiser JL, Moses MA, Fernandez CA, Ghiso N, Cao Y, Klauber N, Frank D, Brownlee M, Flynn E, Parangi S, Byers HR, Folkman J (1997) Oncogenic H-ras stimulates tumor angiogenesis by two distinct pathways. Proc Natl Acad Sci U S A 94:861-6.

5. Bates S, Vousden KH (1996) p53 in signaling checkpoint arrest or apoptosis. Current Opinion in Genetics & Development 6:12-19.

6. Biernat W, Kleihues P, Yonekawa Y, Ohgaki H (1997) Amplification and overexpression of MDM2 in primary (de novo) glioblastomas. J Neuropathol Exp Neurol 56:180-5.

7. Bos JL (1989) ras oncogenes in human cancer: a review. Cancer Res 49:4682-9.

8. Burnett PE, Barrow RK, Cohen NA, Snyder SH, Sabatini DM (1998) RAFT1 phosphorylation of the translational regulators p70 S6 kinase and 4E-BP1. Proc Natl Acad Sci U S A 95:1432-7.

9. Burrows RC, Wancio D, Levitt P, Lillien L (1997) Response diversity and the timing of progenitor cell maturation are regulated by developmental changes in EGFR expression in the cortex. Neuron 19:251-67.

10. Cahill DP, da Costa LT, Carson-Walter EB, Kinzler KW, Vogelstein B, Lengauer C (1999) Characterization of MAD2B and other mitotic spindle checkpoint genes. Genomics 58:181-7.

11. Calver AR, Hall AC, Yu WP, Walsh FS, Heath JK, Betsholtz C, Richardson WD (1998) Oligodendrocyte population dynamics and the role of PDGF in vivo. Neuron 20:869-82.

12. Campbell K, Gotz M (2002) Radial glia: multi-purpose cells for vertebrate brain development. Trends Neurosci 25:235-8.

13. Campbell PM, Der CJ (2004) Oncogenic Ras and its role in tumor cell invasion and metastasis. Semin Cancer Biol 14:105-14.

14. Casanova ML, Larcher F, Casanova B, Murillas R, Fernandez-Acenero MJ,

Villanueva C, Martinez-Palacio J, Ullrich A, Conti CJ, Jorcano JL (2002) A critical role for ras-mediated, epidermal growth factor receptor-dependent angiogenesis in mouse skin carcinogenesis. Cancer Res 62:3402-7.

15. Casper KB, McCarthy KD (2006) GFAP-positive progenitor cells produce neurons and oligodendrocytes throughout the CNS. Mol Cell Neurosci 31:676-84.

16. CBTRUS (2006). Statistical Report: Primary Brain Tumors in the United States. Central Brain Tumor Registry of the United States.

17. Chaffanet M, Chauvin C, Laine M, Berger F, Chedin M, Rost N, Nissou MF, Benabid AL (1992) EGF receptor amplification and expression in human brain tumours. Eur J Cancer 28:11-7.

18. Chang EH, Gonda MA, Ellis RW, Scolnick EM, Lowy DR (1982) Human genome contains four genes homologous to transforming genes of Harvey and Kirsten murine sarcoma viruses. Proc Natl Acad Sci U S A 79:4848-52.

19. Cheng LC, Tavazoie M, Doetsch F (2005) Stem cells: from epigenetics to microRNAs. Neuron 46:363-7.

20. Chernova OB, Somerville RP, Cowell JK (1998) A novel gene, LGI1, from 10q24 is rearranged and downregulated in malignant brain tumors. Oncogene 17:2873-81.

21. Cobrinik D, Lee MH, Hannon G, Mulligan G, Bronson RT, Dyson N, Harlow E, Beach D, Weinberg RA, Jacks T (1996) Shared role of the pRB-related p130 and p107 proteins in limb development. Genes Dev 10:1633-44.

22. Cokgor I, Akabani G, Kuan CT, Friedman HS, Friedman AH, Coleman RE, McLendon RE, Bigner SH, Zhao XG, Garcia-Turner AM, Pegram CN, Wikstrand CJ, Shafman TD, Herndon JE 2nd, Provenzale JM, Zalutsky MR, Bigner DD (2000) Phase I trial results of iodine-131-labeled antitenascin monoclonal antibody 81C6 treatment of patients with newly diagnosed malignant gliomas. J Clin Oncol 18:3862-72.

23. de Bruin A, Wu L, Saavedra HI, Wilson P, Yang Y, Rosol TJ, Weinstein M, Robinson ML, Leone G (2003) Rb function in extraembryonic lineages suppresses apoptosis in the CNS of Rb-deficient mice. Proc Natl Acad Sci U S A 100:6546-51.

24. DeCaprio JA, Ludlow JW, Lynch D, Furukawa Y, Griffin J, Piwnica-Worms H, Huang CM, Livingston DM (1989) The product of the retinoblastoma susceptibility gene has properties of a cell cycle regulatory element. Cell 58:1085-95.

25. Ding H, Roncari L, Shannon P, Wu X, Lau N, Karaskova J, Gutmann DH, Squire JA, Nagy A, Guha A (2001) Astrocyte-specific expression of activated p21-ras results in malignant astrocytoma formation in a transgenic mouse model of human gliomas. Cancer Res 61:3826-36.

26. Dlugosz AA, Hansen L, Cheng C, Alexander N, Denning MF, Threadgill DW, Magnuson T, Coffey RJ Jr, Yuspa SH (1997) Targeted disruption of the epidermal growth factor receptor impairs growth of squamous papillomas expressing the v-ras(Ha) oncogene but does not block in vitro keratinocyte responses to oncogenic ras. Cancer Res 57:3180-8.

27. Doetsch F, Garcia-Verdugo JM, Alvarez-Buylla A (1997) Cellular composition and three-dimensional organization of the subventricular germinal zone in the adult mammalian brain. J Neurosci 17:5046-61.

28. Doetsch F, Petreanu L, Caille I, Garcia-Verdugo JM, Alvarez-Buylla A (2002) EGF converts transit-amplifying neurogenic precursors in the adult brain into multipotent stem cells. Neuron 36:1021-34.

29. Doetsch F, Caille I, Lim DA, Garcia-Verdugo JM, Alvarez-Buylla A (1999) Subventricular zone astrocytes are neural stem cells in the adult mammalian brain. Cell 97:703-16.

30. Dyson N, Buchkovich K, Whyte P, Harlow E (1989) The cellular 107K protein that binds to adenovirus E1A also associates with the large T antigens of SV40 and JC virus. Cell 58:249-55.

31. Eagle LR, Yin X, Brothman AR, Williams BJ, Atkin NB, Prochownik EV (1995) Mutation of the MXI1 gene in prostate cancer. Nat Genet 9:249-55.

32. Ewen ME, Ludlow JW, Marsilio E, DeCaprio JA, Millikan RC, Cheng SH, Paucha E, Livingston DM (1989) An N-terminal transformation-governing sequence of SV40 large T antigen contributes to the binding of both p110Rb and a second cellular protein, p120. Cell 58:257-67.

33. Falls DL (2003) Neuregulins: functions, forms, and signaling strategies. Exp Cell Res 284:14-30.

34. Fraser MM, Zhu X, Kwon CH, Uhlmann EJ, Gutmann DH, Baker SJ (2004) Pten loss causes hypertrophy and increased proliferation of astrocytes in vivo. Cancer Res 64:7773-9.

35. Fricker-Gates RA, Winkler C, Kirik D, Rosenblad C, Carpenter MK, Bjorklund A (2000) EGF infusion stimulates the proliferation and migration of embryonic progenitor cells transplanted in the adult rat striatum. Exp Neurol 165:237-47.

36. Friday BB, Adjei AA (2005) K-ras as a target for cancer therapy. Biochim Biophys Acta 1756:127-44.

37. Fujisawa H, Reis RM, Nakamura M, Colella S, Yonekawa Y, Kleihues P, Ohgaki H (2000) Loss of heterozygosity on chromosome 10 is more extensive in primary (de novo) than in secondary glioblastomas. Lab Invest 80:65-72.

38. Fukuoka M, Yano S, Giaccone G, Tamura T, Nakagawa K, Douillard JY, Nishiwaki Y, Vansteenkiste J, Kudoh S, Rischin D, Eek R, Horai T, Noda K, Takata I, Smit E, Averbuch S, Macleod A, Feyereislova A, Dong RP, Baselga J (2003) Multi-institutional randomized phase II trial of gefitinib for previously treated patients with advanced non-small-cell lung cancer (The IDEAL 1 Trial). J Clin Oncol 21:2237-46.

39. Gangarosa LM, Sizemore N, Graves-Deal R, Oldham SM, Der CJ, Coffey RJ (1997) A raf-independent epidermal growth factor receptor autocrine loop is necessary for Ras transformation of rat intestinal epithelial cells. J Biol Chem 272:18926-31.

40. Garcia-Verdugo JM, Doetsch F, Wichterle H, Lim DA, Alvarez-Buylla A (1998) Architecture and cell types of the adult subventricular zone: in search of the stem cells. J Neurobiol 36:234-48.

41. Ghimenti C, Fiano V, Chiado-Piat L, Chio A, Cavalla P, Schiffer D (2003) Deregulation of the p14ARF/Mdm2/p53 pathway and G1/S transition in two glioblastoma sets. J Neurooncol 61:95-102.

42. Goudar RK, Shi Q, Hjelmeland MD, Keir ST, McLendon RE, Wikstrand CJ, Reese ED, Conrad CA, Traxler P, Lane HA, Reardon DA, Cavenee WK, Wang XF, Bigner DD, Friedman HS, Rich JN (2005) Combination therapy of inhibitors of epidermal growth factor receptor/vascular endothelial growth factor receptor 2 (AEE788) and the mammalian target of rapamycin (RAD001) offers improved glioblastoma tumor growth inhibition. Mol Cancer Ther 4:101-12.

43. Guha A, Feldkamp MM, Lau N, Boss G, Pawson A (1997) Proliferation of human malignant astrocytomas is dependent on Ras activation. Oncogene 15:2755-65.

44. Gutmann DH, Maher EA, Van Dyke T (2006) Mouse Models of Human Cancers Consortium Workshop on Nervous System Tumors. Cancer Res 66:10-3.

45. Hall A, Marshall CJ, Spurr NK, Weiss RA (1983) Identification of transforming gene in two human sarcoma cell lines as a new member of the ras gene family located on chromosome 1. Nature 303:396-400.

46. Hansen R, Oren M (1997) p53; from inductive signal to cellular effect. Current Opinion in Genetics & Development 7:46-51.

47. Harris RC, Chung E, Coffey RJ (2003) EGF receptor ligands. Exp Cell Res 284:2-13.

48. Harris SL, Levine AJ (2005) The p53 pathway: positive and negative feedback loops. Oncogene 24:2899-908.

49. Hatva E, Kaipainen A, Mentula P, Jaaskelainen J, Paetau A, Haltia M, Alitalo K (1995) Expression of endothelial cell-specific receptor tyrosine kinases and growth factors in human brain tumors. Am J Pathol 146:368-78.

50. Henson JW, Schnitker BL, Correa KM, von Deimling A, Fassbender F, Xu HJ,

Benedict WF, Yandell DW, Louis DN (1994) The retinoblastoma gene is involved in malignant progression of astrocytomas. Annals of Neurology 36:714-721.

51. Hermanson M, Funa K, Hartman M, Claesson-Welsh L, Heldin CH, Westermark B, Nister M (1992) - Platelet-derived growth factor and its receptors in human glioma tissue: expression of messenger RNA and protein suggests the presence of autocrine and paracrine loops. Cancer Res 52:3213-9.

52. Hill, R., Song, Y., Cardiff, R. D., and Van Dyke, T. Heterogeneous tumor evolution initiated by loss of pRb function in a preclinical prostate cancer model. Cancer Research 65(22), 10243-54. 2005Ÿ.

53. Holland EC, Celestino J, Dai C, Schaefer L, Sawaya RE, Fuller GN (2000) Combined activation of Ras and Akt in neural progenitors induces glioblastoma formation in mice. Nat Genet 25:55-7.

54. Holland EC (2001) Progenitor cells and glioma formation. Curr Opin Neurol 14:683-8.

55. Hu X, Pandolfi PP, Li Y, Koutcher JA, Rosenblum M, Holland EC (2005) mTOR promotes survival and astrocytic characteristics induced by Pten/AKT signaling in glioblastoma. Neoplasia 7:356-68.

56. Huang HS, Nagane M, Klingbeil CK, Lin H, Nishikawa R, Ji XD, Huang CM, Gill GN, Wiley HS, Cavenee WK (1997) The enhanced tumorigenic activity of a mutant epidermal growth factor receptor common in human cancers is mediated by threshold levels of constitutive tyrosine phosphorylation and unattenuated signaling. J Biol Chem 272:2927-35.

57. Huang MC, Kubo O, Tajika Y, Takakura K (1996) A clinico-immunohistochemical study of giant cell glioblastoma. Noshuyo Byori 13:11-6.

58. Ichimura K, Schmidt EE, Miyakawa A, Goike HM, Collins VP (1998) Distinct patterns of deletion on 10p and 10q suggest involvement of multiple tumor suppressor genes in the development of astrocytic gliomas of different malignancy grades. Genes Chromosomes Cancer 22:9-15.

59. Ichimura K, Schmidt EE, Goike HM, Collins VP (1996) Human glioblastomas with no alterations of the *CDKN2A* (*p16^{INK4A}*, *MTS1*) and *CDK4* genes have frequent mutations of the retinoblastoma gene. Oncogene 13:1065-1072.

60. Jackson EL, Willis N, Mercer K, Bronson RT, Crowley D, Montoya R, Jacks T, Tuveson DA (2001) Analysis of lung tumor initiation and progression using conditional expression of oncogenic K-ras. Genes Dev 15:3243-8.

61. Jeng YM, Hsu HC (2003) KLF6, a putative tumor suppressor gene, is mutated in astrocytic gliomas. Int J Cancer 105:625-9.

62. Jorissen RN, Walker F, Pouliot N, Garrett TP, Ward CW, Burgess AW (2003) Epidermal growth factor receptor: mechanisms of activation and signalling. Exp Cell Res 284:31-53.

63. Kanzawa T, Ito H, Kondo Y, Kondo S (2003) Current and Future Gene Therapy for Malignant Gliomas. J Biomed Biotechnol 2003:25-34.

64. Karlbom AE, James CD, Boethius J, Cavenee WK, Collins VP, Nordenskjold M, Larsson C (1993) Loss of heterozygosity in malignant gliomas involves at least three distinct regions on chromosome 10. Hum Genet 92:169-74.

65. Kesari S, Ramakrishna N, Sauvageot C, Stiles CD, Wen PY (2005) Targeted molecular therapy of malignant gliomas. Curr Neurol Neurosci Rep 5:186-97.

66. Kilic T, Alberta JA, Zdunek PR, Acar M, Iannarelli P, O'Reilly T, Buchdunger E, Black PM, Stiles CD (2000) Intracranial inhibition of platelet-derived growth factor-mediated glioblastoma cell growth by an orally active kinase inhibitor of the 2-phenylaminopyrimidine class. Cancer Res 60:5143-50.

67. Kleihues P, Ohgaki H (1999) Primary and secondary glioblastomas: from concept to clinical diagnosis. Neuro-oncol 1:44-51.

68. Kleihues, P., and Cavenee, W.K. eds. (200). World Health Organization Classification of Tumours of the Nervous System (Lyon: WO/IARC).

69. Knobbe CB, Reifenberger J, Reifenberger G (2004) Mutation analysis of the Ras pathway genes NRAS, HRAS, KRAS and BRAF in glioblastomas. Acta Neuropathol (Berl) 108:467-70.

70. Knobbe CB, Merlo A, Reifenberger G (2002) Pten signaling in gliomas. Neuro-oncol 4:196-211.

71. Kobayashi N, Allen N, Clendenon NR, Ko LW (1980) An improved rat brain-tumor model. J Neurosurg 53:808-15.

72. Koera K, Nakamura K, Nakao K, Miyoshi J, Toyoshima K, Hatta T, Otani H, Aiba A, Katsuki M (1997) K-ras is essential for the development of the mouse embryo. Oncogene 15:1151-9.

73. Kris MG, Natale RB, Herbst RS, Lynch TJ Jr, Prager D, Belani CP, Schiller JH, Kelly K, Spiridonidis H, Sandler A, Albain KS, Cella D, Wolf MK, Averbuch SD, Ochs JJ, Kay AC (2003) Efficacy of gefitinib, an inhibitor of the epidermal growth factor receptor tyrosine kinase, in symptomatic patients with non-small cell lung cancer: a randomized trial. JAMA 290:2149-58.

74. Lee KY, Ladha MH, McMahon C, Ewen ME (1999) The retinoblastoma protein is linked to the activation of Ras. Mol Cell Biol 19:7724-32.

75. Lee MH, Williams BO, Mulligan G, Mukai S, Bronson RT, Dyson N , Harlow E, Jacks T (1996) Targeted disruption of p107: functional overlap between p107 and Rb. Genes Dev 10:1621-32.

76. Levine A (1997) p53, the cellular gatekeeper for growth and division. Cell 88:323-331.

77. Levine A, Momand J, Finlay C (1991) The p53 tumour suppressor gene. Nature 351:453-456.

78. Li DM, Sun H (1997) TEP1, encoded by a candidate tumor suppressor locus, is a novel protein tyrosine phosphatase regulated by transforming growth factor beta. Cancer Res 57:2124-9.

79. Li J, Yen C, Liaw D, Podsypanina K, Bose S, Wang SI, Puc J, Miliaresis C, Rodgers L, McCombie R, Bigner SH, Giovanella BC, Ittmann M, Tycko B, Hibshoosh H, Wigler MH, Parsons R (1997) PTEN, a putative protein tyrosine phosphatase gene mutated in human brain, breast, and prostate cancer. Science 275:1943-7.

80. Listernick R, Charrow J, Gutmann DH (1999) Intracranial gliomas in neurofibromatosis type 1. Am J Med Genet 89:38-44.

81. Maher EA, Furnari FB, Bachoo RM, Rowitch DH, Louis DN, Cavenee WK, DePinho RA (2001) Malignant glioma: genetics and biology of a grave matter. Genes Dev 15:1311-33.

82. Malatesta P, Hartfuss E, Gotz M (2000) Isolation of radial glial cells by fluorescent-activated cell sorting reveals a neuronal lineage. Development 127:5253-63.

83. Malatesta P, Hack MA, Hartfuss E, Kettenmann H, Klinkert W, Kirchhoff F, Gotz M (2003) Neuronal or glial progeny: regional differences in radial glia fate. Neuron 37:751-64.

84. McKay R (1997) Stem cells in the central nervous system. Science 276:66-71.

85. Mellinghoff IK, Wang MY, Vivanco I, Haas-Kogan DA, Zhu S, Dia EQ, Lu KV, Yoshimoto K, Huang JH, Chute DJ, Riggs BL, Horvath S, Liau LM, Cavenee WK, Rao PN, Beroukhim R, Peck TC, Lee JC, Sellers WR, Stokoe D, Prados M, Cloughesy TF, Sawyers CL, Mischel PS (2005) Molecular determinants of the response of glioblastomas to EGFR kinase inhibitors. N Engl J Med 353:2012-24.

86. Miyakawa A, Ichimura K, Schmidt EE, Varmeh-Ziaie S, Collins VP (2000) Multiple deleted regions on the long arm of chromosome 6 in astrocytic tumours. Br J Cancer 82:543-9.

87. Mollenhauer J, Wiemann S, Scheurlen W, Korn B, Hayashi Y, Wilgenbus KK, von Deimling A, Poustka A (1997) DMBT1, a new member of the SRCR superfamily, on chromosome 10q25.3-26.1 is deleted in malignant brain tumours. Nat Genet 17:32-9.

88. Nakamura H, Yoshida M, Tsuiki H, Ito K, Ueno M, Nakao M, Oka K, Tada M, Kochi M, Kuratsu J, Ushio Y, Saya H (1998) Identification of a human homolog of the Drosophila neuralized gene within the 10q25.1 malignant astrocytoma deletion region. Oncogene 16:1009-19.

89. Nakamura M, Watanabe T, Klangby U, Asker C, Wiman K, Yonekawa Y, Kleihues P, Ohgaki H (2001a) p14ARF deletion and methylation in genetic pathways to glioblastomas. Brain Pathol 11:159-68.

90. Nakamura M, Yonekawa Y, Kleihues P, Ohgaki H (2001b) Promoter hypermethylation of the RB1 gene in glioblastomas. Lab Invest 81:77-82.

91. Nister M, Libermann TA, Betsholtz C, Pettersson M, Claesson-Welsh L, Heldin CH, Schlessinger J, Westermark B (1988) Expression of messenger RNAs for platelet-derived growth factor and transforming growth factor-alpha and their receptors in human malignant glioma cell lines. Cancer Res 48:3910-8.

92. Ohgaki H, Dessen P, Jourde B, Horstmann S, Nishikawa T, Di Patre PL, Burkhard C, Schuler D, Probst-Hensch NM, Maiorka PC, Baeza N, Pisani P, Yonekawa Y, Yasargil MG, Lutolf UM, Kleihues P (2004) Genetic pathways to glioblastoma: a population-based study. Cancer Res 64:6892-9.

93. Ohgaki H (2005) Genetic pathways to glioblastomas. Neuropathology 25:1-7.

94. Pao W, Miller VA (2005) Epidermal growth factor receptor mutations, small-molecule kinase inhibitors, and non-small-cell lung cancer: current knowledge and future directions. J Clin Oncol 23:2556-68.

95. - Peeper, D. S., - Upton, T. M., - Ladha, M. H., - Neuman, E., - Zalvide, J., - Bernards, R., - DeCaprio, J. A., and - Ewen, M. E. - Ras signalling linked to the cell-cycle machinery by the retinoblastoma protein [published erratum appears in Nature 1997 Apr 3;386(6624):521]. - Nature 1997 Mar 13;386(6621):177-81 .

96. Plate KH, Breier G, Farrell CL, Risau W (1992) Platelet-derived growth factor receptor-beta is induced during tumor development and upregulated during tumor progression in endothelial cells in human gliomas. Lab Invest 67:529-34.

97. Pruitt K, Der CJ (2001) Ras and Rho regulation of the cell cycle and oncogenesis. Cancer Lett 171:1-10.

98. Pulkkanen KJ, Yla-Herttuala S (2005) Gene therapy for malignant glioma: current clinical status. Mol Ther 12:585-98.

99. Raabe TD, Francis A, DeVries GH (1998) Neuregulins in glial cells. Neurochem Res 23:311-8.

100. Raizer JJ (2005) HER1/EGFR tyrosine kinase inhibitors for the treatment of glioblastoma multiforme. J Neurooncol 74:77-86.

101. Rasheed BK, McLendon RE, Friedman HS, Friedman AH, Fuchs HE, Bigner DD, Bigner SH (1995) Chromosome 10 deletion mapping in human gliomas: a common deletion region in 10q25. Oncogene 10:2243-6.

102. Reardon DA, Egorin MJ, Quinn JA, Rich JN, Gururangan S, Vredenburgh JJ, Desjardins A, Sathornsumetee S, Provenzale JM, Herndon JE 2nd, Dowell JM, Badruddoja MA, McLendon RE, Lagattuta TF, Kicielinski KP, Dresemann G, Sampson JH, Friedman AH, Salvado AJ, Friedman HS (2005) Phase II study of imatinib mesylate plus hydroxyurea in adults with recurrent glioblastoma multiforme. J Clin Oncol 23:9359-68.

103. Reifenberger G, Liu L, Ichimura K, Schmidt EE, Collins VP (1993) Amplification and overexpression of the MDM2 gene in a subset of human malignant gliomas without p53 mutations. Cancer Res 53:2736-9.

104. Reilly, K. M. and Jacks, T. Genetically engineered mouse models of astrocytoma: GEMs in the rough?. [Review] [120 refs]. Seminars in Cancer Biology 11(3), 177-91. 2001.

105. Reilly KM, Loisel DA, Bronson RT, McLaughlin ME, Jacks T (2000) Nf1;Trp53 mutant mice develop glioblastoma with evidence of strain-specific effects. Nat Genet 26:109-13.

106. Rich JN, Reardon DA, Peery T, Dowell JM, Quinn JA, Penne KL, Wikstrand CJ, Van Duyn LB, Dancey JE, McLendon RE, Kao JC, Stenzel TT, Ahmed Rasheed BK, Tourt-Uhlig SE, Herndon JE 2nd, Vredenburgh JJ, Sampson JH, Friedman AH, Bigner DD, Friedman HS (2004) Phase II trial of gefitinib in recurrent glioblastoma. J Clin Oncol 22:133-42.

107. Ritch PA, Carroll SL, Sontheimer H (2003) Neuregulin-1 enhances motility and migration of human astrocytic glioma cells. J Biol Chem 278:20971-8.

108. Robanus-Maandag E, Dekker M, van der Valk M, Carrozza ML, Jeanny JC, Dannenberg JH, Berns A, te Riele H (1998) p107 is a suppressor of retinoblastoma development in pRb-deficient mice. Genes Dev 12:1599-609.

109. Rodriguez-Viciana P, Warne PH, Dhand R, Vanhaesebroeck B, Gout I, Fry MJ, Waterfield MD, Downward J (1994) Phosphatidylinositol-3-OH kinase as a direct target of Ras. Nature 370:527-32.

110. Rodriguez-Viciana P, Warne PH, Khwaja A, Marte BM, Pappin D, Das P, Waterfield MD, Ridley A, Downward J (1997) Role of phosphoinositide 3-OH kinase in cell transformation and control of the actin cytoskeleton by Ras. Cell 89:457-67.

111. Roussel MF (1999) The INK4 family of cell cycle inhibitors in cancer. Oncogene 18:5311-7.

112. Sage J, Mulligan GJ, Attardi LD, Miller A, Chen S, Williams B, Theodorou E, Jacks

T (2000) Targeted disruption of the three Rb-related genes leads to loss of G (1) control and immortalization. Genes Dev 14:3037-50.

113. Sanai N, Alvarez-Buylla A, Berger MS (2005) Neural stem cells and the origin of gliomas. N Engl J Med 353:811-22.

114. Shapiro WR, Basler GA, Chernik NL, Posner JB (1979) Human brain tumor transplantation into nude mice. J Natl Cancer Inst 62:447-53.

115. Sherr CJ, Roberts JM (1999) CDK inhibitors: positive and negative regulators of G1-phase progression. Genes Dev 13:1501-12.

116. Shimizu K, Goldfarb M, Suard Y, Perucho M, Li Y, Kamata T, Feramisco J, Stavnezer E, Fogh J, Wigler MH (1983) Three human transforming genes are related to the viral ras oncogenes. Proc Natl Acad Sci U S A 80:2112-6.

117. Simin K, Wu H, Lu L, Pinkel D, Albertson D, Cardiff RD, Van Dyke T (2004) pRb Inactivation in Mammary Cells Reveals Common Mechanisms for Tumor Initiation and Progression in Divergent Epithelia. PLoS Biol 2:E22.

118. Singh AB, Harris RC (2005) Autocrine, paracrine and juxtacrine signaling by EGFR ligands. Cell Signal 17:1183-93.

119. Soriano P (1999) Generalized lacZ expression with the ROSA26 Cre reporter strain. Nat Genet 21:70-1.

120. Steck PA, Pershouse MA, Jasser SA, Yung WK, Lin H, Ligon AH, Langford LA, Baumgard ML, Hattier T, Davis T, Frye C, Hu R, Swedlund B, Teng DH, Tavtigian SV (1997) Identification of a candidate tumour suppressor gene, MMAC1, at chromosome 10q23.3 that is mutated in multiple advanced cancers. Nat Genet 15:356-62.

121. Suzuki A, Yamaguchi MT, Ohteki T, Sasaki T, Kaisho T, Kimura Y, Yoshida R, Wakeham A, Higuchi T, Fukumoto M, Tsubata T, Ohashi PS, Koyasu S, Penninger JM, Nakano T, Mak TW (2001) T cell-specific loss of Pten leads to defects in central and peripheral tolerance. Immunity 14:523-34.

122. Swenberg JA, Koestner A, Wechsler W (1971) The induction of tumors of the nervous system in rats with intravenous methylnitrosourea (MNU). J Neuropathol Exp Neurol 30:122.

123. Tachibana O, Lampe J, Kleihues P, Ohgaki H (1996) Preferential expression of Fas/APO1 (CD95) and apoptotic cell death in perinecrotic cells of glioblastoma multiforme. Acta Neuropathol (Berl) 92:431-4.

124. Takahashi C, Contreras B, Bronson RT, Loda M, Ewen ME (2004) Genetic interaction between Rb and K-ras in the control of differentiation and tumor suppression. Mol Cell Biol 24:10406-15.

125. Tuzi NL, Venter DJ, Kumar S, Staddon SL, Lemoine NR, Gullick WJ (1991) Expression of growth factor receptors in human brain tumours. Br J Cancer 63:227-33.

126. Ueki K, Ono Y, Henson JW, Efird JT, von Deimling A, Louis DN (1996) CDKN2/p16 or RB alterations occur in the majority of glioblastomas and are inversely correlated. Cancer Res 56:150-3.

127. Watanabe K, Sato K, Biernat W, Tachibana O, von Ammon K, Ogata N, Yonekawa Y, Kleihues P, Ohgaki H (1997) Incidence and timing of p53 mutations during astrocytoma progression in patients with multiple biopsies. Clin Cancer Res 3:523-30.

128. Watanabe K, Tachibana O, Sata K, Yonekawa Y, Kleihues P, Ohgaki H (1996) Overexpression of the EGF receptor and p53 mutations are mutually exclusive in the evolution of primary and secondary glioblastomas. Brain Pathol 6:217-23; discussion 23-4.

129. Wechsler DS, Shelly CA, Petroff CA, Dang CV (1997) MXI1, a putative tumor suppressor gene, suppresses growth of human glioblastoma cells. Cancer Res 57:4905-12.

130. Weickert CS, Blum M (1995) Striatal TGF-alpha: postnatal developmental expression and evidence for a role in the proliferation of subependymal cells. Brain Res Dev Brain Res 86:203-16.

131. Weissenberger J, Steinbach JP, Malin G, Spada S, Rulicke T, Aguzzi A (1997) Development and malignant progression of astrocytomas in GFAP-v-src transgenic mice. Oncogene 14:2005-13.

132. Wen PY, Kesari S (2004) Malignant gliomas. Curr Neurol Neurosci Rep 4:218-27.

133. Westphal M, Meima L, Szonyi E, Lofgren J, Meissner H, Hamel W, Nikolics K, Sliwkowski MX (1997) Heregulins and the ErbB-2/3/4 receptors in gliomas. J Neurooncol 35:335-46.

134. Wong AJ, Bigner SH, Bigner DD, Kinzler KW, Hamilton SR, Vogelstein B (1987) - Increased expression of the epidermal growth factor receptor gene in malignant gliomas is invariably associated with gene amplification. - Proc Natl Acad Sci U S A 1987 Oct;84(19):6899-903. - 84:- 6899-903.

135. Xiao A, Wu H, Pandolfi PP, Louis DN, Van Dyke T (2002) Astrocyte inactivation of the pRb pathway predisposes mice to malignant astrocytoma development that is accelerated by PTEN mutation. Cancer Cell 1:157-68.

136. Yang L, Ng KY, Lillehei KO (2003) Cell-mediated immunotherapy: a new approach to the treatment of malignant glioma. Cancer Control 10:138-47.

137. Yang XD, Jia XC, Corvalan JR, Wang P, Davis CG, Jakobovits A (1999) Eradication

of established tumors by a fully human monoclonal antibody to the epidermal growth factor receptor without concomitant chemotherapy. Cancer Res 59:1236-43.

138. Zhu Y, Guignard F, Zhao D, Liu L, Burns DK, Mason RP, Messing A, Parada LF (2005) Early inactivation of p53 tumor suppressor gene cooperating with NF1 loss induces malignant astrocytoma. Cancer Cell 8:119-30.

139. Zhuo L, Theis M, Alvarez-Maya I, Brenner M, Willecke K, Messing A (2001) hGFAP-cre transgenic mice for manipulation of glial and neuronal function in vivo. Genesis 31:85-94.